DETERMINATION OF TRIACYLGLYCEROLS IN

EDIBLE OILS BY INFUSION ESI/MS AND ESI/MS/MS

DETERMINATION OF TRIACYLGLYCEROLS IN

EDIBLE OILS BY INFUSION ESI/MS AND ESI/MS/MS

By

BIRITAWIT ASFAW, B.A., B.Eng.

A Thesis

Submitted to the School of Graduate Studies

in Partial Fulfillment of the Requirements

for the Degree

Master of Science

McMaster University

MASTER OF SCIENCE (2010)   McMaster University

(Chemistry and Chemical Biology)   Hamilton, Ontario

TITLE: Determination of Triacylglycerols in Edible Oils by Infusion ESI/MS and ESI/MS/MS

AUTHOR: Biritawit Asfaw, B.Eng. (Ryerson University); B.A. (Addis Abeba University, Ethiopia)

SUPERVISOR: Professor B.E. McCarry

NUMBER OF PAGES: xvii, 144

ABSTRACT

Edible oils consist primarily of triacylglycerols (or TAGs), which are triesters of glycerol and fatty acids. Determination of the TAG compositions of edible oils is becoming more important, given the economic value of these oil products and the increasing incidence of adulterating high quality oils with poorer quality oils. In this study we report the development of an analytical protocol using positive ion infusion electrospray mass spectrometry (ESI/MS) in conjunction with tandem mass spectrometry which affords both identification and quantification of TAGs in edible oils samples.

This thesis reports a simple, comprehensive and quantitative method for the analysis of TAGs in edible oils in which the optimized method involves the infusion of an oil sample in chloroform:methanol (1:1) solution (~10-15 μg/mL of oil) in the presence of 0.5 mM LiCl. A sequence of corrections were applied to the raw peak area data of the TAG molecular ions, $[M+Li]^+$, to account for: (1) normalization of peak area data using three internal standards, (2) peak area contributions of M+2 isotopic peaks of TAGs with one more degree of unsaturation and (3) peak area contributions of LiCl adduct ions, $[M+Li+LiCl]^+$, when applicable. The major correction involved multiplication to a given TAG peak area by the appropriate electrospray relative response factor (RRF) for that TAG. The RRFs for all TAGs containing between 48 and 63 carbons in their fatty acyl chains and between 0 and 9 degrees of unsaturation were extrapolated from experimentally determined response factors of a series of standards. The RRFs were found to decrease by 6.7% for each additional acyl chain carbon but increased by 18.6% for each double bond. Comparison of these calculated RRFs to

reported RRFs for a series of TAG standards showed an excellent correlation (1.06% ± 10.20% RSD).

The use of Li$^+$ in TAG analysis followed from the reports by Hsu and Turk [93] and Han and Gross [18] which showed that Li$^+$ afforded more intense MS, and particularly MS/MS, spectra than either H$^+$ or Na$^+$. The enhanced intensities in MS/MS spectra (determined using a triple quadrupole mass spectrometer) were critical for the identification of TAGs, including the identity of the fatty acyl group located at the *sn-2* position. However, this method cannot distinguish unambiguously between isobaric TAGs. This methodology was applied to the profiling of a number of edible oils including canola, olive, sesame, grape seed, walnut and hemp seed oils. The major TAGS in these samples contained 52, 54 and 56 carbons with between 0 and 11 degrees on unsaturation in a given TAG. There were minor amounts of TAGs containing 50, 55 and 57 carbons.

The ability of this method to determine quantitatively the number of degrees of unsaturation in an oil sample was tested by examining a series of partially hydrogenated canola oil samples kindly provided by Bunge Canada. Five oil samples derived from a single feedstock with differing numbers of degrees of unsaturation, measured as iodine values, were subjected to our analytical method. The measured iodine values were compared to iodine values calculated from the number of degrees of unsaturation obtained by our MS-based method. The slope of this correlation was 1.10 with an R^2 = 0.995. Overall, this method is much simpler and more accurate than the protocol

described by Han and Gross [18]. This methodology will be applied as routine method

for the analysis of TAGs in biological samples such as blood samples.

ACKNOWLEDGEMENTS

patiently fulfilled family responsibilities and continually provided me the love and support throughout this journey. Finally, I would like to dedicate my thesis to my oldest sister Rishan who scarified a lot to raise me and my siblings. I am where I am because of you. I am forever grateful and will never forget.

TABLE OF CONTENTS

LIST OF FIGURES

LIST OF TABLES

LIST OF ABBREVIATIONS

CI	chemical ionization
CID	collision-induced dissociation
CRM	charge residue method
DOU	degrees of unsaturation
EI	electron ionization
ELSD	evaporative light scattering detection
ESI	electrospray ionization
ESI/MS	electrospray ionization/ mass spectrometry
ESI/MS/MS	electrospray ionization/ mass spectrometry/ mass spectrometry
FAME	fatty acid methyl ester
FDI	field desorption ionization
FTICR	Fourier transform ion cyclotron resonance
GC/MS	gas chromatography/mass spectrometry
HT-CGC	high temperature capillary gas chromatography
HT-GC/MS	high temperature gas chromatography/mass spectrometry
ICF	isotopic correction factor
IDM	ion desorption method
IS	internal standard
IV	iodine value
LC/MS	liquid chromatography/mass spectrometry
MS/MS	mass spectrometry /mass spectrometry (tandem mass spectrometry)

NMR	nuclear magnetic resoance
PA	peak area
QC	quality control
QToF	quadrupole time-of-flight
RF	response factor
RI	refractive index
RRF	relative response factor
S/N	signal-to-noise ratio
TAG	triacylglycerol

1. INTRODUCTION

1.1 Lipid Definition, Classification, and Nomenclature

The word lipid is used to describe a chemically heterogeneous group of substances which are soluble in non-polar solvents and insoluble in water. Lipids are broadly divided into four major classes (Figure 1.1) commonly referred to as simple lipids, complex lipids, steroids, and prostaglandins and leukotrienes [1]. This thesis will deal with the analysis of simple lipids, the triesters of glycerol, also known as triacylglycerols or TAGs.
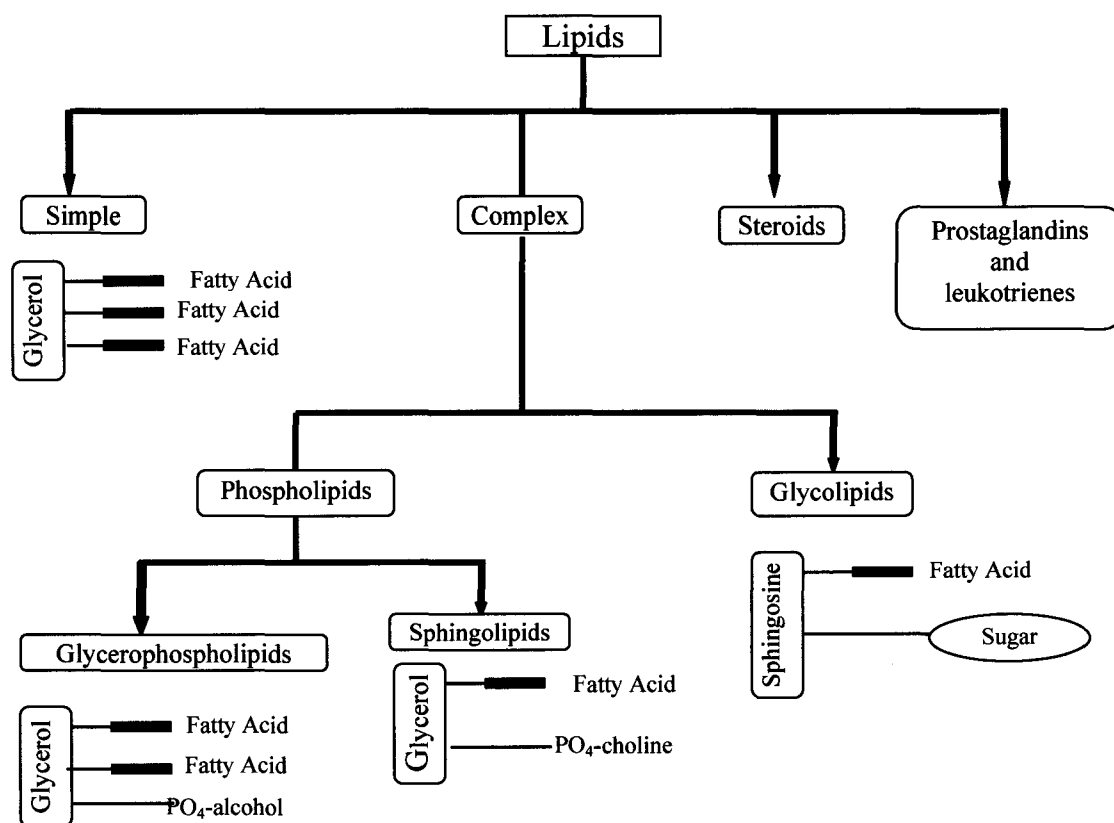
Figure 1.1 *Classification of lipids [1].*

Oils such as vegetable oils and animal fats are mainly mixtures of TAGs which are the most abundant lipids in nature [1-3]. These lipids are triesters of long chain aliphatic carboxylic acids (fatty acids) and glycerol (1,2,3-propanetriol). The chemical structure of a typical TAG molecule, 1-dodecyl-2-octadecyl-3-hexadecyl-*sn*-glycerol, is shown in Figure 1.2.
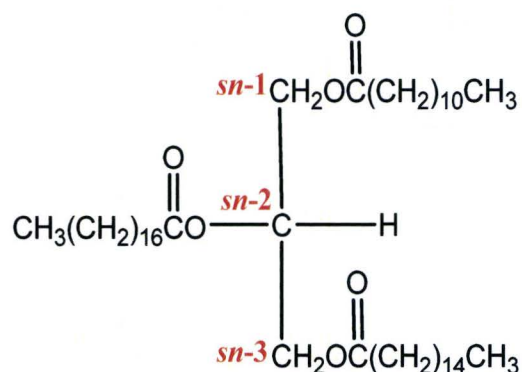
Figure 1.2 *Fischer Projection of a triacyl-sn-glycerol with 3 sn positions identified.*

The total number of carbons in the chains of the acyl groups in TAG molecules in oils ranges from 48-58 carbons [4, 5]. The carbon chains are usually even-numbered, and may contain from 0 to about 9 *cis* (Z) double bonds. The three fatty acyl groups of a TAG molecule can be identical or different, resulting a large number of possible TAG compounds.

TAGs are commonly represented using a simplified notation that indicates the total number of carbon atoms and the total number of double bonds in the three acyl substituents. For example, if a TAG had 54 carbons and 4 double bonds in the 3 fatty acid chains, the notation would be C54:4. TAGs can also be represented using a notation that

indicates the number of carbon atoms and number of double bonds in each of the three fatty acyl groups. For example, for a C48:4 TAG having three hexadecanoic fatty acyl groups whereby two of the acyl groups each has 1 double bond and the third acyl group has 2 double bonds, the notation would be written as C16:1/C16:1/C16:2. The three carbon atoms in the glycerol backbone are identified with the label "*sn*" which stands for "stereochemical numbering" and are numbered as *sn*-1, *sn*-2 and *sn*-3 accordingly. The assignment of the sn-1 and sn-3 positions is not arbitrary. According to IUPAC convention [6], if the middle hydroxyl or ester is shown to the left of middle carbon atom in a Fischer projection of the structure, the carbon above is assigned as carbon-1 and the carbon below is assigned as carbon-3 (Figure 1.2). The prefix "*sn*" is placed before the stem name of the TAG molecules if the stereochemistry of the TAG is known. For instance, the TAG in Figure 1.2 would be named as 1-dodecyl-2-octadecyl-3-hexadecyl-*sn*-glycerol.

The molecular structures of TAGs in edible oils are of great importance as they determine the physical and chemical properties of the oil. Physical properties such as melting point, solubility and viscosity are related to the structures of the TAG species in a food [7, 8]. For example, TAGs with longer carbon chains and fewer double bonds tend to be soft solids, have higher melting points, lower solubility in organic solvents and are less reactive in contrast with TAGs that have shorter carbon chains and more double bonds.

Vegetable oils contain complex mixtures of triacylglycerols with insignificant amounts of monoacylglycerols and diacylglycerols (shown in Figure 1.3) [9, 10].
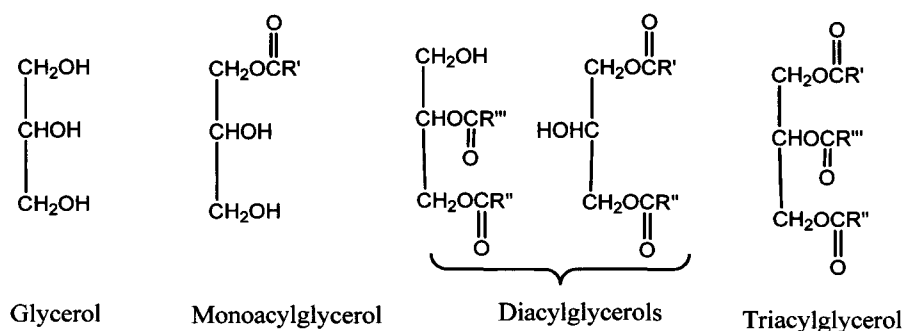
Figure 1.3 *Glycerol and glycerol ester classes.*

The complexity of TAG mixtures arises from the number of possible structural isomers due to the number of different fatty acids and the number of unsaturated fatty acids that a TAG molecule can have [11].

MW=807.3   MW=835.3   MW=863.4   MW=891.5
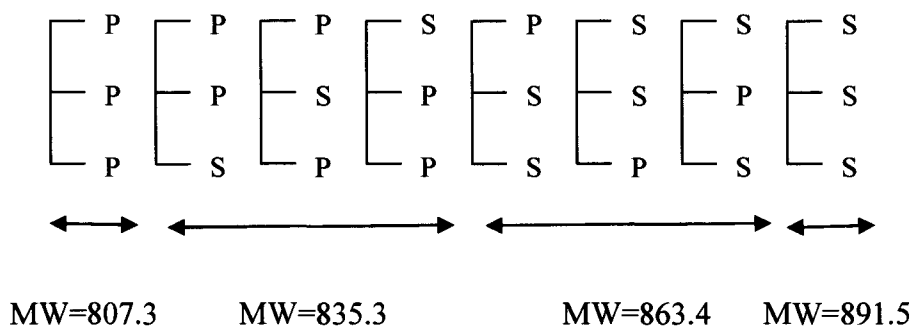
Figure 1.4 *Possible structures for triacyglycerols containing combinations of only two fatty acids, i.e. palmitic acid, (C16:0), (P) and/or stearic acid, (C18:0), (S) (reproduced from [11]).*

For example, a triacylglycerol with only two different fatty acid substituents can have eight different structures as shown in Figure 1.4. Table 1-1 illustrates the possible number of isomeric TAGs that could exist with different numbers of fatty acid substituents.

Table1.1 *The number of possible triacylglycerol isomers when 5, 10 or 20 different fatty acids can be selected from [11].*

	NUMBER OF DIFFERENT FATTY ACYL CHAINS		
	5	10	20
All isomers considered	125	1000	8000
Optical isomers excluded	75	550	4200

1.2 Processing of Edible Oils

In the food industry, vegetable oils are obtained mainly by extracting oils from oilseed crops such as peanuts, sunflowers, canola and soy using solvents such as hexane. The solvent is evaporated to leave the crude oil and is recovered and reused in a continuous extraction process. Additional processing steps are employed to purify the crude oil and also to produce fatty foods for different uses [2].

Vegetable oils are polyunsaturated liquids that can be converted into solids by a hydrogenation process which reduces the degree of unsaturation of the oils. In the food

industry, fully saturated oils have limited utility; therefore, oils are processed to have partial hydrogenation of their double bonds. Some examples of oil products with partial hydrogenation are margarine and shortening. The food industry partially hydrogenates oils so that products: 1) have higher melting points than unprocessed oils which is ideal for baking and high temperature cooking methods [12]; 2) have desirable consistency of creamy and smooth texture as butter and yet are cheaper in price than butter [2, 9]; and 3) have increased oxidative stability which extends shelf life and reduces the potential for rancidity [12]. However, a major disadvantage of high temperature hydrogenation is the conversion of the naturally occurring *Z (cis)* double bonds into E *(trans)* double bonds. The *cis* alkene bonds in the fatty acid chains give a 'kink' to the acyl chain structure which restricts the close packing of the molecules, resulting in flexible molecular structures with lower melting points [2, 13]. In comparison, *trans* bonds are structurally linear and pack into stable crystal forms. The intermolecular forces of the *trans* bonds are stronger than the cis bonds, hence; more energy is needed to melt the molecules resulting in higher melting points. For example, oleic acid (*cis* C18:1 n-9) melts at 13°C whereas elaidic acid (*trans* C18:1 n-9) melts at 45°C [14]. Thus trans fats are solids at human body temperature.

1.3 Oils and Health

Fats and oils are essential constituents of the human diet, along with carbohydrates and proteins. Fats are a major source of energy supplying about 9 calories per gram as opposed to proteins and carbohydrates which each supply about 4 calories

per gram [2, 12]. Fats and oils also aid the absorption of non-polar vitamins such as vitamins A, D, E and K into cells [2, 15].

The quality of oil consumed plays a major role in human health. Consumption of oils which are high in essential fatty acids, (e.g.,linoleic acid, C18:2, and linolenic acid, C18:3), is necessary to maintain proper growth and optimum physiological functions in the body [16]. Since these unsaturated fatty acids are not synthesized by humans, dietary intake of certain unsaturated oils is important to ensure good health. For example, a deficiency in α-linolenic acid has been associated with neurological abnormalities, poor growth and dermatitis [2]. In contrast, higher consumption of *trans* oils/fats and saturated oils/fats contributes to increased blood concentrations of LDL (low density lipoprotein), the so-called "bad cholesterol", resulting in an increased risk of cardiovascular diseases, hypertension and diabetes [12]. Studies have also shown that the *trans* fatty acids in the diet get incorporated into membrane lipids in the brain, altering the ability of neurons to communicate resulting in possible neural degeneration and diminished mental performance [17]. Thus, fast and reliable analytical methods are needed to determine the fatty acid profiles of triacylglycerols not only to ensure that processed oil products have the desired properties and have the chemical constituents claimed by the vendors, but also in the clinical laboratory to determine the profile of triacylglycerols in blood.

1.4 Analytical Techniques Used for the Analysis of Triacylglycerols in Edible Oils

Naturally occurring TAGs exist as a complex mixture of unique molecular species in edible oils and because of the complexity, many researchers have faced extensive

challenges in the identification and quantification of TAGs in lipid samples [18, 19]. Complexity arises due to the number of different fatty acids, which can theoretically produce a large number of TAGs and TAG isomers equal to n^3, where n is the number of available fatty acids. For example, with 5 different fatty acids, 125 TAGs are possible [11, 20]. Furthermore, the quantification of the TAGs is complicated since the signal response of TAGs in mass spectrometric analysis is greatly affected by the length of the carbon chain and number of double bonds on the fatty acyl substituents [18, 19].

Edible oils consist of TAGs that generally exhibit a unique pattern that reflects the characteristics of the oil seeds [21, 22]. However, the fatty acid compositions and the properties of many oils are affected by both environmental and human factors. Environmental factors like climate conditions, degree of fruit ripening and time of harvesting have significant effects on the chemical composition and quality of seed oils [23-25]. Human manipulation (i.e., adulteration) of oils also contributes to variations in the properties of edible oils. Adulteration of food oils has been an increasingly important issue in the food industry, stemming from the mixing of high quality oils with low quality oils [26-29]. Identification and quantification of TAGs are important in terms of the nutritional and functional characteristics of oils [30]. It is therefore essential to monitor the quality of oils and fats that humans consume. There is a need for reliable analytical methods to confirm the purity and integrity of edible oils.

The analytical information required to characterize and quantify intact TAGs in oil samples includes: (a) the determination of molecular masses of the TAG constituents in the oil samples, (b) the number of degrees of unsaturation of the TAG constituents, (c)

the composition of fatty acyl chains, (d) the position of each fatty acyl segment on the glycerol backbone and (e) the location and number of double bonds on each fatty acyl segment. Different analytical techniques have been employed for TAG profile studies of edible oils. Most analysis involve chromatographic, mass spectroscopic and to a lesser extent nuclear magnetic resonance techniques. No single analytical technique is currently available that will provide all of this data as each analytical technique presents its own unique benefits and limitations.

Quantification and structural analysis of TAGs using electrospray ionization mass spectrometry (ESI/MS) and electrospray ionization tandem mass spectrometry (ESI/MS/MS) are described in this thesis. A new aspect introduced in this thesis relates to a set of oil samples consisting of TAGs with fixed carbon number and varying degrees of unsaturation (DOU). Mass spectrometry relative response factors (RRFs) are strongly dependent on the degrees of unsaturation in which RRF increases with increasing DOU. An independent assessment of the degrees of unsaturation had been done on the oil samples by iodine value measurements. This provided an excellent platform from which to test the validity of the developed methodology for the quantification and structural analysis of the oils.

The advantages and limitations of the available analytical techniques are discussed below.

1.4.1 Analysis of Triacylglycerols by Chromatographic Techniques

Gas chromatography (GC) and high performance liquid chromatography (HPLC) with different detection methods are the most widely employed techniques for the separation and detection of TAGs in oil samples [31-35, 36-40].

Gas chromatography is traditionally used for the determination of fatty acid compositions in fats and oils. The analysis involves the release of the fatty acids from the lipids by hydrolysis and derivatization of the fatty acids to obtain volatile fatty acid methyl esters (FAMEs) [41-45]. The FAME mixture is analyzed by GC with flame ionization detection (FID) or mass spectrometric detection and identified based on comparison to authentic standard fatty acid methyl esters [10]. The elution order of FAMEs in GC analysis is based primarily on increasing carbon chain length [46-48]. Gas chromatographic/mass spectrometry (GC/MS) with electron impact (EI) ionization is also frequently used technique in lipid analysis [43], and was initially applied to the analysis of FAMEs as early as 1960 by Ryhage et al. [49] providing spectral information on the FAME molecular ion and its fragments. GC/MS provides sensitive, accurate, high-throughput and automated capabilities for the determination of fatty acid compositions in oil samples. However, the disadvantage of GC/MS are that quantification of intact TAGs is not possible; EI ionization induces excessive fragmentation of the molecular ions which results in total absence or low abundance of the molecular ion in the mass spectrum [43].

For analysis of intact TAG mixtures, high temperature capillary gas chromatography (HT-CGC) with a range of detection systems primarily FID and mass

spectrometric detection has been used [31-35]. HT-CGC utilizes capillary columns with thermally stable stationary phases (up to 380°C) [31]. The degree of polarity of the stationary phase affects the separation of TAG compounds, particularly those containing multiple double bonds. Non-polar stationary phases (having 0 to 5% phenyl content) in methyl polysiloxane coatings provide separations based primarily on boiling points of the analytes, which can be related to molecular masses [48]. On the other hand, polar stationary phases (50 to 65% phenyl content) can provide additional resolution according to the degree of unsaturation of the TAG species [32, 33]. HT-CGC/MS with EI ionization has also been used in the analysis of intact TAGs in which the EI mass spectra of TAGs show fragment ions corresponding to the neutral losses of the fatty acyl substituents which can facilitate the determination of the chemical structures of TAGs [32-34, 50, 51]. However, the mass spectrum is dominated by ions corresponding to the neutral losses of the fatty acyl substituents with very low abundances of molecular ions. Thus, the identities of the TAGs are usually determined from the prevalent diacylglycerol fragments. While HT-CGC has high resolving powers, polyunsaturated TAGs often thermally degrade under the analytical conditions limiting the utility of this method [5, 34, 50].

High performance liquid chromatography has also been used in the analysis of fatty acids, their derivatives (FAMEs) and intact TAGs. The technique is particularly useful for the analysis of the thermally labile higher mass intact TAGs of edible oils [36-40]. Reversed-phase high performance liquid chromatography (RP-HPLC) is widely employed in the separation of TAGs into groups according to total carbon number and

degrees of unsaturation [43, 48, 52, 53]. Hence, TAGs having shorter and more unsaturated carbon chains elute earlier than those having longer and more saturated carbon chains [43, 54, 55]. TAGs in oil samples are highly complex mixtures of compounds due to the number of fatty acids, the number of double bonds and their locations along the carbon chains [56]. This complexity increases the probability of having isobaric and isomeric TAGs that may co-elute. Complete resolution of the TAGs in an oil sample by HPLC is simply not possible due to the efficiencies and peak capacities of typical HPLC columns [5, 57, 58]. Recently new columns with better resolution and faster speed capability are emerging on the market. The new column innovations such as the UPLC® columns [59] using ≤2 μm particles and the Kinetex® UHPLC column [60] also having ≤ 2.6 μm particles with small size core-shell particles that allow shorter diffusion path and narrower particle size distribution would be of great utility in the advancement of HPLC techniques for lipid analysis.

The usual detection methods employed in HPLC are ultraviolet (UV), refractive index (RI), evaporative light scattering (ELS) and mass spectrometry (MS). Detection of fatty acids, FAMEs and intact TAGs using UV detectors is hampered by the absence of strong UV-active chromophores in the molecules [5, 61, 62]. In some cases the fatty acids have been derivatized to aromatic esters to introduce a UV chromophore [43]. RI detectors have also been used for HPLC analyses of underivatized species [52, 63]. However; RI detection is only used with isocratic mobile phases [7, 43, 52]. ELS detection is a universal and mass-sensitive detector that responds to any analyte that is less volatile than the mobile phase, and is also compatible with gradient elution [21, 64].

This can be an alternative to both UV and RI detection systems. However, the main limitation of ELS detection is that detector parameter fluctuation affects the droplet size of the aerosol which indirectly affects the detector response [64].

The utilization of soft ionization techniques particularly ESI has resulted in the application of LC/MS to identify and characterize TAGs in oils [22, 29, 65-67]. One of the disadvantages of LC/MS is the inability to separate co-eluting isobars and isomers; therefore, tandem mass spectrometry may be required for structural information [22, 56]. LC/MS in comparison to direct infusion mass spectrometric methods for TAGs will be discussed in 1.4.2.5.

Two-dimensional chromatographic methods have recently been applied to lipid analysis resulting in improved separations of TAGs [54, 68, 69]. Koning and co-workers have reported techniques such as LC_{TAG} x GC_{TAG} and LC_{TAG} x GC_{FAME} analyses [68, 69]. In the LC_{TAG} x GC_{TAG} technique, the fractions eluting from an LC column are transferred directly onto a GC column via a specially designed side port syringe; the LC pump is stopped and the GC analysis started. This process continues until all the eluents are analyzed [48]. In LC_{TAG} x GC_{FAME}, the TAGs fractioned in the first (LC) dimension are transferred into autosampler vials for transesterification of the TAGs to FAMEs and then the FAMEs are injected into the GC. This technique is not an on-line method like the LC_{TAG} x GC_{TAG} method [48]. The drawback of both methods is that they are rather time consuming (a single analysis can take several hours) which is not often practical for routine quality control analysis in the food industry.

Over all, in addition to the above mentioned limitations, chromatographic methods are time consuming and laborious which limit them as choices of high throughput and automated techniques for the analysis of intact TAGs in oil samples.

1.4.2 Analysis of Triacylglycerols by Mass Spectrometric Techniques

Mass spectrometry provides a direct and rapid method for the identification and structural characterization of lipids. Various ionization techniques such as EI ionization [49, 70], fast atom bombardment (FAB) [71, 72], atmospheric pressure chemical ionization (APCI) [73, 74] and ESI [18, 26, 58, 73, 75, 76] have been utilized to identify and characterize TAGs. The most widely utilized ionization technique is atmospheric pressure ionization (API) with ESI a preferred choice over APCI since in APCI the ionization takes place in a hot vapor chamber resulting in the fragmentation of the ions. Thus ESI is suitable for thermally labile samples such as TAGs and is the most popular ionization technique for lipid analysis as it affords both high sensitivity and quantifiable data. [77]

This thesis work involves direct infusion ESI/MS using a triple quadrupole mass spectrometer for the analysis of TAGs in oil samples. As a result, the rest of the section will be devoted on the development, principles and application of this technique.

1.4.2.1 Development of Electrospray Ionization

The technique of electrospray ionization (ESI) was invented by Dole in 1968 and his pioneering work has been demonstrated in the practical usage of electrospray to ionize intact molecules [78]. However, it was the work of Fenn that ultimately gave recognition to ESI as a potential ionization tool for high molecular mass biological molecules through multiple charging of non-volatile and thermally labile compounds. This method was soon interfaced to liquid chromatography [79, 80]. For his contribution, Fenn earned a shared 2002 Nobel Prize for chemistry. Today ESI/MS is the most widely used analytical technique for biological samples.

1.4.2.2 Principles of Electrospray Ionization Mass Spectrometry

Electrospray ionization is a soft ionization technique that allows molecules to be ionized with little or no fragmentation [81]. Figure1.5 displays the principles of the ESI process. In the ESI technique, ions are produced by directly infusing a sample solution through a capillary tube while applying an electric field to the capillary. With a potential difference of 3-4 kV between the capillary tip and a counter electrode, significant charge accumulation is induced in the solution at the capillary exit. In the positive ion mode, the tip of the capillary tube is positive relative to the mass analyzer. As the solution passes through the capillary tube, the negative ions are held back and the positive ions move forward to produce a mist of highly charged droplets [82, 83]. The charged droplets are then dispersed with the aid of a nebulizer gas such as nitrogen and desolvated by continuous solvent loss due to evaporation [1, 84, 85]. Depending on the instrument

design, additional desolvation gas is used to facilitate the solvent evaporation from the charged droplets. The droplet size decreases with an accompanying increase in charge density on the droplets, resulting in the breaking up of the droplets into smaller droplets due to Coulombic repulsion. This process continues until isolated ions are formed. The ions then pass through a sampling cone, are accelerated into the mass analyzer(s) and analyzed according to their mass-to-charge ratios (m/z).
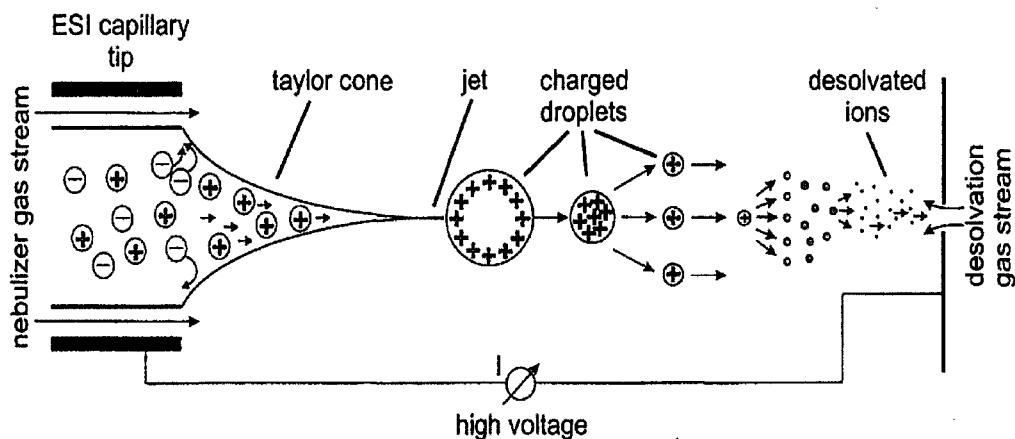
Figure 1.5 *Principles of electrospray ionization [85]*

Mechanism of Ion Formation in ESI

There are two widely accepted mechanisms that explain the formation of the gas phase ions from the charged solvent droplets described earlier [1, 86, 87]. The first

mechanism is the Charge Residue Model (CRM) which states that the droplets diminish in size by solvent evaporation assisted by the flow of drying nitrogen gas. The shrinkage of the droplets results in an increase in charge density on the surface of the droplets, and fission occurs when the droplet reaches the Rayleigh instability limit at which point the magnitude of the charge on the surface is sufficient to overcome the surface tension force that holds the droplet together [1, 82, 84, 85]. Through this Coulombic explosion process, multiple charged fragment droplets are formed, and this process continues until the solvent has evaporated and there is only one charged species (Figure 1.6a). The second mechanism is the Ion Desorption Model (IDM) that has been proposed based on earlier ideas of Iribarne and Thompson [88]. IDM is exactly the same as CRM in terms of the solvent evaporation and subsequent breakage of the droplets. However, the IDM process differs in that at some intermediate droplet size, the repulsive force between the charged ion and the other charges of the droplet is higher than the droplet's cohesive force which then leads to direct ion desorption (Figure 1.6b). Both mechanisms are topics of scientific discussion and research [82], although IDM seems to be currently accepted theory of ESI ion formation [1].
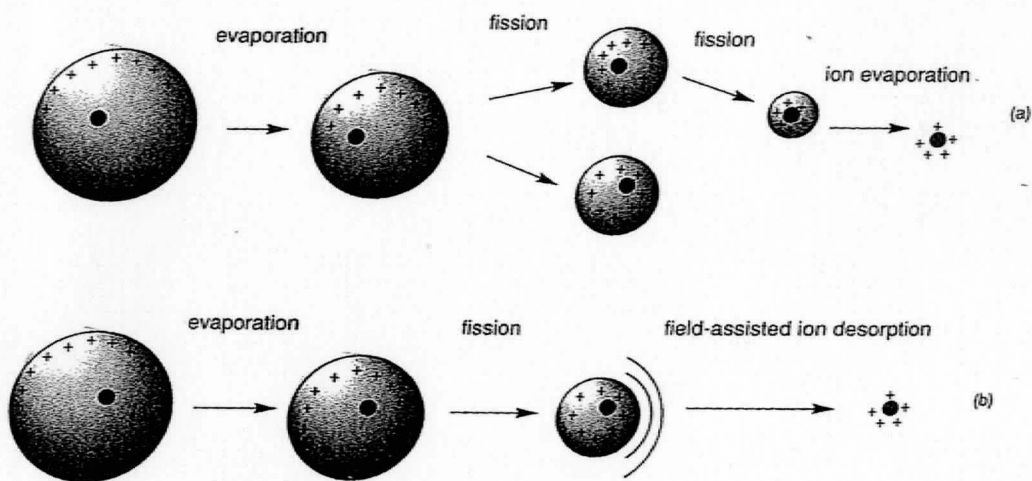
Figure 1.6 *Conceptualization of the process involved in the conversion of ions from droplets into the gas phase: (a) charge residue model and (b) ion desorption model [1]*

1.4.2.3 Tandem Mass Spectrometry

Tandem mass spectrometry (MS/MS) is an instrumental arrangement in which ions are subjected to two or more sequential stages, with the intention of fragmenting the ions. Tandem mass spectrometry can be done in either space or time [89]. Tandem MS in space involves the physical separation of the instrument components as exemplified by a triple quadrupole mass spectrometer (QqQ) or a quadrupole time-of-flight mass spectrometer (QTOF) [89]. Tandem mass spectrometry in time can be performed in an ion trap mass spectrometer. The ions are trapped in the same place with multiple separation steps taking place over time. Two instruments that are used for this type of

analysis are quadrupole ion trap and Fourier transform ion cyclotron resonance (FT-ICR) mass spectrometers [89].

Triple quadrupole mass spectrometers are the most widely used mass spectrometers for MS/MS analysis [90] and this type of instrument is used in this thesis. The configuration of a typical triple quadrupole mass spectrometer consists of three quadrupoles and the middle quadrupole may actually be a hexapole (Figure 1.7). The first (Q1) and third (Q3) quadrupoles are mass analyzers that separate ions based on their mass-to-charge ratio while the second quadrupole (Q2) functions as a collision chamber [91] with an inert gas such as argon being admitted to collide with the ions resulting in ion decomposition.
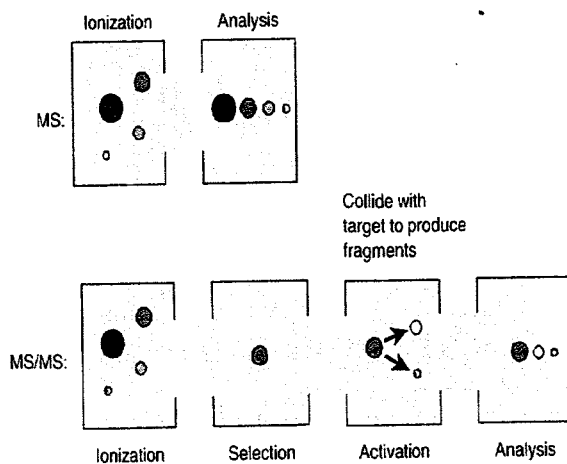
Figure 1.7 Single-stage MS and tandem MS/MS [92].

Quadrupole MS is suited to ESI since it can handle the relatively high analyzer pressure resulting from the atmospheric pressure in which the ions are produced [80]. Another advantage of an ESI quadrupole mass spectrometer is that in its being amenable to analysis of large intact biological molecules through multiple charging; however, its main limitation is that it is a low resolution (a unit mass) system.

There are three common MS/MS scan modes [91]: 1) the product ion scan or daughter ion scan is performed by setting first quadrupole (Q1) to allow only ions with one specific m/z value to pass through. The ion is fragmented in the second quadrupole (Q2) and the fragment ions are analyzed by scanning the third quadrupole (Q3). This scan is the most widely used MS/MS mode and is applied to obtain structural information of analytes. The product ion scan was employed in the experimental part of this thesis to gather structural information of TAGs in the oil samples; 2) the precursor ion scan or parent ion scan is performed by setting Q3 to a selected m/z while Q1 is scanned. Only those ions from Q1 which upon fragmentation in Q2 produce the selected ion in Q3 will be detected. This method is useful to provide m/z values of analytes that produce the selected product ion and 3) the neutral loss scan is performed by scanning both Q1 and Q3 simultaneously with a constant mass difference or defect (x) between the two selected ions. A selected ion with mass (m) in Q1 will be detected in Q3 only if the ion yields a fragment ion of mass (m-x) in Q2. This scan mode is used to screen for mixture compounds that lose a common neutral component [91].

1.4.2.4 Application of ESI/MS and ESI/MS/MS for Triacylglycerol Analysis in Edible Oils

Electrospray mass spectrometry has been used in lipid analysis since the mid 1990s and the "shotgun lipidomics" approach allowed the direct analysis of lipids from solutions as cationized intact molecules without prior chromatographic separations [18, 19, 27, 83, 84, 87, 91, 93-96]. Traditionally, lipids were analysed by chromatographic methods which involved two-stage chromatographic separations. First, complex lipid mixtures are separated into lipid classes and then each lipid class undergoes a second chromatographic separation to obtain even better resolution. However, this approach is laborious, time-consuming and prone to analyte losses limiting the sensitivity, particularly for minor analytes [97]. Since edible oils constitute primarily a single complex lipid class, i.e., TAGs, only a one-stage chromatographic separation is needed for the separation of the TAG species. In comparison, the direct infusion mass spectrometric method provides an intrasource separation of the molecular ions without prior use of chromatographic separation; hence, the use of LC is not necessary [98]. It is worth mentioning that in both methods, direct infusion MS and LC/MS, the overlapping of isobaric and isomeric TAG species is prevalent; thus, for complete structural characterization the use of tandem mass spectrometry is necessary.

The direct infusion method of ESI/MS and ESI/MS/MS has played a leading role in the identification, quantification and characterization of lipids and oils [83, 98-101]. First, the mass spectrometer serves as a separation device based on separations of ions by their m/z values. Second, there is no need for extensive sample preparation. Third, the

"soft" nature of the ionization results in minimal fragmentation allowing intact molecular ion identification. Fourth, tandem mass spectrometry has high sensitivity (DL about fmol/µL) and fifth, mass spectrometry methods have large dynamic ranges down to lower concentration regions (<10pmol/µL).

Although the direct infusion methodology has greatly simplified and facilitated the analysis of complex TAG mixtures in oil samples, identification and quantification of TAGs is a challenging task [18, 19, 27, 67, 75, 87, 91, 93]. There are a few issues that need to be addressed which include: 1) the intrasource separation technique cannot determine the composition of isobaric TAG species; tandem mass spectrometry can provide some useful information on isobaric species [18, 75, 83, 93, 98]; 2) the relative response of a given lipid class is dependent on the number of carbons and double bonds on the fatty acyl moieties, isotopic overlaps and total lipid concentration. To overcome this challenge the application of correction factors and utilization of an appropriate analysis concentration range is needed as mentioned in the previous paragraph [18, 83] and 3) this high throughput method generates a large amount of data in a relatively short time requiring a great deal of time to analyze the information [98]. Therefore, the use of tandem mass spectrometry and a quantitative model to deal with these incredibly complicated and large data sets is needed.

In this work, the analyses were performed using positive ion ESI/MS and ESI/MS/MS with triple quadrupole mass spectrometry for quantification and structural information of TAGs in oil samples. The rest of this section will focus on these techniques and provide a review of the literature on the types of cations used in the

ionization of TAGs, the methods of quantification and the structural determination of TAGs.

1.4.2.4.1 Cations Used for the Ionization of Triacylglycerols

TAGs are very weak bases and are not readily protonated. Duffin et al. [75] and Segall et al. [56] reported that the addition of formic acid into a solution of TAG standards produces a weak ion current corresponding to the protonated TAGs. One of the most useful aspects of ESI is that it can be used to analyze molecules which do not possess ionizable sites through the formation of adduct ions [56, 75, 83, 93, 102]. Cations such as Li^+, Na^+ and NH_4^+ have been used to increase the ionization efficiency of TAGs in positive ion mode analyses [56, 75, 93, 102]. Complexation of metal-cations with carbonyl bases has been previously investigated, showing that the cations are electrostatically bonded to the carbonyl oxygen which has unshared electrons [103, 104] through an ion-dipole attraction [104]. The adduct formation is based on interactions of the weak acid cations with the oxygens of the ester groups of the TAG species which have lone pairs of electrons; ester functional group form charge transfer complexes with the cations [104, 105].

The charge density of the cation determines the strength of the attachment of the ion to the TAGs. The greater the charge density (smaller ionic radius) of a cation, the easier that cation can polarize the electron density of the functional group, and form a bond between the cation and the ester oxygen of the TAG molecule [104, 105]. Lithium has an advantage over sodium and ammonium as a cationizing agent. Under collision

induced dissociation (CID) conditions, lithiated TAG adducts provide more structural information than either sodiated or ammoniated TAGs. Researchers have used these cations in the analysis of TAGs in lipids and a review of these works is presented in the following paragraphs.

ESI/MS analyses of TAG solutions in the presence of sodium acetate produced sodium adduct TAG ions, $[M+Na]^+$ [75, 106]. However, the sodiated molecular ions gave rather weak MS/MS spectra [75, 106]. Segall et al. [106] found that the MS/MS analysis of sodiated TAGs did not produce ions corresponding to fatty acids or monoacylglycerols, limiting the structural information in these spectra. As to the determination of regiospecific distribution of the fatty acids on the glycerol backbone of TAGs using the relative abundance of the diacylglycerol fragments, conflicting results have been reported. Both Duffin et al. and Segall et al. reported that the relative abundance of the diacylglycerol fragment resulting from the loss of fatty acid from position *sn*-2 is not significantly different from the *sn*-1 and *sn*-3 positions. However, Hvattum [102] reported that the intensity of the diacylglycerol fragment from loss of fatty acid from the *sn*-2 position is less than from losses of fatty acids from *sn*-1 and *sn*-3 positions.

Infusion of TAG molecules in the presence of ammonium acetate under ESI conditions yielded ammoniated TAGs, $[M+NH_4]^+$ [75, 76]. Duffin et al. [75] and Cheng et al. [76] reported that the MS/MS spectra of ammoniated TAGs at low energy collision energies produced fragment ions, $[M+NH_4-RCOONH_4]^+$ and $[RCO]^+$; these fragment ions provided information on carbon chain length and double bond number of each acyl

moiety but did not distinguish between the positions of the fatty acyl substituents [75, 76].

Turk et al. [93] were the first to show that ESI/MS/MS spectra of lithiated TAGs, $[M+Li]^+$ produced very useful ESI/MS/MS spectra at low collision energies using a triple quadrupole instrument. These analyses yielded characteristic ion fragmentations that allowed the determination of both the fatty acyl groups' identities and their regio-chemistry [93]. Thus, lithium salts have a distinct advantage over protonated, sodium and ammonium salts in the analysis of TAGs by producing more structurally useful product ions that allow the identification and determination of the position of the fatty acid substituents relative to the sodiated and ammoniated TAGs. The structural analysis of lithiated TAGs will be described in section 1.4.2.4.3.

1.4.2.4.2 Quantification of Lithiated Triacylglycerols

Previous MS studies of TAGs have mentioned that number of carbons and degrees of unsaturation of TAG molecules have significant effects on the relative ionization responses [18, 35, 36, 74, 101, 106-109]. Byrdwell et al. [74] and Kemppinen et el. [35] have reported the quantification of TAGs in lipid samples based on the fatty acid compositions using an LC/APCI/MS technique and the application of molar correction factors for the fragmented ions of TAGs using a GC/EI/MS technique, respectively. Han and Gross [18] have developed a mathematical model to quantify TAGs from biological samples using ESI/MS, and to the best of our knowledge they are the only group that dealt with the quantification of TAGs by the application of correction

factors in a comprehensive way. Their model includes correction factors for ionization efficiency otherwise known as relative response factors (RRFs). The TAGs were quantified by direct comparison of ESI/MS peak areas to that of an internal standard, TAG 54:1 after correction for ^{13}C isotope effects that arise from the carbon number difference between a given TAG and the internal standard. Han and Gross also addressed the quantitative effect of M+2 isotopic overlaps on molecular ions which were 2 mass units higher than the M$^+$ ions. The M+2 contribution was determined using only the ^{13}C isotope effect. The natural abundances of ^{18}O, ^{17}O and ^{2}H isotopes were not taken into consideration for the determination of their M+2 contributions. There was no correction for LiCl adduct ions either. Moreover, the Han and Gross quantitative model was based on standard TAGs and was never applied to real samples with an independent assessment of degree of unsaturation.

1.4.2.4.3 Structural Characterization of Lithiated Triacylglycerols Using Collision Induced Dissociation

Fragmentation of lithiated TAG ions under CID conditions has been studied by Hsu and Turk [93]. The product ion spectra of [M+Li]$^+$ ions produced abundant fragment ions that reflect the identities and positions of the fatty acid moieties of TAG species. However in oil samples where a complex mixture of TAGs exists, the structural analysis is not straightforward. The complication in the analysis is due to the presence of large number of isobaric and isomeric structures arising from the different combinations of fatty acids at different positions [18, 75, 110].

In this thesis, the Hsu and Turk methodology is utilized to determine the identification of the fatty acid substituents of the TAG species and the possible identification of isobars. The following sub sections will summarize the structural characterization of lithiated TAGs as demonstrated by Hsu and Turk.

Fragment Ions to Determine Fatty Acid Identities

Upon CID, lithiated TAG molecular species fragment to provide structural information that allows the identification of the fatty acyl substituents based on the fragment ions corresponding to $[M+Li-R_nCOOH]^+$ and $[M+Li-R_nCOOLi]^+$. The losses of the individual fatty acyl substituents were detected as free fatty acids and as lithiated salts of the fatty acids, respectively as shown in Figure 1.8. The fragment ion pairs were detected at a mass difference of 6 units due to the presence of Li^+ and H^+. For example in Figure 1.8A, the TAG (C16:0/C18:0/C18:1) yielded three ion pairs at m/z (611, 605), m/z (583, 577) and m/z (585, 579) reflecting the neutral losses of C16:0, C18:0 and C18:1 as fatty acids and their lithium salts from the $[M+Li]^+$ ion, m/z 867. Hsu and Turk identified additional diagnostic fragment ions that reflect the fatty acid compositions of the TAG molecules, and these fragment ions were observed at m/z $[R_nCOOH+Li]^+$, R_nCO^+ and R_nCO^+-18. For example in Figure1.8A, the $[R_nCOOH+Li]^+$ ions for the three fatty acid substituents, C16:0, C18:0 and C18:1, were detected at m/z 263, 291 and 289, respectively. Similarly the acylium ions R_nCO^+ produced from the fatty acid substituents were detected at m/z 239, 267, and 265, respectively.
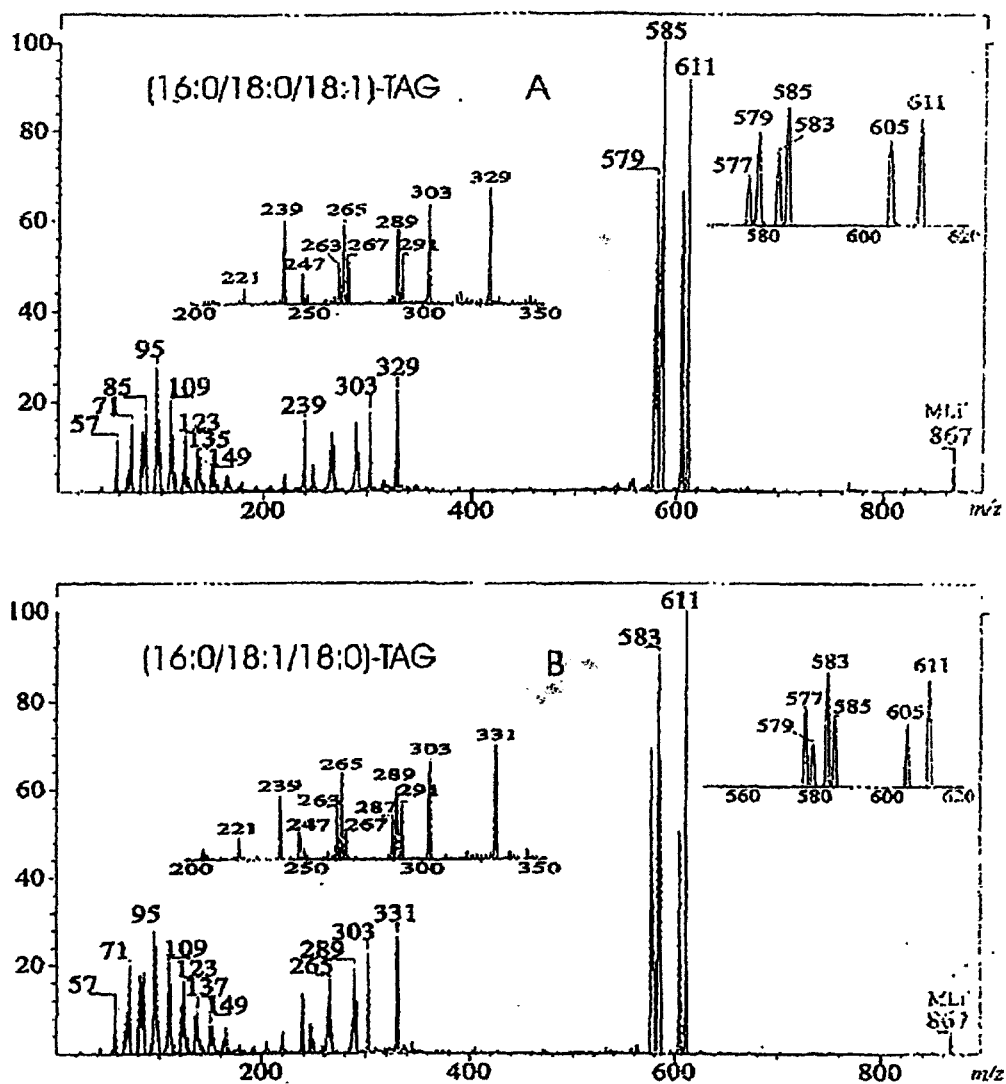
Figure 1.8 *Tandem mass spectra of lithiated adducts of two positional isomeric TAG species following CID of the [M+Li]⁺ species at m/z 867. Panels A and B are tandem mass spectra of the lithiated adducts of (C16:0/C18:0/C18:1) TAG and of (C16:0/C18:1/C18:0)-TAG, respectively [93].*

Fragment Ions to Determine Fatty Acid Positions

The regiospecific (positional) characterization of lithiated TAGs under CID condition has been reported by Hsu and Turk and others [18, 93, 111-114] and was based on two findings:

1) ***The preferential formation of fragment ions resulting from the loss of the acyl chain from the sn-1/sn-3 positions over the loss from the sn-2 position:*** The fragment ion intensities that originated from the losses of fatty acids from the *sn*-1 and *sn*-3 positions were more abundant than the fragment ions which originated from the loss of fatty acids from the *sn*-2 position. For example in Figure 1.8A, the abundance of the fragment ion pair m/z (611, 605) and m/z (585, 579) that originated from the losses of C16:0 from *sn-1* position and C18:1 from *sn-3* positions, respectively, were equal and more abundant than the fragment ion pair m/z (583, 577) that originated from the loss of C18:0 from *sn*-2 position. Therefore, this approach provides both the determination of the identities and relative positions of the fatty acid substituents on the TAG glycerol backbone.

2) ***Preferential combined elimination of sn-1/sn-3 fatty acyls as fatty acids and sn-2 fatty acyl as α,β-unsaturated fatty acids:*** Fragment ions produced from the combined losses of *sn*-1/*sn*-3 fatty acyl substituents as free fatty acids followed by the elimination of the *sn*-2 fatty acyl substituent as α,β-unsaturated fatty acids can be used to determine the position of the fatty acid substituents. Hsu and Turk reported

that the combined loss of *sn*-1 and *sn*-3 was not observed. The two fragment ions which resulted from the combined losses of the substituents from the (*sn*-1 and *sn*-2) and (*sn*-3 and *sn*-2) positions were identified in the spectrum with a mass difference which was equal to the mass difference between *sn*-1 and *sn*-3 substituents. For example, in Figure 1.8A, the two fragment ions were detected at m/z 329 and m/z 303 representing the combined losses of the substituents from the *sn*-1 and *sn*-2 positions and the *sn*-3 and *sn*-2 positions, respectively. The mass difference between m/z 329 and m/z 303 is 26 mass units reflecting the mass difference between C16:0, m/z 256, at the *sn*-1 position and C18:1, m/z 282 at *sn*-3 the position. Combined losses of the *sn*-1 and *sn*-3 substituents at m/z 331 were not observed in the mass spectrum.

1.4.3 Analysis of Intact Triacylglycerols by Nuclear Magnetic Resonance (NMR)

Both proton NMR (^{1}H-NMR) and carbon-13 NMR (^{13}C-NMR) have been used in lipid analyses, with ^{1}H-NMR being more frequently used compared to ^{13}C-NMR which requires larger amounts of sample. NMR methods are particularly useful in determining the location of double bonds in fatty acyl substituents of TAG standards [10, 43, 115]. The drawback of this technique is that it is only suited to the analysis of single TAGs, not complex mixtures of TAGs, and needs technical expertise for structural interpretation of the spectral data. NMR is never used in a routine quality control (QC) analysis laboratory supporting a production facility [116].

1.5 Research Goals

Based on the literature, we decided to use a triple quad mass spectrometer and lithium chloride as a cationizing agent for the analysis of the oil samples; we will also use correction factors: relative response factor (RRF), isotopic, internal standard normalization and lithium chloride adduct for the quantitative determination of the TAGs in the oil samples. The correction factors will be applied to a set of partially hydrogenated samples with measured iodine values (measure of degree of unsaturation) to assess the robustness of the quantitative method. The numbers of carbons in this set of samples are the same and it is only the degrees of unsaturation changing. Since the relative response factors (RRFs) of TAGs are strongly dependent on the degrees of unsaturation, this set of samples would provide us an ideal opportunity to test and validate our quantitative model.

The overall objective of this thesis is to develop a rapid and reliable positive ion ESI/MS and ESI/MS/MS techniques to characterize and quantify complex TAG mixtures in edible oil samples. To achieve this overall goal, individual goals were identified as follows:

a) To develop a reliable intrasource method for the infusion ESI/MS and ESI/MS/MS analysis of triacylglycerols (TAGs) in complex oil samples.

b) To determine whether the structures of TAGs can be determined using ESI/MS/MS analysis of lithiated TAGs.

c) To determine relative response factors for TAGs and compare these data to reported values.

d) To create a protocol to provide quantitative analyses for TAGs that accounts for the relative response factor, peak overlaps of isotopic peaks and any other confounding factors.

e) To develop a spreadsheet method which would apply successive correction factors to raw MS peak area data to provide quantitative values for TAGs and percentage composition data for complex mixtures of TAGs.

f) To apply this method to the analysis of a series of partially hydrogenated commercial oil samples and to compare the number of double bonds in each sample calculated using ESI/MS data with the number of double bonds as determined by iodine value measurements.

2. EXPERIMENTAL METHODS

2.1 Chemicals, Solvents and Gasses

All synthetic triacylglycerol standards were purchased from Nu Check Prep, Inc. (Elysian, MN) and have >99% purity. The standards include: 1,3-dihexadecanoyl-2-octadecenoyl glycerol (C16:0/C18:1/C16:0), 1-dodecanoyl-2-[cis-9-octadecenoyl]-3-hexadecanoyl-rac-glycerol (C12:0/(cis-9)C18:1/C16:0), tritridecanoin glycerol (C13:0/C13:0/C13:0), tripentadecanoin glycerol (C15:0/C15:0/C15:0), trihexadecanoin glycerol (C16:0/C16:0/C16:0), triheptadecanoin glycerol (C17:0/C17:0/C17:0), trioctadecanoin glycerol (C18:0/C18:0/C18:0), trinonadecanoin glycerol (C19:0/C19:0/C19:0), trieicosanoin glycerol (C20:0/C20:0/C20:0), triheneicosanoin glycerol (C21:0/C21:0/C21:0), trioctadecenoin glycerol (Δ9 cis) (C18:1/C18:1/C18:1), trioctadecadienoin glycerol (Δ9,12 cis)(C18:2/C18:2/C18:2), and trioctadecatrienoin glycerol (C18:3/C18:3/C18:3). The unsaturated lipid standards were provided in sealed glass ampoules under inert atmosphere. The saturated lipid standards were provided in powder form. Solvents used were HPLC grade (methanol and chloroform) and were purchased from Caledon Laboratories Ltd. (Georgetown, ON, Canada). LiCl (>99.9% purity) was obtained from Sigma-Aldrich, Mississauga, ON. Ultra high purity argon gas was obtained from Praxair Canada Inc, Hamilton, ON.

2.2 Provision of Samples

Four partially hydrogenated canola oil samples labeled as CA67, CA37, CA09, CA04, and the original canola oil used to prepare them were kindly provided by Bunge

Canada, Oakville, ON. The iodine values of these samples had been determined by Bunge Canada and were 63, 73, 86, 89 and 115, respectively. Five commercial edible oils were purchased from a local grocery store and included: grape seed oil (Loriva, California, USA), hempseed oil (Manitoba Harvest, Manitoba, Canada), olive oil (Bertolli pure classico, Italy), walnut oil (Vilux, B.C., Canada) and toasted sesame oil (Loriva, California, USA).

2.3 Instrumentation

A Waters Quattro Ultima triple quadrupole mass spectrometer (Waters Micromass, UK) equipped with a standard electrospray ion source was used for all analyses. The mass spectrometer used was not dedicated to the project; therefore; the possibility of having interfering ions from previous uses was high. Thus, before running samples, the ion source was dismantled and washed in formic acid, deionized water and acetonitrile for 15 minutes each using a sonic bath. The parts were dried with nitrogen and reassembled. Blank solvent ($CHCl_3$:CH_3OH (v/v 1:1)) was infused and usually no ions were detected over the mass range of interest. All samples were infused at a flow rate of 5µL/min using a Harvard syringe pump. Waters MassLynx mass spectrometry software was used to acquire and process all mass spectral data. All experiments were performed in the positive ion mode in the presence of LiCl.

2.4 Electrospray Mass Spectrometry Protocols

Full scan mass spectra were obtained for all standards and complex oil samples by infusion of $CHCl_3$:CH_3OH solutions (1:1) at a flow rate of 5µL/min in the presence of 0.5mM LiCl. In typical experiments, mass spectral data of the oil samples were acquired over m/z range from 800-1050 at a scan rate of 125 m/z per second. For each experiment 100 mass spectra were acquired and averaged to give a single mass spectrum. Tandem mass spectra of selected ions were obtained by collision induced dissociation (CID) in the positive ion mode. A lithiated precursor ion ($[M+Li]^+$) was selected in the first mass analyzer (Q1), collided with argon gas in Q2 and the product ions detected in Q3. The operational parameters for these experiments are listed in Table 2-1.

Table 2.1 *Instrument operational parameters for ESI/MS and ESI/MS/MS analysis.*

Capillary voltage	3.5kV
Cone voltage	140V
Cone gas flow	40L/hr
Capillary temperature	250°C
CID voltage	35V
Desolvation temperature	350°C
Desolvation flow rate	540L/hr
Low mass resolution (Q1)	14
High mass resolution (Q1)	14
Ion energy 1	0.1
Low mass resolution (Q2)	15
High mass resolution (Q2)	15
Ion energy 2	1.0

2.5 Materials Handling Procedures

The following precautions were taken in order to ensure the quality and integrity of the lipid standards and analyte samples:

a) All standards were stored neat at -20°C in a freezer and were allowed to equilibrate to room temperature before weighing.

b) The solvents were purged with argon in order to remove oxygen.

c) Stock solutions of standards were stored in the fridge (+4°C).

d) Solutions of samples and standards were prepared in glass vials prior to MS experiments and the caps were lined with Teflon.

e) Graduated glass pipettes were used to transfer solvents.

f) Stock solutions of unsaturated TAG standards were checked before use (as these solutions may degrade with time due to oxidation). A solution of four C54 standards (C54:0, C54:3, C54:6 and C54:9) was analyzed each time analyses were performed and the response factors compared to those obtained previously from freshly prepared standards. Typically, after about six months a small decrease in the response of the most highly unsaturated standard (C54:9) was observed. When the response of C54:9 had decreased by 5%, all standards were discarded and replaced with freshly prepared standards.

2.6 Preparations of Standards and Samples

2.6.1 Preparation of Solutions of Triacylglycerol Standards

Stock solutions of authentic triacyglycerol C54 standards (C54:9, C54:6, C54:3 and C54:0) and saturated standards (C48:0, C51:0 C54:0, C57:0, C60:0 and C63:0) were prepared in solvent; stock solutions of the saturated TAGs were prepared using chloroform while unsaturated TAGs were dissolved in $CHCl_3:CH_3OH$ (1:1). The standards were weighed using a Mettler M5SA balance with microgram accuracy and made up in 10 mL volumetric flasks. Stock solutions of all TAG standards were prepared individually in the 0.5 to 2 mM range and were mixed sand diluted to prepare mixed sets of saturated and unsaturated standards at concentrations of about 20 μM each in $CHCl_3:CH_3OH$ (1:1). For calibration, solutions of the mixed unsaturated standards were prepared in the mixed solvent over a range of concentrations from 0.1 to 10 μM in the presence of 0.5mM LiCl. For the saturated standards, a solution of mixed standards was prepared in the mixed solvent with each TAG at 2.5 μM in the presence of 0.5mM LiCl.

2.6.2 Preparation of Oil Samples

Stock solutions of Bunge oil samples and commercial vegetable oils were prepared by diluting a 25mg sample of each oil with chloroform:methanol (1:1, v/v) in a 10 mL volumetric flask. Prior to analysis, these solutions were diluted about 200-fold to 12.5 μg/mL in the presence of 0.5 mM LiCl. A TAG internal standard (IS) mixture containing C51:0, C57:0 and C63:0 TAGs was added to each oil sample such that the

final concentration of each TAG IS was about 2.5μM. The oil samples were then infused

into the mass spectrometer at 5μL/min.

2.7 Determination of Linear Dynamic Range of the Triacylglycerol Assay

The solutions of four C54 standards (C54:9, C54:6, C54:3 and C54:0) that had

been prepared in section 2.6.1 at concentrations ranging from 0.1 to 10 μM were used to

determine the linear dynamic range of the TAG assay. Five infusions were performed at

each concentration. The linear dynamic range extends from 0.3 to 2.5 μM. The slopes and

coefficient of determination (R^2) values were calculated using Excel (see Figure 3.4 and

section 3.2.1).

2.8 Determination of Relative Response Factors

The relative response factors (RRFs) of the TAG standards were determined from

the calibration plots for each standard (section 2.7). The plots of sample concentration

versus peak area (Figure 3.4) were linear and the slope of the line represented the

response factor (RF) of that TAG standard as shown by the relationship in equation 2.1.

The RRF of each standard was determined using equation 2.2. The RRF of C57:0 was set

at 1.00.

RF (response factor) = peak area/ mass of analyte TAG   (2.1)

RRF= (RF of CX:#)/(RF of C57:0)   (2.2)

3. ANALYTICAL METHOD DEVELOPMENT

The main goal of this thesis is to develop a rapid, sensitive and robust analytical method for the qualitative identification and quantitative analysis of TAGs in edible oils. A typical positive ion ESI/MS spectrum of an oil sample after the addition of LiCl is shown in Figure 3.1. The spectrum displays clusters of peaks which correspond to the $[M+Li]^+$ adduct ions of the triacylglycerol species. Adduct ion formation involves the complexation of electron-rich carbonyl groups of TAGs with lithium cation.
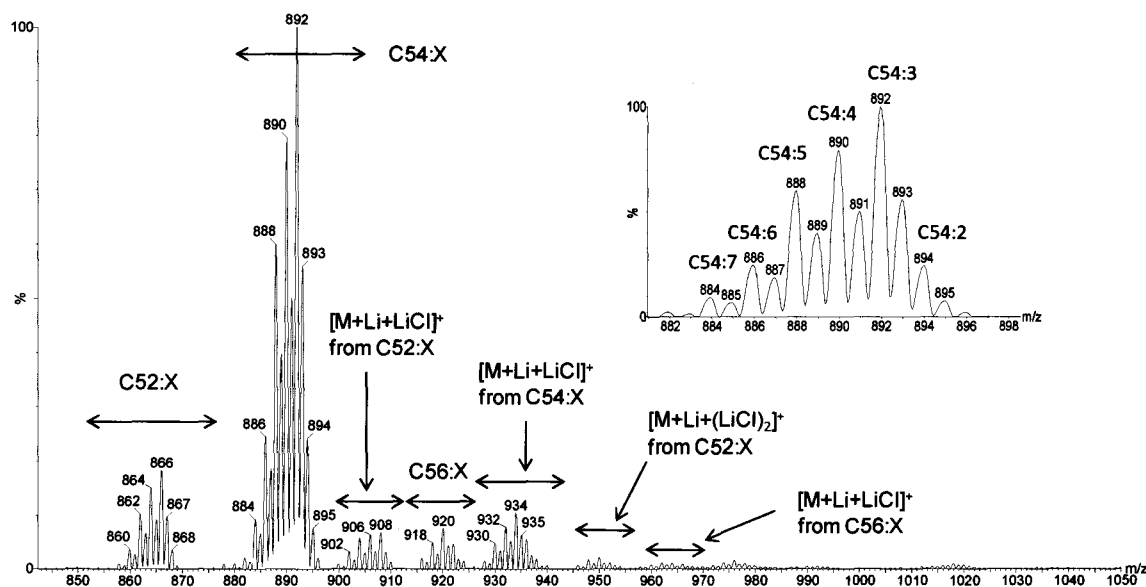
Figure 3.1 *Infusion ESI/MS positive ion mass spectrum of a canola oil feedstock solution showing lithiated TAG adduct ions (C52:X, C54:X and C56:X) and the inset shows the C54:X TAG group. The LiCl adduct ions are also labeled. (canola oil concentration: 12.5 µg/mL with 0.5mM LiCl).*

The mass spectrum revealed three separate clusters of peaks; each major cluster corresponds to TAG species having the same number of carbons but different numbers of double bonds. The three TAG groups are C52:X, C54:X and C56:X, as labeled in Figure 3.1. Within a cluster, TAGs are separated by 2 mass units due to different numbers of double bonds in the fatty acyl moieties (see Figure 3.1 insert). In addition to the abundant $[M+Li]^+$ ions, there were also weak ion clusters corresponding to $[M+Li+LiCl]^+$ and $[M+Li+(LiCl)_2]^+$ species. Furthermore, these LiCl adducts showed peaks due to the presence of ^{35}Cl and ^{37}Cl, i.e., $[M+Li+(Li^{35}Cl)_n]^+$ and $[M+Li+(Li^{37}Cl)_n]^+$. These latter ions are detected at masses 42 and 44 mass units greater than the corresponding lithiated molecular ion, $[M+Li]^+$.

Several challenges are faced in the analysis of TAGs using electrospray spectrometry. Firstly, the mass spectrometric analysis of triacylglycerols can suffer from lack of specificity if isobaric TAGs are present [18]. In complex mixtures, multiple isobaric species are possible depending on the fatty acyl groups present, the positional distribution of fatty acyl groups and the locations of double bonds on the fatty acyl groups [19]. Secondly, the instrumental responses of TAGs are greatly affected by two factors: (1) the total number of carbons in the fatty acyl chains and; (2) the number of degrees of unsaturation in the TAG. Thirdly, mass spectrometric analyses of TAGs are often complicated by isotopic overlaps [107] and the overlap of an $[M+Li]^+$ ion of a given TAG with $[M+Li+LiCl]^+$ ion of another TAG with 3 fewer CH_2 groups.

To address these challenges, the following issues will be discussed in this chapter:

a) Determination of the ESI/MS spectra for molecular mass identification of

lithiated TAG standards.

b) Determination of ESI/MS/MS spectra and characteristic fragment ions of lithiated TAG standards [93].

c) Determination of calibration curves, relative response factors (RRFs) and detection limits of TAG standards with different carbon chain lengths and degrees of unsaturation.

d) Determination of correction factors for the peak area contributions of M+2 isotope peaks to the lithiated molecular ions of TAGs with one less degree of unsaturation.

e) Determination of the optimum LiCl concentration for TAG analysis while minimizing the formation of LiCl adduct ions.

f) Determination of the correction factor for the LiCl adduct formation based on the ion intensities of $[M+Li+LiCl]^+$ ions versus $[M+Li]^+$ ions.

3.1 Qualitative Determination of Triacylglycerol Standards

3.1.1 ESI/MS of Triacylglycerol Standards

Triacylglycerols in chloroform:methanol (1:1) solution were infused directly into the electrospray ionization source using a Harvard syringe pump at a flow rate of 5 µL/min in the presence of 0.5mM LiCl and analyzed in the positive ion mode. In typical experiments, mass spectral data were acquired from m/z 800-1050 at a scan rate of 125 m/z per second (see Figure 3.1). This mass range was selected because it was sufficient to include the five major TAG groups identified in all oil samples. For each spectrum, 100

scans were acquired and averaged to give a single spectrum. This protocol was used for all samples to reduce the presence of artifacts in the spectra and provide spectra with improved signal-to-noise ratios (S/N).

The ESI/MS spectrum of a TAG yielded a cluster of peaks that reflect the isotopic distribution of the TAG molecule with the base peak representing the monoisotopic peak ion, $[M+Li]^+$. The mass spectrum of a standard TAG, trioctadecanoin glycerol (C18:0/C18:0/C18:0), is shown in Figure 3.2 at m/z 898, together with its isotopic clusters corresponding M+1, M+2 and M+3 peaks at m/z 899, 900 and 901, respectively is presented. Note that the $[M+2+Li]^+$ ion intensity is significant at this m/z value. The issue of making corrections due to the peak area contribution of isotopic peaks will be discussed in detail in section 3.2.4.
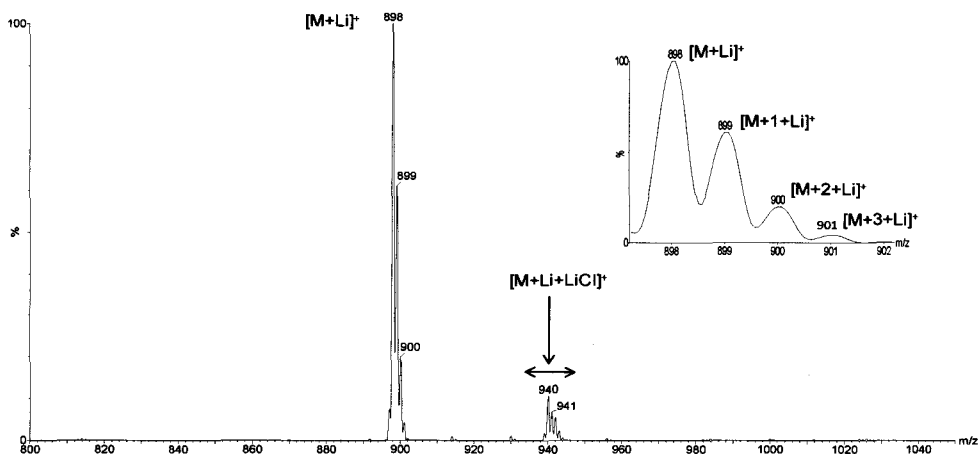
Figure 3.2 *ESI/MS positive ion mass spectrum of* trioctadecanoin glycerol (C18:0/C18:0/C18:0) at m/z 898. *The inset is an enlarged spectrum showing the isotopic distribution of the TAG.*

3.1.2 ESI/MS/MS of Triacylglycerol Standards

A tandem mass spectrum of a lithiated TAG standard with three different fatty acyl groups, 1-dodecanoyl-2-[cis-9-octadecenoyl]-3-hexadecanoyl-rac-glycerol (12:0/(cis)-9,18:1/16:0), obtained by collision induced dissociation (CID) in the positive ion mode is shown in Figure 3.3. The experiment was performed with argon as the collision gas and the instrument parameters as listed in Table 2.1. For this particular analysis, a collision energy of 50V reduced the intensity of the $[M+Li]^+$ ion at m/z 784 to < 10% of its original intensity. The dissociation of the $[M+Li]^+$ species showed characteristic losses of the three fatty acids both as free fatty acids $[M+Li-R_nCOOH]^+$ and as lithium salts of these fatty acids $[M+Li-R_nCOOLi]^+$ where "n" stands for 1, 2 and 3 reflecting the three fatty acyl substituents of the TAG.
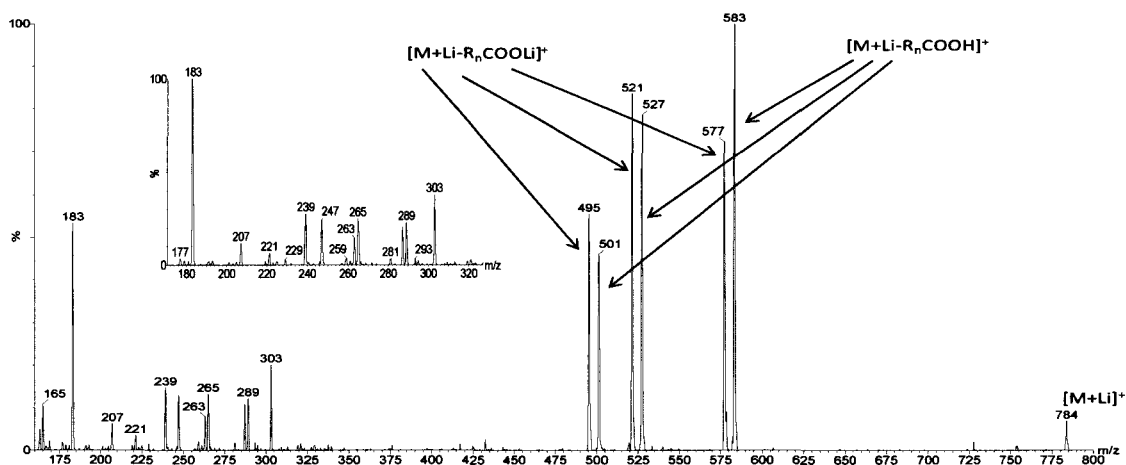
Figure 3.3 *ESI/MS/MS of 1-dodecanoyl-2-[cis-9-octadecenoyl]-3-hexadecanoyl-rac-glycerol (12:0/(cis)-9,18:1/16:0).*

The spectrum in Figure 3.3 displayed three pairs of fragment ions corresponding to losses of the three fatty acyl chains. The paired product ions at m/z 583 and 577, m/z 501 and 495 and m/z 527 and 521 reflect the neutral losses of the fatty acids, dodecanoic acid (C12:0), octadecenoic acid (C18:1) and hexadecanoic acid (C16:0) as losses of free fatty acids and as losses of lithium salts of the fatty acids, respectively.

The positions of the fatty acid substituents on the glycerol backbone of the TAG standard were confirmed from the relative fragment ion intensities. The intensities of the fragment ion pair due to losses of the octadecenoic acid, C18:1, from position *sn*-2 (m/z 495 and 501) were the least intense of all. The fragment ion intensities due to losses of either the dodecanoic acid, C12:0, (577, 583) or the hexadecanoic acid, C16:0, (521, 527) from positions *sn*-1 and *sn*-3, respectively were similar (Figure 3.3).

The positions of the fatty acid substituents were also consistent with the fragments derived from combined losses of adjacent substituents, i.e., *sn*-1/2 and *sn*-3/2 as a free fatty acid plus an α,β-unsaturated fatty acid. The combined losses of C12:0 and C18:1 (*sn*-1/2) produced a fragment ion at m/z 303, while the combined losses of C16:0 and C18:1 (*sn*-3/2) produced a fragment ion at m/z 247. Together these data confirmed that the C18:1 substituent was at *sn*-2. The mass difference between the two fragments (56 Da) is equal to the molecular mass difference between C12:0 and C16:0. Notice that the combined losses of C12:0 and C16:0 (*sn*-1/3) had not occurred as the expected fragment ion at m/z 327 was not detected in the mass spectrum.

Additional diagnostic fragments were also observed in the CID spectrum. Lithiated fatty acid fragment ions, $[R_nCO_2H+Li]^+$, were detected at m/z 207, 289 and

263, corresponding to C12:0, C18:1 and C16:0 fatty acids, respectively. Similarly, acylium fragment ions, R_nCO^+ arising from the fatty acid substituents C12:0, C18:1 and C16:0 were revealed at m/z 183, 265 and 239, respectively.

In summary, ESI/MS spectra allow the identification of TAG molecules. However, this MS analysis alone is not capable of differentiating overlapping isobaric TAGs; hence, structural characterization of the TAGs using tandem ms method is necessary; fragmentation of the TAGs and using the product ion scan mode provide MS/MS spectra which elucidates the fatty acid compositions of the TAGs and the identification of isobaric TAGs if they exist.

3.2 Quantitative Determination of Triacylglycerol Standards

3.2.1 Linear Dynamic Range

The calibration curves for four C54 TAG standards with different degrees of unsaturation, (C54:9, C54:6, C54:3 and C54:0) are shown in Figure 3.4. Quintuplicate infusions were performed for each TAG at concentrations over the range from 0.1-10 µM. The linear dynamic range extended from 0.3 - 2.5 µM. Relative standard deviations of the five runs ranged from 3.0% to 29.7% and averaged 16.3%.
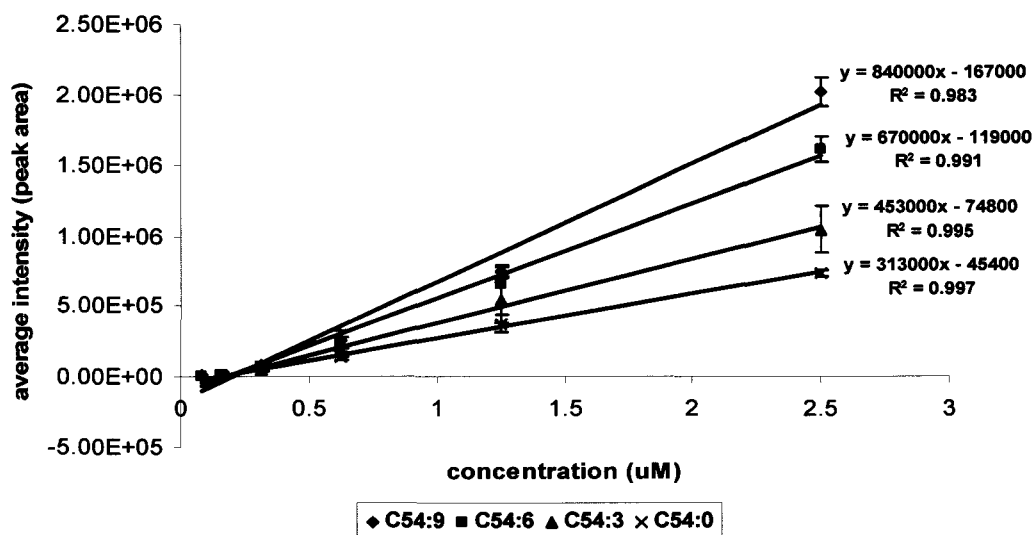
Figure 3.4 *Plots of average peak area versus concentration (μM) of four 54-carbon standard TAGs (C54:9, C54:6, C54:3 and C54:0) from 0.1 to 2.5 μM.*

The least squares lines of best fit over the 0.3 μM to 2.5 μM range are shown in Figure 3.4 along with the coefficient of determination (R^2) values of 0.983, 0.991, 0.995 and 0.997 for C54:9, C54:6, C54:3 and C54:0, respectively.

3.2.2 Detection Limits

In this study, detection limits were defined as the amount of substance that would give a signal-to-noise (S/N) ratio of 3:1. The detection limits for the C54:X standards were found to range from 0.06 μM to 0.10 μM.

3.2.3 Prediction of Relative Response Factors

Several lipid researchers have mentioned that the mass spectral response for TAGs increases as the number of degrees of unsaturation increases; response factors (RF) are also known to decrease with increasing carbon chain length [18, 35, 74, 75, 94, 109]. Byrdwell et al. [74] and Kemppinen et al. [35] have reported the quantification of TAG compositions in lipid samples. Byrdwell et al. used LC/APCI/MS to determine the correction factors for TAGs based on the fatty acid compositions of TAGs, while Kemppinen et al. used GC/EI/MS to determine the correction factors of TAGs in butterfat samples based on correction factors for the fragmented ions, $[M-RCOO]^+$. Han and Gross [18] have developed a mathematical model to predict the relative response factors (RRFs) of TAGs and these values were used to quantify TAGs in biological samples using ESI/MS. To the best of our knowledge this report is the only one that dealt with the quantification of TAGs with the application of calculated RRFs that are based on the mass spectral peak areas of known TAGs. Their methodology is similar to ours; therefore, comparison of their data with ours will provide a reliable comparison with our methodology. A table of our RRFs along with the corresponding RRFs from Han and Gross is shown at the end of this section in Table 3.2.

In this thesis, a selection of unsaturated and saturated TAG standards was analyzed to determine their relative response factors. Mixtures of the four C54 TAG standards with different degrees of unsaturation (C54:0, C54:3, C54:6 and C54:9) together with a selection of saturated TAGs with different total carbons in their acyl chains (C48:0, C51:0, C57:0, C60:0 and C63:0) were prepared and analyzed as per

section 2.6. Plots of raw peak area versus concentration of the C54:X series were shown in Figure 3.4. In a similar manner the responses of the saturated TAGs were also determined (Figure 3.5).

The slope of each standard plot represented the sensitivity (response) of the TAG standard. From the plots, the response of the C54:9 TAG was the greatest, while the response of the C54:0 was the least. The relative response factor (RRF) of each standard was determined by normalizing the response factor (slope of the line) of the individual standard TAG to that of C54:0 TAG.

In order to calculate the RRF values of all TAGs ranging from C48 to C63 with degrees of unsaturation from 0 to 9, the increase in RRF due to the addition of one double bond was determined using equation 3.1. Accordingly, the C54:9 RRF (2.68) minus the C54:0 RRF (1.00) divided by the difference in double bonds between C54:9 and C54:0 (9 double bonds) afforded the incremental RRF value due to the presence of one double bond (DB) in a TAG's fatty acyl substituents. This value was determined to be 0.187 and was used to calculate RRFs of the unsaturated TAGs. These RRF increases were assumed to be additive and led to the formulation of Table 3.1.

$$\text{Increase in RRF due to 1DB} = \frac{((\text{slope of C54:9 - slope of C54:0})/\text{ slope of C54:0})}{\text{difference in double bonds (9 - 0)}} \quad (3.1)$$

Where "DB" stands for double bonds.

Saturated TAG standards (C48:0, C51:0 C54:0, C57:0, C60:0 and C63:0) were also used to determine the RRFs of TAGs based on carbon chain length. Five analyses were conducted of each TAG and the responses were averaged. The RRF of a given TAG standard was expressed as the ratio of its average peak area compared to the average peak area of the C57:0 standard. The C57:0 standard was assigned an RRF = 1.00. The RRF values of the C48:0, C51:0 C54:0, C57:0, C60:0 and C63:0 standards were 1.54, 1.36, 1.18, 1.00, 0.77 and 0.54, respectively. A plot of these RRF values versus the carbon number revealed a linear least squares line of best fit drawn through the six data points with an $R^2 = 0.996$ (Figure 3.5). In order to extrapolate the RRF values of the TAGs in between, the decrease in RRF due to addition of one carbon chain was determined using equation 3.2. Accordingly C48:0 RRF (1.54) minus the C63:0 RRF (0.54) divided by the difference in carbon number between C63:0 and C48:0 (15 carbons) afforded the RRF value due to the addition of one carbon chain in a saturated TAG's fatty acyl substituents. This value was determined to be 0.067. In other words the RRF decreased by 6.7% for each additional acyl carbon atom while the RRF increased by 18.7% for addition of a double bond.

Decrease in RRF due to 1 carbon = $\dfrac{\text{(RRF C48:0 - RRF C63:0)}}{\text{difference of carbons (63 - 48)}}$ (3.2)

For the TAG range that we are interested in, C48:0 to C57:0 the RRF decreased by 6.0% for each additional acyl carbon atom.

The plot shows:

$$y = -0.0664x + 4.75$$
$$R^2 = 0.996$$

with y-axis labeled RRF (from 0.20 to 1.80) and x-axis labeled carbon number (from 45 to 65).
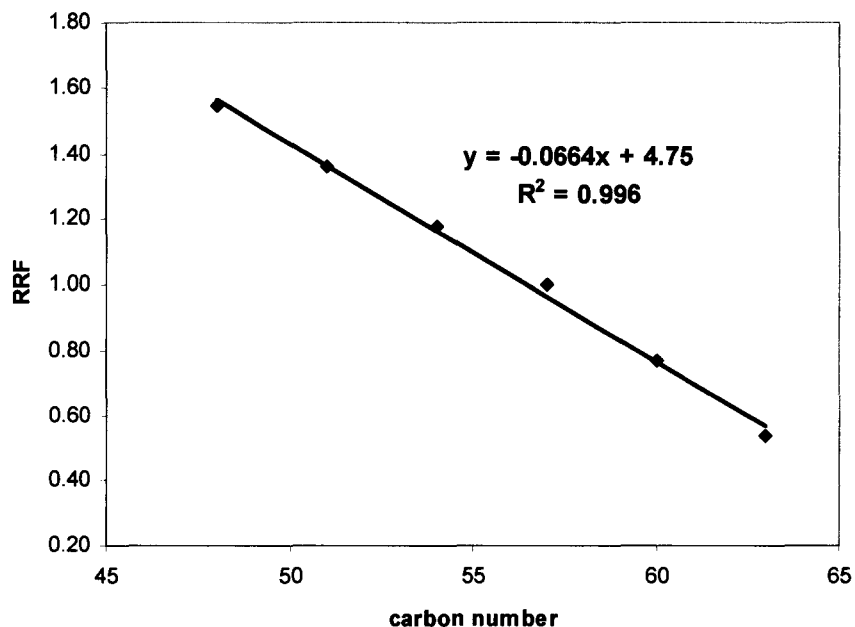
Figure 3.5 *Plot of RRF versus carbon number of saturated* standard TAGs *(C48:0, C51:0 C54:0, C57:0, C60:0 and C63:0).*

Combining the values from the saturated and unsaturated TAG standards, it was possible to calculate RRF values of TAG species from C48 to C63 with 0 to 9 double bonds. The RRF values of the TAGs were expressed relative to the RRF of the C57:0 TAG which was arbitrarily set as 1.00. These RRF values are reported in Table 3.1 and plotted in Figure 3.6 showing the measured and predicted RRF values.

Table 3.1 *Experimentally determined RRF values of TAG standards (in bold face type) and calculated RRF values that are determined by linear extrapolation.*

DOU	C48:X	C49:X	C50:X	C51:X	C52:X	C53:X	C54:X	C55:X	C56:X	C57:X	C58:X	C59:X	C60:X	C61:X	C62:X	C63:X
0	**1.54**	1.48	1.42	**1.36**	1.30	1.24	**1.18**	1.12	1.06	**1.00**	0.92	0.85	**0.77**	0.69	0.62	**0.54**
1	1.73	1.67	1.61	1.55	1.49	1.43	1.37	1.31	1.25	1.19	1.11	1.03	0.96	0.88	0.80	0.73
2	1.91	1.85	1.79	1.73	1.67	1.61	1.55	1.49	1.43	1.37	1.30	1.22	1.14	1.07	0.99	0.91
3	2.10	2.04	1.98	1.92	1.86	1.80	**1.74**	1.68	1.62	1.56	1.48	1.41	1.33	1.25	1.18	1.10
4	2.29	2.23	2.17	2.11	2.05	1.99	1.93	1.87	1.81	1.75	1.67	1.59	1.52	1.44	1.36	1.29
5	2.48	2.42	2.36	2.30	2.24	2.18	2.12	2.06	2.00	1.94	1.86	1.78	1.70	1.63	1.55	1.47
6	2.66	2.60	2.54	2.48	2.42	2.36	**2.30**	2.24	2.18	2.12	2.05	1.97	1.89	1.82	1.74	1.66
7	2.85	2.79	2.73	2.67	2.61	2.55	2.49	2.43	2.37	2.31	2.23	2.16	2.08	2.00	1.93	1.85
8	3.04	2.98	2.92	2.86	2.80	2.74	2.68	2.62	2.56	2.50	2.42	2.34	2.27	2.19	2.11	2.04
9	3.22	3.16	3.10	3.04	2.98	2.92	**2.86**	2.80	2.74	2.68	2.61	2.53	2.45	2.38	2.30	2.22

*DOU stands for degrees of unsaturation.
Bold face type values are the experimentally determined RRFs.
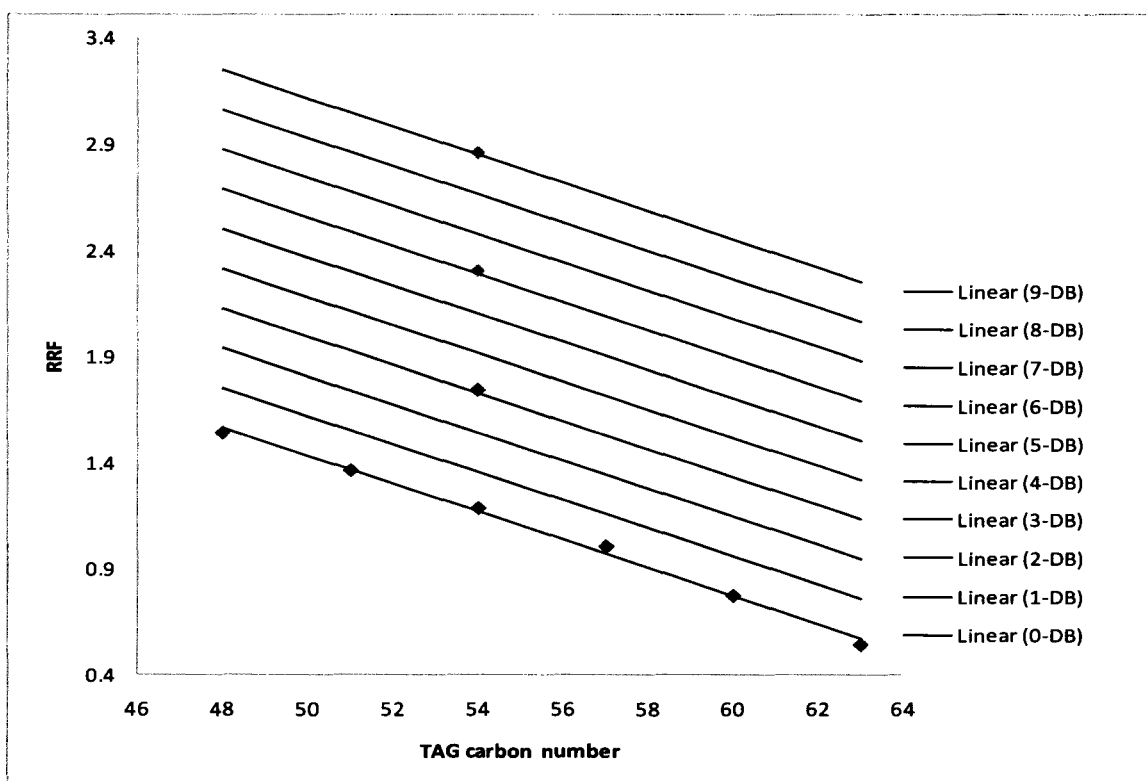
Figure 3.6 *Plots of thesis predicted (lines) and measured (data points) RRF values versus TAG carbon numbers for standards with carbon number ranging from 48 to 63 and degree of unsaturation ranging from 0 to 9.*

Han and Gross [18] have reported a similar set of predicted TAG RRFs based on the RRFs of a larger selection of TAG standards. The RRFs of eighteen TAGs were converted to the scale used in this thesis (i.e., C57:0 = 1.00). Their measured data and our measured data (bold face type in Table 3.2) are essentially identical except for TAG C60:0 in which our number is 21.5% lower than the Han and Gross measured value. Figure 3.7 displays the correlation of Han and Gross measured RRF values to our

predicted values for the selected set of TAGs listed in Table 3.2.

Table 3.2 *Comparison of Han and Gross and thesis predicted TAG RRF values to Han and Gross measured TAG RRF values [18].*

TAG	Thesis measured RRF values	Han&Gross measured RRF values	% difference between Han and Gross measured and predicted RRF values	% difference between Han and Gross measured and thesis predicted RRF values
C48:0	**1.54**	**1.54**	**0.00**	**0.00**
C48:3		2.23	2.00	-5.91
C50:0		1.38	1.61	2.62
C50:1		1.58	2.82	1.60
C51:3		2.23	-9.00	-13.97
C52:1		1.45	3.08	2.71
C52:4		2.01	4.44	2.06
C54:0	**1.18**	**1.20**	**-1.85**	**-2.09**
C54:2		1.47	6.06	5.22
C54:3	**1.74**	**1.81**	**-3.70**	**-3.75**
C54:5		1.98	5.62	6.73
C54:6	**2.30**	**2.30**	**10.75**	**10.81**
C56:4		1.61	9.72	12.63
C56:6		1.90	9.41	14.91
C56:8		2.14	12.50	19.48
C60:0	**0.77**	**0.98**	**2.27**	**-21.59**
C60:3		1.47	-7.58	-9.71
C60:6		1.94	-11.49	-2.67
%Mean difference and standard deviation			2.04% ± 6.80%	1.06% ± 10.20%

Both predicted RRF values show over estimation compared to Han and Gross measured RRF values, with our predicted values showing better predictability by almost a factor of two. The standard deviation which shows the degree of variation of the data from the mean is calculated as 6.80% for Han and Gross and 10.20% for our thesis;

hence, the data spread is a bit larger for our data. Both prediction values are similar to the measured values and overall the two methods are comparable.
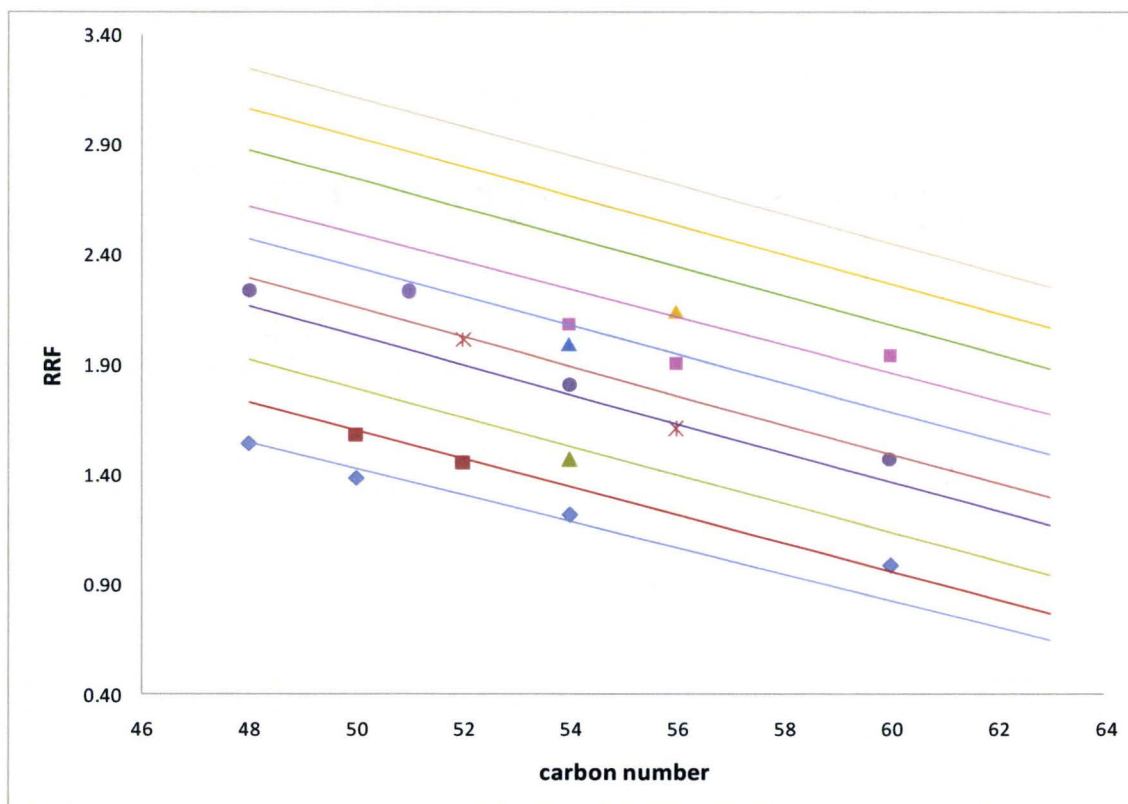
Figure 3.7 *Plots of RRF values versus TAG carbon numbers for standards with carbon number ranging from 48 to 63 and degree of unsaturation ranging from 0 to 9. The lines show the correlation of the thesis predicted RRF values for TAGs with degree of unsaturation ranging from 0 to 9, and the scattered data show the correlation of the measured RRF values from Han and Gross experiment. The color of the lines and scattered data is similar for TAGs with the same degree of unsaturation.*

3.2.4 Determination of Isotopic Peak Area Correction Factors

The lithiated molecular ions of TAGs in a typical ion cluster are separated by 2, 4, 6, etc. mass units corresponding to differences of one degree of unsaturation (see Figure 3.1). The ESI/MS mass spectra of TAGs showed molecular ions with significant intensities in the M+1, M+2 and M+3 isotopic peaks [107]. The natural abundances of the H, C and O heavy isotopes are 0.015% for ^{2}H, 1.10% for ^{13}C, 0.04% for ^{17}O and 0.2% for ^{18}O. The isotope peak distribution and the relative abundances of the C54:0 molecular ions are shown in Figure 3.8.
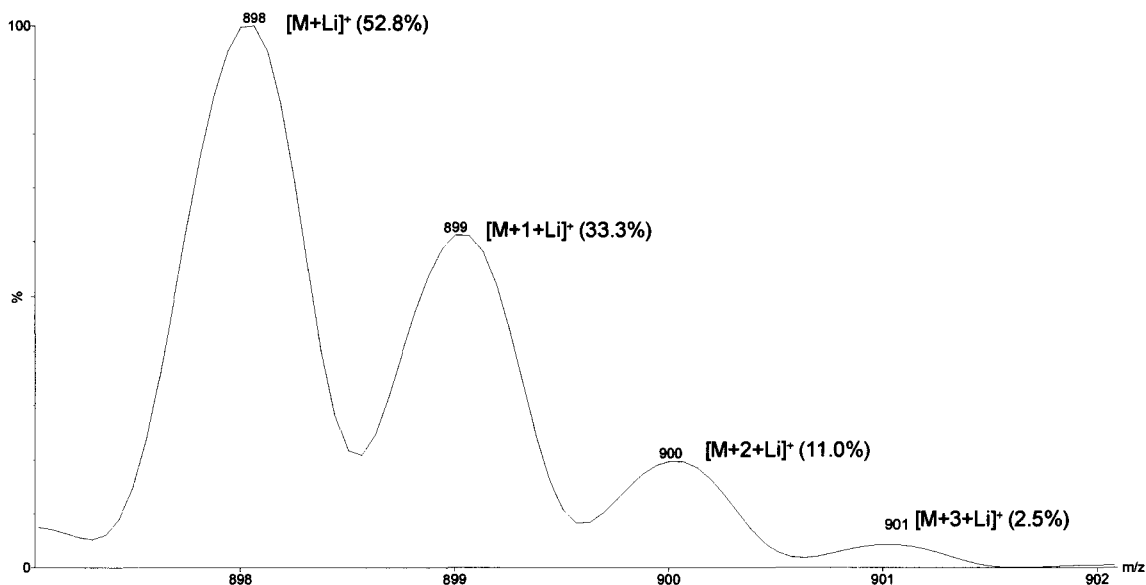
Figure 3.8 *Isotopic pattern of the C54:0 TAG standard (2.5µM with 0.5 mM LiCl).*

The isotopic contributions of odd mass isotope peaks (M+1 and M+3) do not

afford any interference. The contributions of M+4 peaks are also extremely low since their relative abundances are <0.5% of the total. However, the M+2 peak of a given TAG will have the same nominal m/z value as M peak of the TAG 2 mass units greater, i.e., a TAG with one less degree of unsaturation. Figure 3.8 shows that 52.8% of the total intensity of the molecular ion cluster of the C54:0 TAG is observed at m/z 898 $[M+Li]^+$ while 11.0% is detected at m/z 900 $[M+2+Li]^+$. In other words, the $[M+2+Li]^+$ ion is corresponding to about 20% of the peak area of the $[M+Li]^+$ peak.

The M+2 contributions to neighboring TAG peak areas can be significant in some instances. The C54 cluster in an olive oil sample illustrates this point (Figure 3.9).
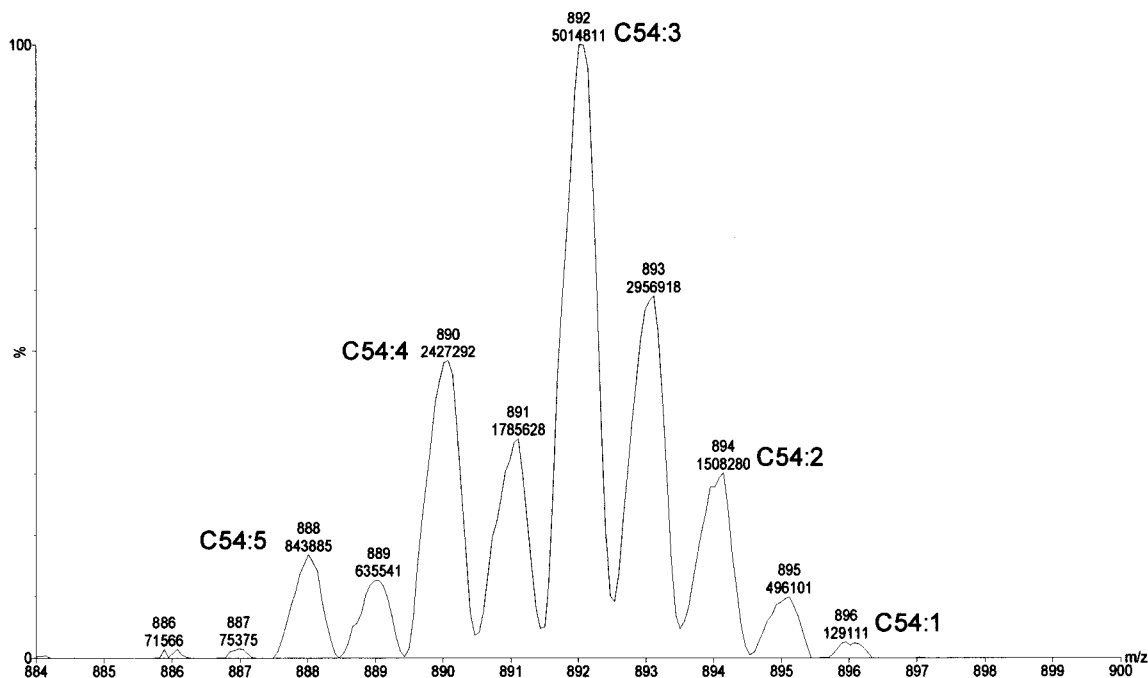
Figure 3.9 *TAG C54:X cluster in olive oil sample (sample concentration of 12.5μg/mL with 0.5 mM LiCl).*

Working from the left hand side of the spectrum, the TAG with the highest degree of unsaturation (C54:5, m/z 888) has no isotopic peak interferences since there is almost no C54:6 TAG in the sample. The M+2 peak of the C54:5 TAG (m/z 890) has the same nominal mass as the molecular ion of C54:4 (m/z 890). The (M+2) peak from C54:5 accounts for about 10% of the total ion intensity of the m/z 890 peak (see Figure 3.10). This contribution needs to be subtracted from the measured m/z 890 peak area to give the corrected peak area from the [M+Li]$^+$ ion of the C54:4 TAG. Similarly the M+2 signal from C54:4 (m/z 892) overlaps on to the C54:3 molecular ion (m/z 892). The C54:4 M+2 isotopic contribution needs to be subtracted from the measured peak area of C54:3 lithiated molecular ion. This process continues until the last TAG ion in the cluster has been dealt with. The contribution of the C54:3 M+2 isotopic peak to C54:2 is about 60% of the C54:2 total peak area; interestingly there is no C54:1 in the sample; the peak at m/z 896 is due only to the contribution from the M+2 isotope ion of the C54:2 TAG (Figure 3.10). This indicates that the peak areas of minor TAGs with lower degrees of unsaturation suffer the greatest correction.
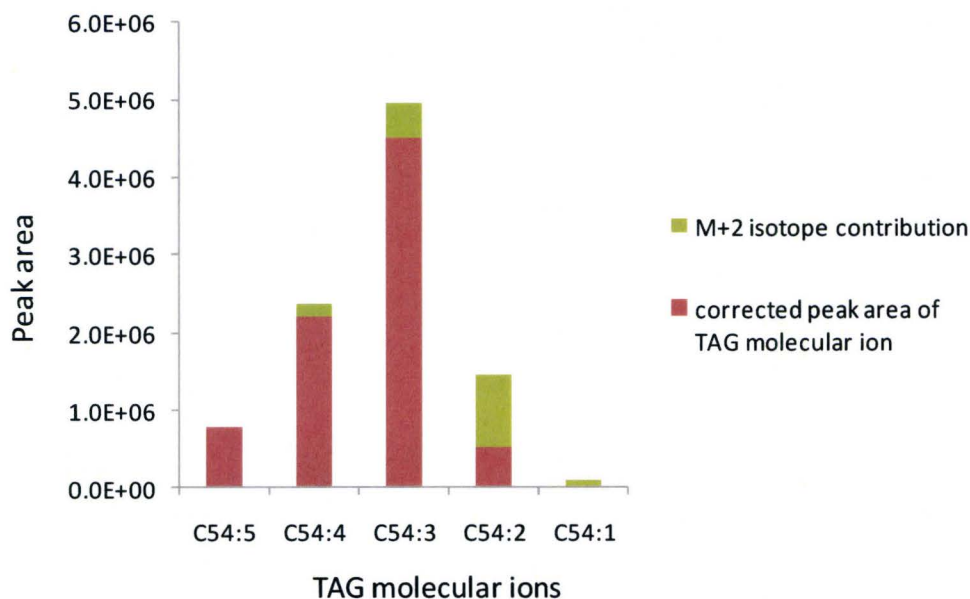
Figure 3.10 *M+2 isotopic peak area contributions to neighboring molecular ions with 2 mass units greater in TAG C54:X cluster in olive oil sample.*

Isotopic correction factors for the M+2 contributions need to be applied to all TAG cluster ions. The isotopic correction factor (ICF) is the ratio of the (M+2) to (M) portions of the total peak area of a lithiated TAG ion and is calculated using formula 3.3. The M+2 contribution is then calculated by multiplying the peak area of the monoisotopic peak (M) by the isotopic correction factor. This M+2 peak area value is then subtracted from the measured peak area of the TAG at the same nominal mass. The ICF values for various TAG classes are listed in Table 3.3.

ICF= % total isotopic abundance (M+2) / % total isotopic abundance (M)   (3.3)

Table 3.3 *M+2 Isotopic correction factors (ICF) for triacylglycerols based on the isotopic abundance ratios of M and M+2 ions.*

TAG ID	Isotope mass	% isotopic abundance	M+2 correction factors
C50:0	M=834.7677	55.1	0.181
	M+2=836.7744	10.0	
C52:0	M=862.7989	54.0	0.194
	M+2=864.8057	10.5	
C54:0	M=890.8302	52.8	0.208
	M+2=892.8370	11.0	
C55:0	M=904.8459	52.2	0.215
	M+2=906.8502	11.2	
C56:0	M=918.8615	51.7	0.221
	M+2=920.8683	11.4	
C57:0	M=932.8772	51.0	0.229
	M+2=934.8839	11.7	

For TAG groups with the same carbon number but different numbers of double bonds, the isotopic correction factor for that carbon number is used for all members of the series. For example, for all TAGs with carbon number 50 and different degree of unsaturations, the correction factor used is 0.181. This is because the M+2 contribution arising from the ^2H atom is insignificant with the addition of few hydrogen atoms. However, with the addition of carbon atoms the ICF increases due to the significant

effect of the ^{13}C on the M+2 contribution. For example, for C52 TAGs, the ICF is 0.194 which is greater than the ICF of C50 TAGs (0.181) and smaller than ICF of the C54 TAGs (0.208).

3.2.5 Corrections for LiCl Adduct Ion Formation

In this study, it has been observed that LiCl forms adducts with lithiated TAG species $[M+Li]^+$ giving rise to $[M+Li+(LiCl)]^+$ ions, consisting of $[M+Li+(Li^{35}Cl)]^+$ and $[M+Li+(Li^{37}Cl)]^+$ ions (see Figure 3.11). The LiCl adducts are 42 and 44 mass units greater than the corresponding lithiated molecular ion $[M+Li]^+$. These adduct ion formations result in two problems: 1) decreased $[M+Li]^+$ ion intensities and 2) the potential for overlap with TAG species which are 42 or 44 mass greater in molecular mass.
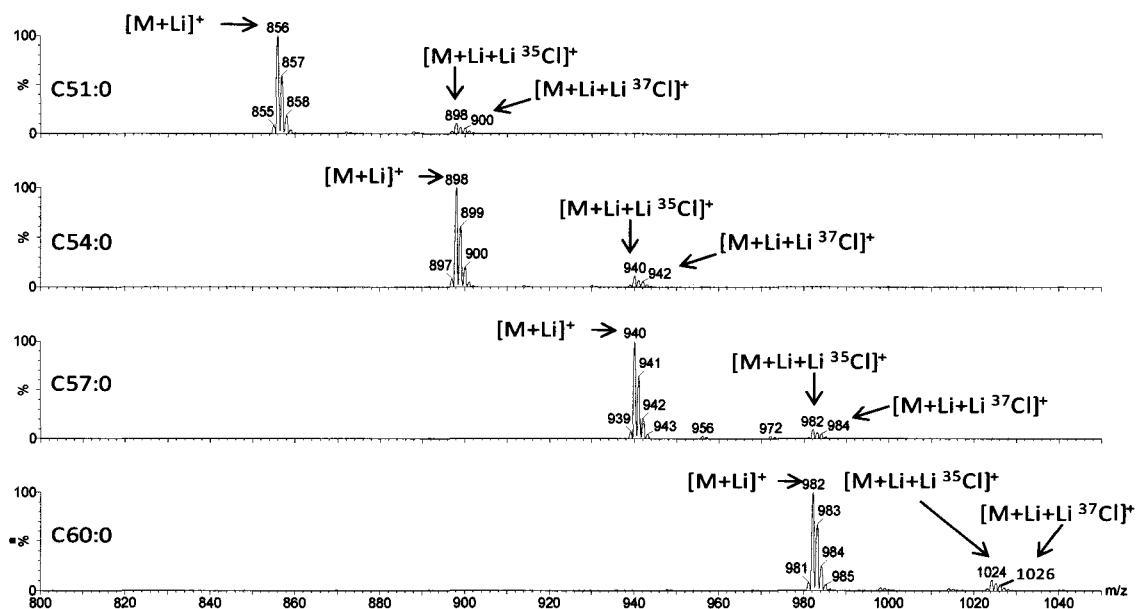
Figure 3.11 *ESI/MS of four TAG standards (C51:0 C54:0, C57:0 and C60:0) showing the detection of LiCl adducts at 42 and 44 mass units greater than their corresponding lithiated TAG standard ions.*

Figure 3.11 shows infusion electrospray mass spectra of C51:0, C54:0, C57:0 and C60:0 TAGs. The $[M+Li+LiCl]^+$ ion intensities are about 5% of the $[M+Li]^+$ intensities. In addition, there is an overlap of the mass values of the $[M+Li+LiCl]^+$ adducts with the lithiated molecular ion, $[M+Li]^+$ which have the same nominal masses. For example, the C51:0 $[M+Li+(Li^{35}Cl)]^+$ ion appears at m/z 898 which is identical to the m/z value for the C54:0 $[M+Li]^+$ ion. While this occurrence is relatively rare in the analysis of complex TAG mixtures, there needs to be a correction applied where necessary. To the best of our knowledge this quantitative correction has not been reported before.

3.2.5.1 Determination of Optimum LiCl Concentration

The relative intensities of $[M+Li]^+$ lithiated molecular ions and $[M+Li+LiCl]^+$ adduct ions showed some dependency on the LiCl concentration as shown in Figures 3.12 and 3.13. A study was undertaken to determine the optimum and minimum LiCl concentration needed for the analysis of TAGs. Solutions of the C54:3 TAG standard were prepared (2.5μM) and infused in the presence of varying concentrations of LiCl (0.25mM to 10mM). Five sets of averaged spectra were collected at each LiCl concentration. Figure 3.13 is a plot of the data from these experiments. The maximum peak area was observed at 0.5 mM LiCl; this concentration was used for the analyses of all the samples and standards.
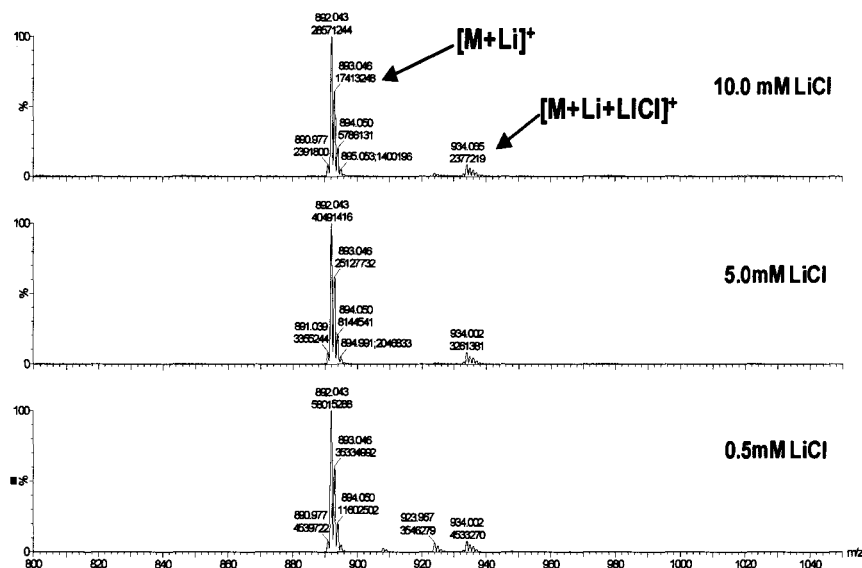
Figure 3.12 *Effect of LiCl concentration on the signal intensity as demonstrated with C54:3 TAG standard (2.5μM).*
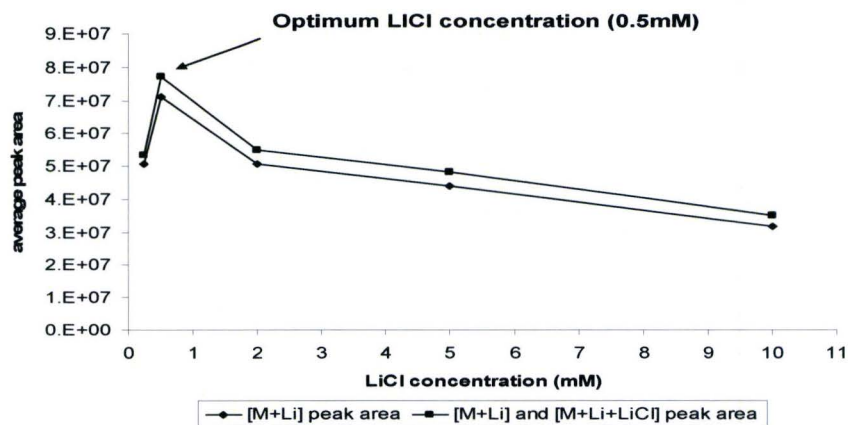
Figure 3.13 *Plots of average peak intensity of lithiated molecular ion $[M+Li]^+$ (bottom) and total ion ($[M+Li]^+$, $[M+Li+Li^{35}Cl]^+$ and $[M+Li+Li^{37}Cl]^+$) (top) of standard C54:3 (2.5µM) versus LiCl concentration in mM, (n=3).*
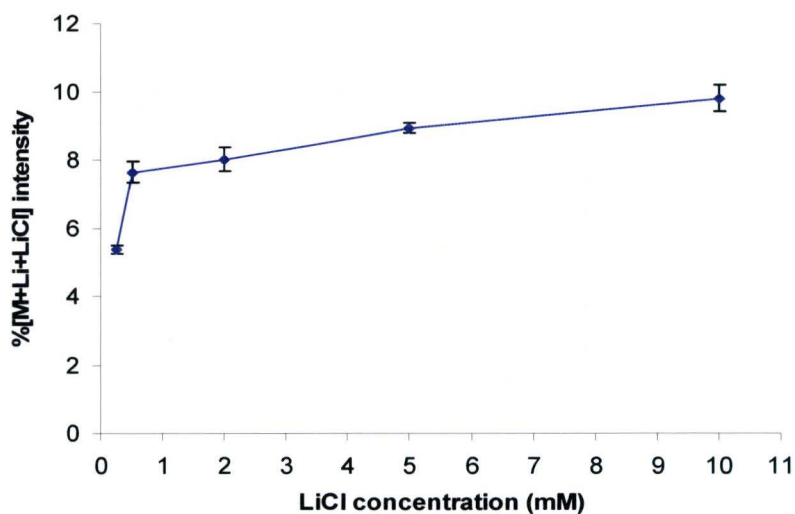
Figure 3.14 *Percentage of $[M+Li+LiCl]^+$ intensity as a function of total ion intensity.*

Figure 3.14 shows the percentage of LiCl adduct ion formation as a function of LiCl concentration. The formation of $[M+Li+LiCl]^+$ adduct ions reduces the peak area of the corresponding $[M+Li]^+$ ions. The lowest degree of $[M+Li+LiCl]^+$ adduct formation was observed at 0.5 mM. LiCl (4.8%).

3.2.5.2 Determination of LiCl Adduct Ion Correction Factors

The formation of $[M+Li+LiCl]^+$ adduct ions reduces $[M+Li]^+$ ion intensities. A correction factor to account for this loss of ion intensity is needed if it is desired to develop a quantitative method for TAG analysis. However, there was no way to determine response factors for $[M+Li+(Li^{35}Cl)]^+$ and $[M+Li+(Li^{37}Cl)]^+$ ions; it was felt reasonable to assume that the response factors for these ions were similar to the $[M+Li]^+$ ions of the corresponding TAG molecules.

In order to determine the $[M+Li+LiCl]^+$ adduct correction factors, we investigated the effect of degrees of unsaturation and concentration of TAGs on $[M+Li+LiCl]^+$ adduct formations. Standards with the same number of carbons but different degrees of unsaturation were selected; these were C54:X series of standards with 0, 3, 6 and 9 degree of unsaturation. These four TAGs were infused at concentrations of 0.625μM, 1.25μM 2.5μM and 5μM, and the mean (n=5) of the $[M+Li]^+$, $[M+Li+Li^{35}Cl]^+$ and $[M+Li+Li^{37}Cl]^+$ ions were determined. The percent total LiCl adduct ion intensities ($[M+Li+Li^{35}Cl]^+$ and $[M+Li+Li^{37}Cl]^+$) were calculated using equation 3.4. The results are presented in Table 3.4.

% total LiCl adduct intensity = $\dfrac{(\,PA[M+Li+Li^{35}Cl]^{+} + PA\,[M+Li+Li^{37}Cl]^{+})*100}{(PA\ of\ [M+Li]^{+} + PA[M+Li+Li^{35}Cl]^{+} + PA\,[M+Li+Li^{37}Cl]^{+})}$ (3.4)

Where "PA" stands for peak area.

Table 3.4 *Calculated percentage of total LiCl adduct ion intensities, ([M+Li+Li^{35}Cl]$^{+}$ and [M+Li+Li^{37}Cl]$^{+}$, using unsaturated TAGs (0.625-5µM analyte concentration in the presence of 0.5mM LiCl). (Mean ± SD, n=5).*

Concentration (µM)	% average total LiCl adduct ion intensity			
	C54:0	C54:3	C54:6	C54:9
0.625	7.0 ± 1.1	4.0 ± 1.2	4.1 ± 0.7	3.0 ± 0.7
1.25	4.2 ± 0.9	4.5 ± 2.2	4.0 ± 2.6	3.3 ± 1.3
2.50	6.4 ± 1.9	5.5 ± 0.6	4.8 ± 1.3	3.6 ± 0.8
5.00	5.2 ± 1.9	5.1 ± 1.9	7.3 ± 2.1	4.8 ± 2.1
Total average (n=20)	**5.7 ± 1.8**	**4.7 ± 1.6**	**5.1 ± 2.1**	**3.4 ± 1.3**

The data in Tables 3.4 shows that the percentage of [M+Li+LiCl]$^{+}$ ion formation slightly decreases with the increasing number of degrees of unsaturation. Changing the TAG concentrations from 0.625 to 5.0µM had no statistically meaningful effect on the abundance of the LiCl adducts. The average percentage of LiCl adduct intensities were 3.4 ± 1.3, 5.1 ± 2.1, 4.7 ± 1.6 and 5.7% ± 1.8 for C54:9, C54:6, C54:3 and C54:0, respectively.

A pair-wise comparison of the mean of the TAGs was conducted by calculating the p-values (Table 3.5). All p-values were $\geq$ 0.05 except two data points shown with asterisks at 0.03 and 0.04. Overall, the p-values showed that there were no significant differences in the distributions. Thus considering a single mean value (4.8%) of $[M+Li+LiCl]^+$ ion formation from the corresponding $[M+Li]^+$ ion was acceptable.

Table 3.5 *Calculated p-values for the pair-wise comparisons of the lithiated adduct intensities for C54 TAG standards. (Mean $\pm$ SD, n=5).*

% average total LiCl adduct ion intensity		p-value
C54:0; 5.7 $\pm$ 1.8	C54:3; 4.7 $\pm$ 1.6	0.1
C54:0; 5.7 $\pm$ 1.8	C54:6; 5.1 $\pm$ 2.2	0.5
C54:0; 5.7 $\pm$ 1.8	C54:9; 3.4 $\pm$ 1.3	0.03*
C54:3; 4.7 $\pm$ 1.6	C54:6; 5.1 $\pm$ 2.1	0.6
C54:3; 4.7 $\pm$ 1.6	C54:9; 3.4 $\pm$ 1.3	0.1
C54:6; 5.1 $\pm$ 2.1	C54:9; 3.4 $\pm$ 1.3	0.04*

The interpretation of the data in Table 3.5 is that an average of 4.8% peak area of all $[M+Li]^+$ ions were detected as $[M+Li+LiCl]^+$ adduct ions; hence, there is a proportional loss of intensity across all the TAGs in a given sample. The 4.8% $[M+Li+LiCl]^+$ adduct ion formation can be divided in a 3:1 ratio based on the isotope ratio of $[M+Li+Li^{35}Cl]^+$ and $[M+Li+Li^{37}Cl]^+$ intensities. Therefore the average

percentage of $[M+Li+Li^{35}Cl]^+$ and $[M+Li+Li^{37}Cl]^+$ adduct ion intensities would be 3.6% and 1.2%, respectively. These adducts could interfere with the signals of $[M+Li]^+$ ions which have the same nominal masses. Thus the overlapped peak areas must be subtracted from the $[M+Li]^+$ ions in order to determine their accurate amount in a given oil sample.

The method developed in this chapter will be applied to data from real oil samples and the results will be discussed and presented in the following chapter.

4. RESULTS AND DISCUSSION

This chapter will discuss the application of the methods developed in Chapter 3 to the qualitative and quantitative analyses of TAG species in commercial oils. The TAGs in the oil samples were identified and structures elucidated using ESI/MS and ESI/MS/MS, respectively in the positive ion mode. The real test of the ESI/MS and ESI/MS/MS methodology will be provided by the quantification the TAGs in a set of partially hydrogenated canola oil samples for which the iodine values are known. Using mass spectrometry methods it is possible to determine the percentage composition and degree of unsaturation of each TAG in the canola oil samples; using these data an iodine value for each oil sample will be calculated. These calculated iodine values will be compared to the measured iodine values provided by Bunge Canada (Table 4.1). Similarly, the iodine values of five edible oils will also be calculated from experimental ESI/MS and ESI/MS/MS data and compared to literature values.

As described in Chapter 3, intense lithiated adduct ions, $[M+Li]^+$, can be generated during ESI positive ion mode infusion of the oil solution in the presence of lithium chloride. Peak identities were assigned to the lithiated TAG species based on their mass-to-charge ratios. The total number of carbons and double bonds in each TAG were determined using the m/z values of the adduct TAG ions.

Upon CID, the $[M+Li]^+$ ions afforded product ion spectra that contained diagnostic fragment ions. These fragment ions assisted in determining the fatty acyl substituents of each TAG species as described in section 3.2. The location of the fatty acyl moieties on the glycerol backbone cannot be determined in this work.

Quantification of TAG species in the oil samples involved the application of a series of correction factors to the raw ESI/MS data. The responses of TAGs were shown to be highly dependent on the number of double bonds and the carbon chain length of the acyl components. The set of relative response factors (RRFs) determined in Chapter 3 will be applied to the TAGs in the oil samples to compensate for the signal variations that arise from the structural differences. Additional correction factors: M+2 isotopic contributions, instrument signal fluctuations (internal standard normalization) and LiCl adduct ion formation will be factored in as well.

In summary, the mass spectral data will be processed in the following way:

1) Determine the molecular masses and identities of TAG species in the oil samples using infusion ES/MS and ESI/MS/MS methods.

2) Apply individual correction factors to the raw peak area data and evaluate and compare the relative effect of the single correction factor on the quantification of TAGs in oil samples.

3) Determine the final percentage compositions of TAG species in the oils by sequentially applying the four correction factors (internal standard normalization, M+2 isotopic contributions, LiCl adduct ion formation and RRF) on to the raw peak area data.

4) Calculate the iodine value of an oil sample using the degree of unsaturation and percentage compositions of the TAGs in the sample.

4.1 Qualitative Analysis of Triacylglycerols in Oil Samples

Four partially hydrogenated oil samples were kindly provided by Bunge Canada and were derived from a single canola oil feed stock. The oils had been subjected to increasing degrees of hydrogenation resulting in a sequential decrease in the degree of unsaturation of each sample. Table 4.1 lists the iodine values that were provided by Bunge Canada for the canola oil feedstock and the four partially hydrogenated samples. Since iodine reacts with double bonds of the TAG molecules, the greater the degrees of unsaturation, the higher the iodine values of an oil sample would be. Iodine values are discussed further at the end of this chapter.

Table 4.1 *Iodine values measured at Bunge Canada of a canola oil feedstock and four canola oil samples that had increasing degrees of hydrogenation.*

Bunge oil samples	Measured iodine values (grams of iodine consumed by 100 grams of oil)
Canola oil feedstock	115
CA04	89
CA09	86
CA37	73
CA67	63

In addition to the Bunge Canada samples, five commercial edible oils: grape seed oil (Loriva, California, USA), hemp seed oil (Manitoba Harvest, Manitoba, Canada), olive oil (Bertolli pure classico, Italy), walnut oil (Vilux, B.C., Canada) and sesame oil (Loriva, California, USA) were purchased from a local grocery store and analyzed using the same method. The Bunge oil samples will be discussed first while the edible oil samples will be presented later in section 4.1.2.

4.1.1 Identification of Triacylglycerols in Bunge Oil Samples

The positive ion mode electrospray mass spectrometric analyses of the five Bunge oil samples yielded a complex mixture of TAG ions (Figure 4.1). In the presence of lithium ion, the TAG molecular ions in the oil samples afforded abundant $[M+Li]^+$ ions which provided the molecular masses of the TAG species. However, molecular masses of intact TAGs are not unique identifiers as isobaric TAGs could be detected as a single ion peak [11, 19]. Thus the use of tandem mass spectrometry is indispensable to determine the presence of isobaric TAGs in each $[M+Li]^+$ ion.

ESI/MS data provided the molecular mass of the individual TAG from which the total acyl carbons and double bonds was determined using expected fatty acyl moieties. For example in Figure 4.1, m/z 890 ion corresponded to lithiated TAG with 54 acyl carbons and 4 double bonds i. e. C54:4. Within a given TAG group, the TAG molecular ions were separated by 2 mass units corresponding to the difference in one degree of unsaturation. For example, in the C54:X group, C54:4 and C54:3 corresponded to mass-to-charge ratios of 890 and 892, respectively.
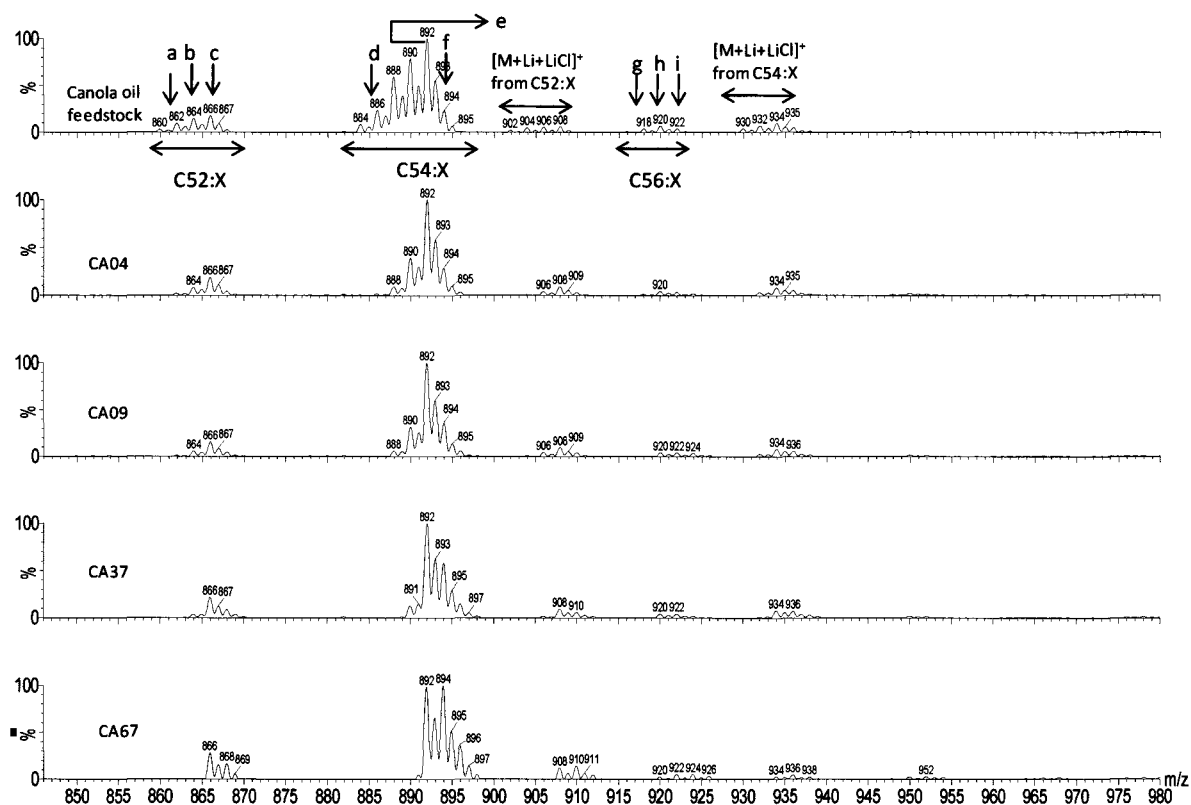
a=C52:4, b=C52:3, c=C52:2, d=C54:6, e=C54:3, f=C54:2, g=C56:4, h=C56:3, i=C56:2

Figure 4.1 *Positive ion ESI/MS mass spectra of the five Bunge oil samples. Few of the TAGs are labeled using letters a through i. The labels, C52:X, C54:X and C56:X correspond to the three main TAG groups. [M+Li+LiCl]$^+$ adduct ions corresponding to the C52:X and C54:X series are noted. Sample and LiCl concentrations were 12.5 μg/mL and 0.5mM, respectively.*

The ESI/MS mass spectra of Bunge oil samples revealed three major TAG groups, each containing the same total number of carbons, i.e., C52, C54 and C56 (Figure 4.1 and Table 4.2). As expected, the numbers of double bonds decreased with increasing

degrees of hydrogenation. The addition of hydrogen results in the conversion of the highly unsaturated TAGs to lesser unsaturated TAGs in a group. For example, the changing patterns (shifting intensities from left to right) in the mass spectra of the C54 TAGs in the five Bunge oils reflected the decreasing degrees of unsaturation of the TAG molecules in these samples. Similar patterns were observed in the C52 and C56 series.

Table 4.2 *Distributions of TAGs in Bunge oil samples identified from the ESI/MS spectra.*

$[M+Li]^+$ (Da)	TAGs				
	canola oil feedstock	CA04	CA09	CA37	CA67
860	C52:5				
862	C52:4				
864	C52:3	C52:3	C52:3	C52:3	
866	C52:2	C52:2	C52:2	C52:2	C52:2
868	C52:1	C52:1	C52:1	C52:1	C52:1
870					C52:0
882	C54:8				
884	C54:7				
886	C54:6	C54:6			
888	C54:5	C54:5	C54:5		
890	C54:4	C54:4	C54:4	C54:4	C54:4
892	C54:3	C54:3	C54:3	C54:3	C54:3
894	C54:2	C54:2	C54:2	C54:2	C54:2
896	C54:1	C54:1	C54:1	C54:1	C54:1
898			C54:0	C54:0	C54:0
916	C56:5				
918	C56:4				
920	C56:3	C56:3	C56:3	C56:3	C56:3
922	C56:2	C56:2	C56:2	C56:2	C56:2
924	C56:1	C56:1	C56:1	C56:1	C56:1
926					C56:0

The TAGs identified in the five Bunge samples are listed in Table 4.2. The number of TAG species identified in each canola oil sample follows the sample name in brackets: canola oil feedstock (18), CA04 (12), CA09 (12), CA37 (12) and CA67 (13).

Other peaks were observed in the ESI/MS spectra of the oil samples corresponding to the $[M+Li+LiCl]^+$ adduct ions (see Figure 4.1). Increasing the cone voltage and lowering the LiCl concentration reduced LiCl adduct ion formation but did not entirely eliminate these adducts. The signals of the LiCl adduct ions, $[M+Li+Li^{35}Cl]^+$ and $[M+Li+Li^{37}Cl]^+$, were detected at 42 and 44 mass units higher than the corresponding lithiated molecular ion, $[M+Li]^+$. For example, the LiCl adduct ions that arose from the C52:X and C54:X TAGs were detected in the mass ranges between m/z 902-912 and 928-936, respectively as shown in Figure 4.1. There were no overlaps between LiCl adduct ions and $[M+Li]^+$ ions in these samples so no correction needed to be applied.

4.1.2 Structural Elucidation of Triacylglycerols in Bunge Oil Samples

We have shown that upon CID, the mass spectra afforded sufficient information to determine the structural composition of TAG species. The CID of lithiated TAG ions of oil samples generated abundant diacylglycerol ions: the neutral losses of the acyl moieties as free fatty acids, $[M+Li-RCOOH]^+$, and as the lithium salts of the fatty acids, $[M+Li-RCOOLi]^+$. These two fragment ions allowed us to identify unambiguously the fatty acyl compositions of the TAGs in the oils. To illustrate, ESI/MS/MS spectra of typical TAGs in oil samples with different structural composition (symmetric, asymmetric and isobaric) are presented in Figure 4.2.
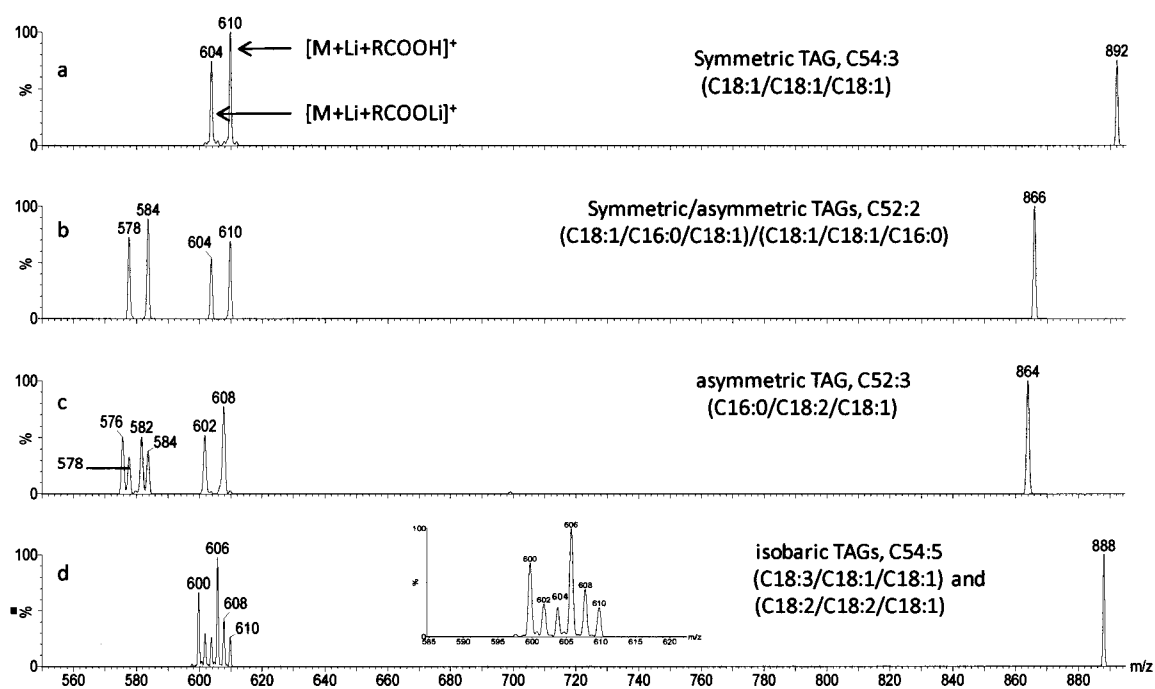
Figure 4.2 *Product ion mass spectra of selected TAGs observed in Bunge canola oil feedstock sample showing characteristic fragment ions. Interpretation of the fragment ion pattern afforded the following structural assignment: a) symmetric TAG with three identical fatty acyl substituents b) symmetric/asymmetric TAG with two different fatty acyl substituents depending on the position of the fatty acyl substituents on the glycerol backbone c) asymmetric TAG with three different fatty acyl substituents and d) isobaric TAGs where two TAGs with identical nominal masses detected as a single ion.*

Figure 4.2a is the product ion scan of the symmetric lithiated TAG species C54:3 (m/z 892). The CID spectrum contained a single pair of product ions at m/z 610 and 604 which corresponded to the neutral loss of a single fatty acid (C18:1) as a free fatty acid (m/z 610) and as the loss of lithium salt of the fatty acid (m/z 604). Notice that the pair fragments were detected at a mass difference of 6 Da. The intensity of the fragment due

to the neural loss of the fatty acyl substituent as a free fatty acid (m/z 610) was greater than the intensity of the fragment due to the neutral loss of the fatty acyl substitute as the lithium salt of the acid (m/z 604) consistent with observations in the method development section of this work. Since the fragments resulted from a single fatty acyl loss, the structure of the C54:3 TAG was assigned as C18:1/C18:1/C18:1.

Figure 4.2b illustrates the CID spectrum of a symmetric/asymmetric TAG C52:2 (m/z 866); two pairs of product ions arising from the neutral losses of two fatty acyl substituents as the free fatty acids and as the lithium salts of the fatty acids were observed. Accordingly, one pair (m/z 610 and 604) and a second pair (m/z 584 and 578) were assigned to the neutral losses of fatty acids and the lithium salts of C16:0 and C18:1, respectively. Since the fragments resulted from two fatty acyl losses, the structure of the C52:2 TAG was assigned as C18:1/C16:0/C18:1 or C18:1/C18:1/C16:0 representing a symmetric or an asymmetric TAG, respectively. Notice that the position of the C16:0 substituent determines the symmetry of the TAG molecules.

Figure 4.2c illustrates the CID spectrum of an asymmetric TAG C52:3 (m/z 864) with three pairs of product ions arising from the neutral losses of three fatty acyl substituents as the free fatty acids and as the lithium salts of the fatty acids. Accordingly, first pair (m/z 608 and 602), second pair (m/z 584 and 578) and third pair (m/z 582 and 576) were assigned to the neutral losses of fatty acids and the lithium salts of C16:0, C18:1 and C18:2, respectively. Since the fragments were resulted from three fatty acyl losses, the structure of the C52:3 TAG was assigned as C16:0/C18:2/C18:1 with no specification as to the *sn* positions.

Figure 4.2d exhibits the product ion spectrum of isobaric TAG C54:5 (m/z 888). Several fragment ions were observed. Constructing the possible isobaric TAGs from the fragment ions required matching of the identified fatty acids in order to come up with TAGs that had an m/z value of 888 and five double bonds. From the fragment pairs, the compositions of the fatty acids of the isobaric TAGs were determined. There were three fragment pairs: the first pair (m/z 610 and 604), the second pair (m/z 608 and 602) and the third pair (m/z 606 and 600). The corresponding fatty acids responsible for the formation of the fragment ions were C18:3, C18:2 and C18:1, respectively. From the mass spectral information shown in Figure 4.2d, it was possible to determine that there were two isobaric TAGs at m/z 888, which had the structural compositions of C18:3/C18:1/C18:1 and C18:2/C18:2/C18:1.

The diacyl fragment ion pairs, fatty acyl components and possible compositions of TAGs in the Bunge oil samples are listed in Table 4.3.

Table 4.3 *Fatty acyl substituents of the identified lithiated TAG molecular species in Bunge oil samples as determined by ESI/MS/MS; identification of more than one TAG species of a given [M+Li]⁺ ion confirmed the presence of isobars.*

TAG ID	[M+Li]⁺ m/z	MS/MS product ion pairs *	Masses of fatty acid substituents	TAG Compositions				
				canola oil feed stock	CA04	CA09	CA37	CA67
C52:5	860	**604,598** **610,604** 578,572 580,574 582,576	**256(C16:0)** **250(C16:3)** 282(C18:1) 280(C18:2) 278(C18:3)	C16:3/C18:1/C18:1 C16:0/C18:2/C18:3	ND	ND	ND	ND
C52:4	862	**606,600** 580,574 582,576 584,578	**256(C16:0)** 282(C18:1) 280(C18:2) 278(C18:3)	C16:0/C18:2/C18:2 C16:0/C18:1/C18:3	ND	ND	ND	ND
C52:3	864	**608,602** **610,604** 582,576 584,578	**256(C16:0)** **254(C16:1)** 282(C18:1) 280(C18:2)	C16:1/C18:1/C18:1 C16:0/C18:2/C18:1	C16:1/C18:1/C18:1 C16:0/C18:2/C18:1	C16:1/C18:1/C18:1 C16:0/C18:2/C18:1	C16:1/C18:1/C18:1 C16:0/C18:2/C18:1	ND
C52:2	866	**610,604** 584,578	**256(C16:0)** 282(C18:1)	C16:0/C18:1/C18:1	C16:0/C18:1/C18:1	C16:0/C18:1/C18:1	C16:0/C18:1/C18:1	C16:0/C18:1/C18:1
C52:1	868	**612,606** 584,578 586,580	**256(C16:0)** 284(C18:0) 282(C18:1)	C16:0/C18:0/C18:1	C16:0/C18:0/C18:1	C16:0/C18:0/C18:1	C16:0/C18:0/C18:1	C16:0/C18:0/C18:1
C52:0	870	**614,608** 586,580	**256(C16:0)** 284(C18:0)	ND	ND	ND	ND	C16:0/C18:0/C18:0
C54:8	882	602,596 604,598	280(C18:2) 278(C18:3)	C18:2/C18:3/C18:3	ND	ND	ND	ND
C54:7	884	602,596 604,598 606,600	282(C18:1) 280(C18:2) 278(C18:3)	C18:2/C18:2/C18:3 C18:1/C18:3/C18:3	ND	ND	ND	ND
C54:6	886	602,596 604,598 606,600 608,602	284(C18:0) 282(C18:1) 280(C18:2) 278(C18:3)	C18:0/C18:3/C18:3 C18:1/C18:2/C18:3 C18:2/C18:2/C18:2	C18:0/C18:3/C18:3 C18:1/C18:2/C18:3 C18:2/C18:2/C18:2	ND	ND	ND
C54:5	888	606,600 608,602 610,604	282(C18:1) 280(C18:2) 278(C18:3)	C18:2/C18:2/C18:1 C18:1/C18:1/C18:3	C18:2/C18:2/C18:1 C18:1/C18:1/C18:3	C18:2/C18:2/C18:1 C18:1/C18:1/C18:3	ND	ND
C54:4	890	606,600 608,602 610,604 612,606	284(C18:0) 282(C18:1) 280(C18:2) 278(C18:3)	C18:2/C18:1/C18:1 C18:2/C18:2/C18:0 C18:0/C18:1/C18:3	C18:2/C18:1/C18:1 C18:2/C18:2/C18:0 C18:0/C18:1/C18:3	C18:2/C18:1/C18:1 C18:2/C18:2/C18:0 C18:0/C18:1/C18:3	C18:2/C18:1/C18:1 C18:2/C18:2/C18:0 C18:0/C18:1/C18:3	C18:2/C18:1/C18:1 C18:2/C18:2/C18:0 C18:0/C18:1/C18:3
C54:3	892	610,604	282(C18:1)	C18:1/C18:1/C18:1	C18:1/C18:1/C18:1	C18:1/C18:1/C18:1	C18:1/C18:1/C18:1	C18:1/C18:1/C18:1
C54:2	894	610,604 612,606	284(C18:0) 282(C18:1)	C18:0/C18:1/C18:1	C18:0/C18:1/C18:1	C18:0/C18:1/C18:1	C18:0/C18:1/C18:1	C18:0/C18:1/C18:1
C54:1	896	612,606 614,608	284(C18:0) 282(C18:1)	C18:0/C18:0/C18:1	C18:0/C18:0/C18:1	C18:0/C18:0/C18:1	C18:0/C18:0/C18:1	C18:0/C18:0/C18:1
C54:0	898	614,608	284(C18:0)	ND	ND	C18:0/C18:0/C18:0	C18:0/C18:0/C18:0	C18:0/C18:0/C18:0
C56:5	916	636,630 ***608,600***	280(C18:2) ***310(C20:1)***	C18:2/C18:2/C20:1	ND	ND	ND	ND
C56:4	918	636,630 638,632 ***608,602***	282(C18:1) 280(C18:2) ***310(C20:1)***	C18:1/C18:2/C20:1	ND	ND	ND	ND
C56:3	920	638,632 ***610,604***	282(C18:1) ***310(C20:1)***	C18:1/C18:1/C20:1	C18:1/C18:1/C20:1	C18:1/C18:1/C20:1	C18:1/C18:1/C20:1	C18:1/C18:1/C20:1
C56:2	922	638,632 640,634 ***612,606***	284(C18:0) 282(C18:1) ***310(C20:1)***	C18:0/C18:1/C20:1	C18:0/C18:1/C20:1	C18:0/C18:1/C20:1	C18:0/C18:1/C20:1	C18:0/C18:1/C20:1
C56:1	924	640,634 ***614,608***	284(C18:0) ***310(C20:1)***	ND	ND	ND	ND	C18:0/C18:0/C20:1

*MS/MS product ion pairs corresponding to the fatty acyl losses as free fatty acids and lithium salts of the acids.
ND stands for not detected
Bold face type represents the MS/MS product ion pairs and fatty acid substituents of C16:X.
Italics type represents the MS/MS product ion pairs and fatty acid substituents of C18:X.
Italics bold face type represents the MS/MS product ion pairs and fatty acid substituents of C20:X

The identified fatty acid substituents were assembled for each TAG species in the oil samples. Columns 1 and 2 of Figure 4.3 display the TAG identities and corresponding mass-to-charge ratios, respectively. Columns 3 and 4 of Figure 4.3 display the diacyl product ion pairs and corresponding fatty acids that contributed to the fragment ion formation, respectively. Columns 5 to 9 display the possible TAG compositions in the five Bunge oils. For TAGs which had more than two fatty acyl chains, the existence of isobars was confirmed.

The list of possible TAG molecular species was determined by combining the identified fatty acyl substituents for each $[M+Li]^+$ TAG ion such that the total number of carbons and degree of unsaturations (number of double bonds) would be equal to the molecular mass of the TAG. For example, the MS/MS spectra of TAG C54:6 (m/z 886) of canola oil feed stock and CA04 samples yielded four product ion pairs at m/z (602, 596), (604, 598), (606, 600) and (608, 602) corresponding to the losses of fatty acyl substituents of C18:0, C18:1, C18:2 and C18:3, respectively. Three possible isobaric TAGs were determined by combining the available fatty acyl substituents that would give the TAG molecular ion C54:6 (m/z 886). Accordingly, the identified TAG isobars were C18:0/C18:3/C18:3, C18:1/C18:2/C18:3 and C18:2/C18:2/C18:2.

Although the method development section demonstrated that the position of the fatty acyl moieties on the glycerol backbone can be determined from the relative intensities of the diacyl fragments using standard TAGs, for the oil samples the complexity of the TAGs was a hindrance in achieving this. Most of the identified TAGs were isobaric TAGs containing more than three diacyl fragments; hence, an intensity

comparison could not be applied for the determination of the fatty acyl positions. For the non isobaric TAGs which were comprised one or two fatty acids, the ratio of the intensities did not match the theoretical ratios reported by Hsu and Turk [93]. As a result, it was difficult to determine conclusively the positions of the fatty acyl substituents based on the peak intensities of the fragment ions. However, regardless of this drawback, we were able to determine the fatty acyl moieties of the TAGs and to quantify the TAG species which eventually used to calculate the iodine values of the oil samples.

4.1.3 Identification and Structural Characterization of Triacylglycerols in Edible Oils

The ESI/MS spectra of the edible oil samples (Figure 4.3 and Table 4.4) were similar to the ESI/MS spectra of the Bunge oil samples in which two major TAG groups C52:X and C54:X were detected. However, unlike the Bunge oils, two minor TAG groups containing odd number carbons, C55:X and C57:X, were detected in all five oil samples. An additional TAG group, C50:X was also detected in the olive oil sample and to a lesser extent in the sesame oil sample. LiCl salt adduct ions were also detected in the edible oil spectra, as shown in Figure 4.3.
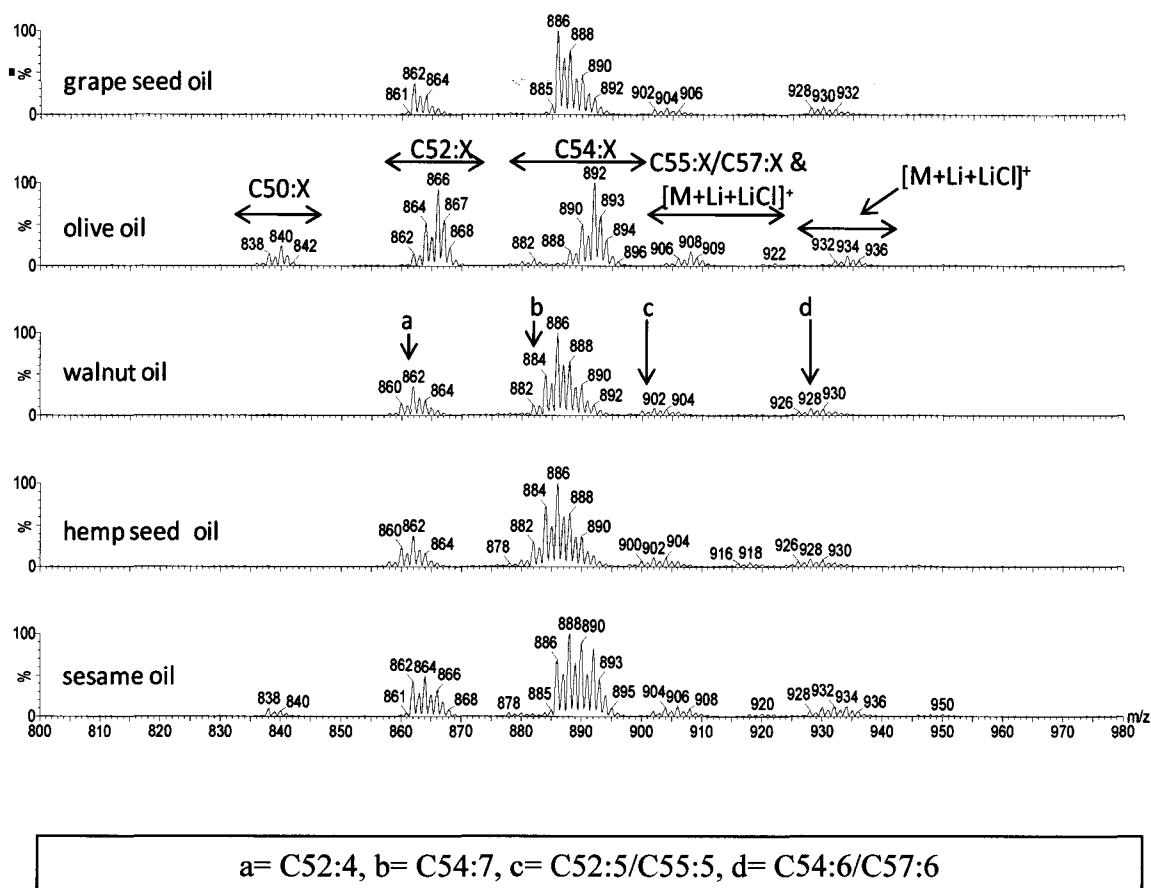
Figure 4.3 *Positive ion ESI/MS mass spectra of the five edible oil samples. The labels, (C50:X, C52:X, C54:X, C55:X and C57:X), indicate the TAG groups of the edible oil samples, and a, b, c, and d represent TAG ions corresponding to the TAG groups, respectively. [M+Li+LiCl]⁺ adduct ions were observed in the mass range m/z 900-930 (overlapping the lithiated molecular adducts of C55:X and C57:X) and m/z 928-936. Sample concentration and LiCl concentration were 12.5 µg/mL and 0.5mM, respectively.*

Table 4.4 *Distributions of TAGs in edible oil samples identified from the ESI/MS spectra.*

[M+Li]$^+$ (Da)	TAGs				
	olive oil	Walnut oil	Hemp seed oil	Sesame oil	Grape seed oil
838	C50:2				
840	C50:1				
860	C52:5	C52:5	C52:5		
862	C52:4	C52:4	C52:4	C52:4	C52:4
864	C52:3	C52:3	C52:3	C52:3	C52:3
866	C52:2			C52:2	
876		C54:11	C54:11		
878		C54:10	C54:10	C54:10	
880		C54:9	C54:9	C54:9	
882		C54:8	C54:8	C54:8	
884		C54:7	C54:7	C54:7	
886		C54:6	C54:6	C54:6	C54:6
888	C54:5	C54:5	C54:5	C54:5	C54:5
890	C54:4	C54:4	C54:4	C54:4	C54:4
892	C54:3	C54:3	C54:3	C54:3	C54:3
894	C54:2			C54:2	
898					
900		C55:6	C55:6		C55:6
902		C55:5	C55:5		C55:5
904		C55:4	C55:4	C55:4	C55:4
906	C55:3	C55:3	C55:3	C55:3	C55:3
908	C55:2			C55:2	C55:2
926		C57:7	C57:7		
928		C57:6	C57:6		
930		C57:5	C57:5		

The number of TAG species identified in each edible oil sample follows the sample name in brackets: olive oil (12), walnut oil (19), hemp seed oil (19), sesame oil (15) and grape seed oil (11).

The TAGs identified in the five edible oil samples are listed in Table 4.4. The most unsaturated TAGs are observed in the C54 groups containing 5 to 11 double bonds. Walnut oil and hemp seed oil contain C54:11 TAGs. Sesame oil, grape seed oil and olive oil contain C54:10, C54:6 and C54:5 TAGs, respectively.

LiCl salt adduct ions were detected in the edible oil spectra and these adduct ions overlapped with the C55:X and C57:X TAG ions of the edible oils. These species were readily distinguished by their characteristic CID fragment ions as shown in Figures 4.4 and 4.5.

The tandem mass spectra of the C52:3 (m/z 864) TAG olive oil produced fragments due to the neutral losses of the fatty acids as free fatty acids at mass units: 610 (C16:1), 608 (C16:0), 584 (C18:2) and 582 (C18:1) as shown in Figures 4.4 and 4.5. Rearrangement of the identified fatty acids resulted in the presence of two possible isobaric TAGs namely C16:0/C18:2/C18:1 and C16:1/C18:1/C18:1 representing the molecular ion C 52:3 (m/z 864).
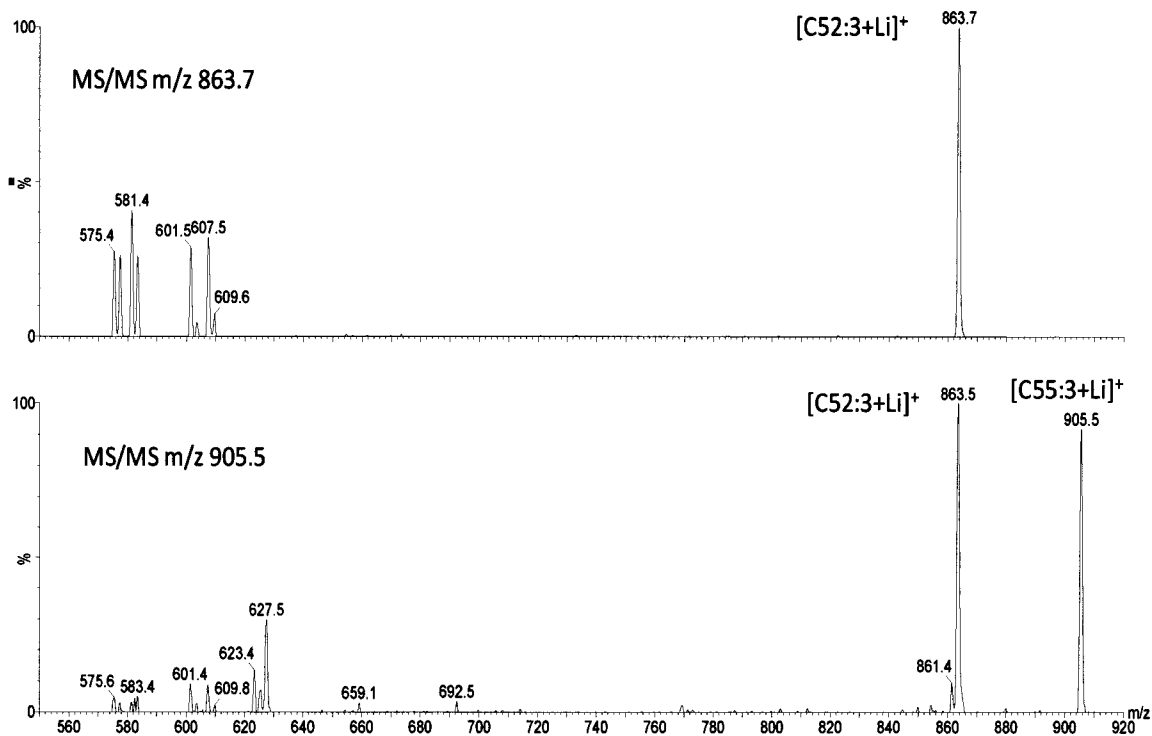
Figure 4.4 *ESI/MS/MS spectra of TAGs C52:3 (m/z 863.7) and C55:3 (m/z 905.5) in olive oil. TAG C55:3 has the same nominal mass as the LiCl adduct ion C55:3.*
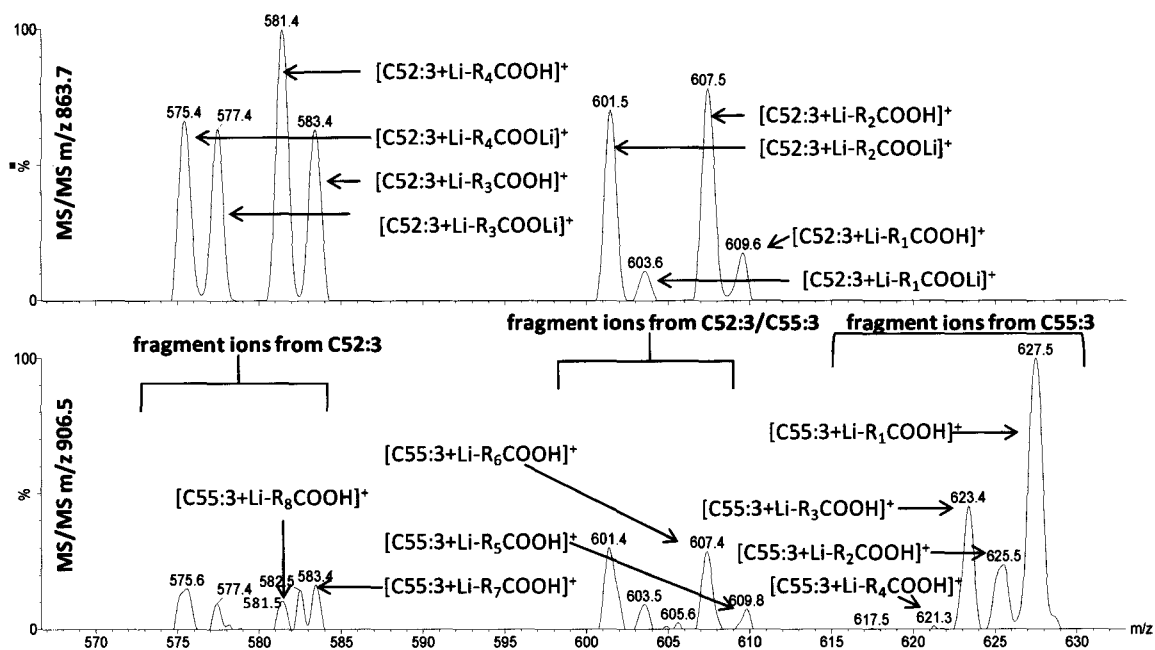
Figure 4.5 *An expanded region of Figure 4.4. MS/MS of m/z 863.7 (top) revealed four fragment pair ions resulted from the neutral losses of the four fatty acids: R_1=C16:1, R_2=C16:0, R_3=C18:2 and R_4=C18:1. MS/MS of m/z 905.5 (bottom) revealed seven fragment pair ions resulted from the neutral losses of the seven fatty acids: R_1=C18:3, R_2=C18:2, R_3=C18:1, R_4=C18:0, R_5=C19:1, R_6=C19:0, R_7=C21:2 and R_8=C21:1. The neutral losses of the fatty acids as free lithium salts of the acids were not marked in the bottom spectrum.*

On the other hand, the tandem mass spectra of the C55:3 (m/z 906) produced additional fragment ions besides to the fragment ions that arose from C52:3 (m/z 864). The fragment ions from TAG C55:3 resulted from the neutral losses of the fatty acids

with mass units: 628 (C18:3), 626 (C18:2), 624 (C18:1), 622 (C18:0), 610 (C19:1), 608 (C19:0), 584 (C21:2) and 582 (C21:1) (see Figures 4.4 and 4.5). Rearrangement of the fragment fatty acid moieties confirmed the presence of additional four isobaric TAGs (C18:3/C19:0/C18:0, C18:1/C19:1/C18:1, C18:0/C19:1/C18:2 and C18:1/C19:0/C18:2) in conjunction with the two isobaric TAGs that arose from the fragmentation of TAG C52:3 (m/z 864). The two identified fatty acids. C21:1 and C21:2 could not make a TAG with m/z 906 and 3 degrees of unsaturation in combination with the other identified fatty acids. Therefore, it can be concluded that the fragment ions at m/z 582 and 584 were obtained solely from the CID fragmentation of TAG molecular ion C52:3, representing the neutral losses of the fatty acids C18:1 and C18:2 as free fatty acids, respectively. It is worth mentioning that the intensities of the fragments due to the neutral losses of the fatty acids, C18:3, C18:2, C18:1 and C18:0 as lithium salt of the fatty acids of the m/z 906 ion are very weak (see Figure 4.5).

ESI/MS/MS analyses were used to determine the structural composition of TAGs in the five edible oils and their compositions are listed in Appendix 3.

4.2 Quantitative Analysis of Triacylglycerols in Oil Samples

In an attempt to attain high quality data for each analyte, specific analytical procedures were conducted in collecting and processing the data. The data processing involved implementing sequential corrections to the raw peak area data of TAGs in oil samples.

4.2.1 Data Collection

A mass spectrum of each oil sample was acquired and each peak in the mass spectrum was identified by its m/z value. One hundred mass spectra were collected and averaged to afford a single mass spectrum. The advantage of acquiring a high number of mass spectra was to improve the signal-to-noise ratio of the peaks. Each sample was run five times and each run was blank subtracted. A mean intensity and relative standard deviation were calculated for each m/z value of interest.

4.2.2 Data Processing with the Application of Correction Factors

Data processing of each sample involved the application of the four correction factors to the raw peak area data as discussed in the method development section of the thesis. It is worth mentioning that the "raw peak area" data in this thesis is the "uncorrected trace peak area" data obtained from the mass spectra. The four correction factors were internal standard normalization, isotopic correction factors, corrections for $[M+Li+LiCl]^+$ contributions and relative response factors (RRFs).

In order to determine the importance of each of the four correction factors in the quantification of the TAG species in the oil samples, each correction factor will be applied to the ESI/MS raw peak area data, and the percentage compositions of TAGs before and after the correction will be compared. This protocol should allow a determination of the relative importance of the four correction factors for the quantification of the TAG species in the oil samples.

Using the final percentage compositions and degree of unsaturations of the TAGs

in the oil samples, the corresponding iodine values of the samples can be calculated. The calculated iodine values will be compared with the measured iodine values. A similar procedure will be conducted in the quantitative evaluation of the edible oil samples. The remaining section of this chapter will focus on the detailed quantification process as outlined above.

4.2.2.1 Normalization of Peak Area Data

The response of mass spectrometric detectors may change for a variety of reasons from run to run or over time. Therefore internal standards are used to compensate for signal drift and for instrument response changes during the sample analysis. By normalizing TAG peak areas to the peak areas of internal standards, more reproducible data are obtained [1]. In this thesis, odd carbon number saturated TAGs (C51:0, C57:0 and C63:0) were added as internal standards. The primary reason for the selection of these internal standards was that odd carbon number saturated TAGs occur rarely in nature [1]; these TAGs were not observed in any of the oil samples used in this project (see Figure 4.6).

The molecular masses of the first two internal standards (C51:0, m/z 856 and C57:0, m/z 940) bracketed the mass range of the major TAG groups in the oil samples (Figure 4.6). The TAG raw peak area data from the C52:X and C54:X clusters were normalized by dividing each peak area by the peak area of the TAG C51:0, and for the normalization of the TAGs in the C56:X clusters, TAG C57:0 was used. Table 4.5

compares the percentage compositions of TAGs in the Bunge canola oil feedstock sample

using raw peak area data and internal standard-normalized peak area data.
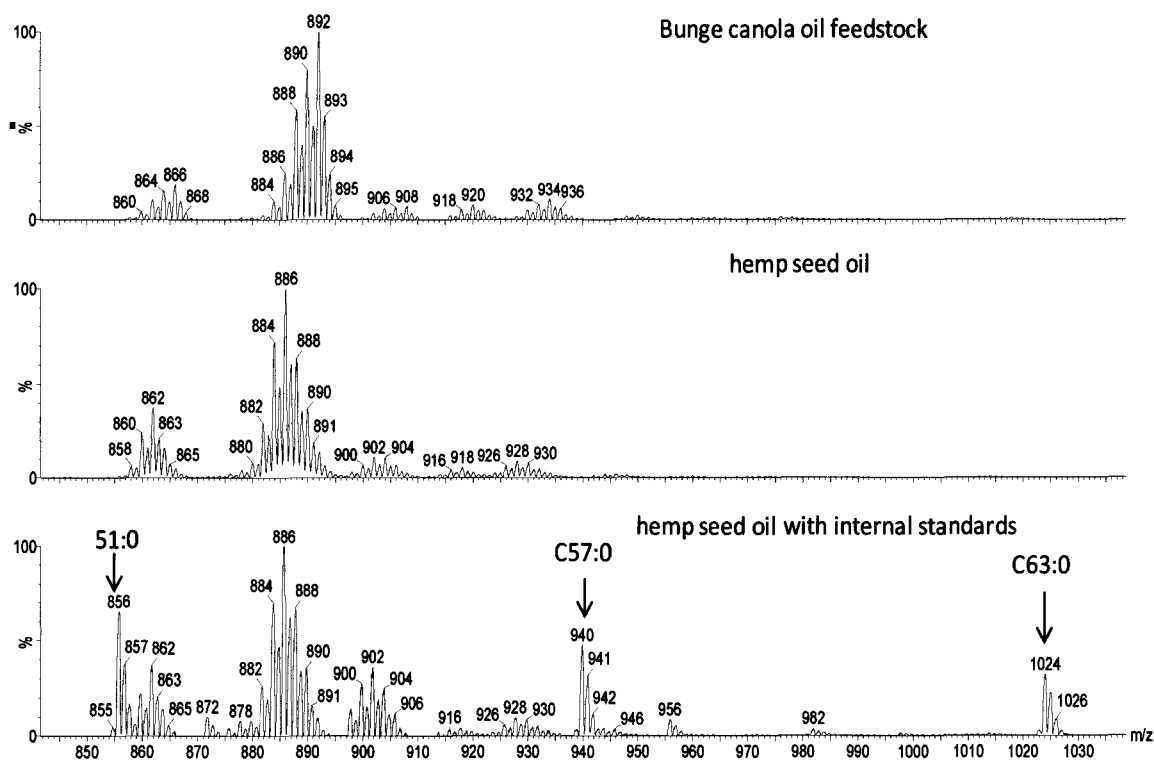
Figure 4.6 *ESI/MS spectra of Bunge canola oil feed stock, hemp seed oil and hemp seed oil with internal standards (C51:0, C57:0 and C63:0) illustrating the absence of the internal standard TAGs in the representative Bunge oil samples (canola oil feedstock) and edible oil samples (hemp seed oil). The internal standard TAGs were not detected in any of the oil samples studied in this thesis.*

Table 4.5 *Comparison of the percentage compositions of TAGs in a Bunge canola oil feedstock sample calculated using raw peak area data and internal standard normalized peak area ESI/MS data.*

TAG ID	m/z	%TAG using raw peak area (Mean ± %RSD; n=5)	%TAG using internal standard normalized peak area (Mean ± %RSD; n=5)
C52:5	860	1.1 ± 7.2%	0.9 ± 3.0%
C52:4	862	2.7 ± 7.2%	2.4 ± 1.9%
C52:3	864	4.0 ± 7.2%	3.5 ± 2.2%
C52:2	866	4.7 ± 6.5%	4.1 ± 1.6%
C52:1	868	1.0 ± 7.4%	0.9 ± 1.5%
C54:8	882	1.1 ± 3.2%	1.1 ± 6.9%
C54:7	884	2.9 ± 4.9%	3.0 ± 3.0%
C54:6	886	6.9 ± 6.2%	7.0 ± 6.4%
C54:5	888	15.8 ± 7.5%	16.1 ± 1.6%
C54:4	890	20.5 ± 7.7%	20.9 ± 1.2%
C54:3	892	25.7 ± 7.5%	26.3 ± 1.3%
C54:2	894	6.5 ± 7.1%	6.7 ± 1.1%
C54:1	896	0.9 ± 6.0%	0.9 ± 2.8%
C56:5	916	0.9 ± 5.3%	0.9 ± 3.2%
C56:4	918	1.5 ± 5.1%	1.6 ± 2.9%
C56:3	920	2.3 ± 6.3%	2.3 ± 1.9%
C56:2	922	1.5 ± 4.6%	1.5 ± 3.6%

As shown in Table 4.5, the use of an internal standard usually resulted in reduced %RSD values. Repeatability of the five runs of the canola oil feedstock was determined by %RSD and the average % RSD for the percentage compositions of TAGs calculated using raw peak areas and normalized peak areas were 6.5% and 2.5%, respectively.

4.2.2.2 Use of Isotopic Correction Factors to Peak Area Data

ESI/MS analysis of the oil samples revealed overlapping of the M+2 isotopic peaks with the $[M+Li]^+$ monoisotopic ions which had the same nominal masses. Therefore, for accurate quantification of the TAG components, the application of the isotopic correction factors was necessary.

Isotopic corrections were made starting from the lowest mass $[M+Li]^+$ ion in an ion cluster. The peak area of the M+2 peak was calculated using the isotopic correction factors listed in Table 3.3. This calculated peak area value was then subtracted from the area of the peak 2 mass units higher to afford a corrected peak area for the adjacent TAG's $[M+Li]^+$ ion. This process was continued sequentially across the ion cluster until there were no TAG peaks. This isotopic correction process was easily accomplished using an Excel spreadsheet (see Appendix 1). As an example the percentage compositions of TAGs in Bunge canola feed stock oil sample based on raw peak area data and isotopically corrected peak area data are presented in Table 4.6.

Table 4.6 *Comparison of the percentage compositions of TAGs in a Bunge canola oil feedstock sample calculated using raw peak area data and isotope corrected data.*

TAG ID	m/z	%TAG using raw peak area (Mean ± %RSD; n=5)	%TAG using isotopic corrected peak area (Mean ± %RSD; n=5)	p-value
C52:5	860	1.1± 7.2%	1.3 ± 7.2%	1.0
C52:4	862	2.7 ± 7.2%	3.1 ± 7.2%	0.13
C52:3	*864*	*4.0 ± 7.2%*	*4.2 ± 7.3%*	*0.023**
C52:2	*866*	*4.7 ± 6.5%*	*4.8 ± 6.4%*	*0.0051**
C52:1	**868**	**1.0 ± 7.4%**	**0.3 ± 12.9%**	**0.00001***
C54:8	882	1.1 ± 3.2%	1.3 ± 3.2%	1.0
C54:7	884	2.9 ± 4.9%	3.3 ± 5.1%	0.037*
C54:6	886	6.9 ± 6.2%	7.6 ± 6.4%	0.066
C54:5	888	15.8 ± 7.5%	17.4 ± 7.6%	0.11
C54:4	*890*	*20.5 ± 7.7%*	*21.0 ± 7.7%*	*0.012**
C54:3	*892*	*25.7 ± 7.5%*	*26.6 ± 7.5%*	*0.013**
C54:2	**894**	**6.5 ± 7.1%**	**2.3 ± 6.7%**	**0.00001***
C54:1	**896**	**0.9 ± 6.0%**	**0.6 ± 6.7%**	**0.00001***
C56:5	916	0.9 ± 5.3%	1.1 ± 5.3%	1.0
C56:4	918	1.5 ± 5.1%	1.6 ± 5.1%	0.0031*
C56:3	920	2.3 ± 6.3%	2.4 ± 6.5%	0.0091*
C56:2	922	1.5 ± 4.6%	1.3 ± 4.1%	0.00001*

*Mean values are significantly different between the raw peak area data and the isotopically corrected data ($p < 0.05$).
Bold italic shows relatively major components.
Bold face shows relatively minor components.

As shown in the above table, application of isotopic correction factors on raw peak area data resulted in peak area corrections with resultant changes in minor TAG components (bold face type) or in major TAG components (bold faced italics). For example, TAGs C52:1 and C54:2 were confounded by the M+2 peaks of the abundant ions of C52:2 and C54:3, respectively, resulting in an increase in their percentage compositions of about 2 fold. On the other hand, corrections of abundant TAGs (e.g.,

C54:3 and C54:4) was not significant. Although C54:3 was confounded by the C54:4 M+2 ion, the percentage compositions of C54:3 after the isotopic correction was not impacted significantly. The p-values for each pair of corrected and uncorrected data are included in Table 4.6. Overall, the application of the isotopic correction factors was important for these data sets.

4.2.2.3 Corrections for LiCl Adduct Ion Intensities

The formation and intensities of $[M+Li+LiCl]^+$ adduct ions were discussed in chapter 3. Overall, the peak area of the $[M+Li+LiCl]^+$ ions averaged about 4.8% of the peak area of the originating molecular ion $[M+Li]^+$. The $[M+Li+Li^{35}Cl]^+$ and $[M+Li+Li^{37}Cl]^+$ peak areas were 3.6% and 1.2% of the $[M+Li]^+$ ion total peak area respectively reflecting the 3:1 isotopic ratio.

In developing LiCl adduct ion correction factors, two issues had to be dealt with. The first issue was to determine the sum of the $[M+Li+LiCl]^+$ plus the $[M+Li]^+$ ion total peak area intensities to obtain the total adduct ion intensity. This summation of data was done based on the assumption that the mass spectral response factors of the $[M+Li]^+$ and the $[M+Li+LiCl]^+$ were identical. The second issue was if the $[M+Li]^+$ ion of one TAG was isobaric with the m/z value of a $[M+Li+Li^{35}Cl]^+$ or $[M+Li+Li^{37}Cl]^+$ ion of a second TAG, the intensity of the $[M+Li+LiCl]^+$ ion would need to be subtracted to determine the intensity of the $[M+Li]^+$ ion. This issue was particularly relevant to the edible oil samples. For instance, in Figures 4.5 and 4.6, the MS/MS spectrum of the ion at m/z 905.5 revealed the presence of $[M+Li]^+$ ion of TAG C55:3 in addition to the

$[M+Li+Li^{35}Cl]^+$ ion of the LiCl adduct of C52:3. The peak area of the $[M+Li+Li^{35}Cl]^+$ ion was subtracted from the peak area of the $[M+Li]^+$ ion of C55:3. The peak area subtracted for the $[M+Li+Li^{35}Cl]^+$ contribution corresponded to 3.6% of the total peak area of C52:3 (m/z 863.7) in which the $[M+Li+Li^{35}Cl]^+$ ion originated.

Mass spectral data from a walnut oil sample was used to show the effect of the application of LiCl adduct ion corrections on the accuracy of TAG contents in the oil sample. Table 4.7 presents a comparison of the percentage compositions of TAGs in walnut oil with and without the peak area corrections applied. Only a small subset of peaks showed significant changes (i.e., $p < 0.05$); these entries were noted with an asterisk. The overall changes to the percentage composition profile were very modest and impacted only three low abundance TAGs.

Table 4.7 *Comparison of the percentage compositions of TAGs in a walnut oil sample calculated using raw peak area data and LiCl adduct overlap corrected data.*

TAG ID	m/z	%TAG using raw peak area (Mean ± %RSD; n=5)	%TAG using LiCl overlap corrected peak area (Mean ± %RSD; n=5)	p-value
C52:5	860	2.6 ± 49%	2.7 ± 49%	0.91
C52:4	862	6.6 ± 14%	6.9 ± 12%	0.67
C52:3	864	3.5 ± 12%	3.6 ± 11%	0.64
C54:11	876	1.5 ± 18%	1.5 ± 18%	1.0
C54:10	878	2.9 ± 21%	2.9 ± 21%	1.0
C54:9	880	1.8 ± 19%	1.9 ± 19%	1.0
C54:8	882	2.8 ± 11%	2.8 ± 11%	1.0
C54:7	884	9.6 ± 14%	10.1 ± 14%	0.61
C54:6	886	18.8 ± 14%	19.8 ± 14%	0.61
C54:5	888	12.7 ± 12%	13.4 ± 13%	0.57
C54:4	890	6.6 ± 13%	6.6 ± 13%	1.0
C54:3	892	2.4 ± 14%	2.4 ± 14%	1.0
C55:6	900	5.4 ± 17%	5.4 ± 17%	1.0
C55:5	902	8.8 ± 20%	8.8 ± 20%	0.94
C55:4	904	6.2 ± 20%	5.4 ± 27%	0.39
C55:3	906	3.3 ± 18%	3.1 ± 20%	0.59
C57:7	**926**	**1.1 ± 12%**	**0.7 ± 15%**	**0.03***
C57:6	**928**	**1.8 ± 13%**	**1.0 ± 12%**	**0.0004***
C57:5	**930**	**1.8 ± 13%**	**1.1 ± 15%**	**0.0008***

*Mean values are significantly different between the raw peak area data and the LiCl overlap corrected peak area data (p< 0.05).
Bold face shows relatively minor components.

Table 4.7 showed the presence of odd carbon number TAGs in walnut oil samples. Odd carbon TAGs were present in all the edible oil samples studied in this work. This was surprising as natural TAGs usually only contain even carbon numbers.

In summary, the application of the LiCl adduct correction factors did not result in significant changes as shown by the p-values with the exception of few minor TAGs

shown in asterisk. Even though these corrections were not significant for many TAGs, the corrections were applied to all samples.

4.2.2.4 Application of Relative Response Factors to Peak Area Data

The ionization efficiencies of TAG molecules are largely influenced by the degree of unsaturation and to a lesser extent by the carbon chain length of the acyl moieties [18, 74, 75, 91, 100]; as a result, raw peak intensities of TAGs do not reflect their relative molar abundances in samples. For the quantitative determination of TAGs, it was critical to determine the relative response factors (RRF) for TAGs as a function of total carbon number and degrees of unsaturation.

The RRFs of a wide range of TAG species were calculated previously and converted to a look up table (Table 3.2). Using these RRF values, the percentage compositions of the TAGs in the Bunge canola oil feed stock sample were calculated and these data were compared with percentage compositions of the TAGs calculated based on the uncorrected raw peak area data (Table 4.8). Again the purpose of this comparative data was to show the significance of the RRF corrections on the quantification of the TAG species in the oils samples. Table 4.8 shows the comparison of the percentage composition of TAGs in a Bunge canola oil feed stock sample based on the raw peak area data and the RRF corrected data.

Table 4.8 *Comparison of the percentage compositions of TAGs in a Bunge canola oil feed stock sample calculated using raw peak area data and RRF corrected peak area data.*

TAG ID	m/z	%TAG using raw peak area (Mean ± %RSD; n=5)	%TAG using RRF corrected peak area (Mean ± %RSD; n=5)	p-value
C52:5	860	1.0 ± 7.2%	0.9 ± 6.4%	8.5E-06*
C52:4	862	2.7 ± 7.2%	2.5 ± 4.4%	9.8E-06*
C52:3	864	4.0 ± 7.2%	4.0 ± 6.7%	1.3E-05*
C52:2	866	4.7 ± 6.5%	5.3 ± 5.6%	1.2E-05*
C52:1	868	1.0 ± 7.4%	1.3 ± 4.5%	7.5E-05*
C54:8	882	1.1 ± 3.2%	0.8 ± 1.1%	1.4E-07*
C54:7	884	2.9 ± 4.9%	2.2 ± 2.8%	1.0E-06*
C54:6	886	6.9 ± 6.2%	5.6 ± 4.5%	3.8E-06*
C54:5	888	15.8 ± 7.5%	14.0 ± 7.0%	1.1E-05*
C54:4	890	20.5 ± 7.7%	19.8 ± 7.3%	1.6E-05*
C54:3	892	25.7 ± 7.5%	27.7± 6.3 %	2.3E-05*
C54:2	894	6.5 ± 7.1%	7.8 ± 6.5%	3.8E-05*
C54:1	896	0.9 ± 6.0%	1.2 ± 5.8%	7.1E-05*
C56:5	916	0.9 ± 5.3%	0.8 ± 6.0%	1.8E-06*
C56:4	918	1.5 ± 5.1%	1.6 ± 5.6%	1.8E-06*
C56:3	920	2.3 ± 6.3%	2.6 ± 5.8%	1.2E-05*
C56:2	922	1.5 ± 4.6%	2.0 ± 2.4%	4.9E-06*

*Mean values are significantly different between the raw peak area data and the RRF corrected data (p< 0.05).

The percentage compositions of almost all of the TAGs showed significant changes after application of RRF correction factors. The p-values for all data were <0.05 suggesting that difference of the two data distributions was very significant. The use of RRFs was the most significant correction factor that affected the quantification of the TAGs in the oil samples.

4.2.3 Application of the Combined Correction Factors to Raw Peak Area Data

Examination of the data in Table 4.9 revealed the net effect of the sequential application of the four correction factors on the quantification of the TAGs in a Bunge canola oil feed stock sample. The percentage compositions of all TAGs were significantly changed. The average %RSD of the final corrected percentage compositions of the TAGs improved by a factor of 2, i.e., 6.3 %RSD versus 3.2 %RSD for the raw and final corrected percentage compositions, respectively. In conclusion, the data correction steps that were implemented were necessary for the accurate quantification of the TAGs in the oil samples. The LiCl adduct correction factor did not have a significant effect on the percentage composition values of the TAGs in oil samples.

Table 4.9 *Comparison of the percentage compositions of TAGs in a Bunge canola oil feedstock sample calculated using raw peak area data and final corrected data using all four correction factors.*

TAG ID	m/z	%TAG using raw peak area (Mean ± %RSD; n=5)	%TAG using final corrected peak area (Mean ± %RSD; n=5).	p-value
C52:5	860	1.1 ± 7.2%	0.9 ± 3.0%	8.5E-06*
C52:4	862	2.7 ± 7.2%	2.5 ± 1.9%	9.8E-06*
C52:3	864	4.0 ± 7.2%	3.8 ± 2.5%	1.3E-05*
C52:2	866	4.7 ± 6.5%	4.8 ± 1.5%	1.2E-05*
C52:1	868	1.0 ± 7.4%	0.3 ± 8.7%	7.5E-05*
C54:8	882	1.1 ± 3.2%	0.9 ± 6.9%	1.4E-07*
C54:7	884	2.9 ± 4.9%	2.5 ± 2.7%	1.0E-06*
C54:6	886	6.9 ± 6.2%	6.4 ± 1.5%	3.8E-06*
C54:5	888	15.8 ± 7.5%	16.0 ± 1.3%	1.1E-05*
C54:4	890	20.5 ± 7.7%	21.2 ± 1.3%	1.6E-05*
C54:3	892	25.7 ± 7.5%	29.6 ± 1.2%	2.3E-05*
C54:2	894	6.5 ± 7.1%	2.9 ± 2.9%	3.8E-05*
C54:1	896	0.9 ± 6.0%	0.8 ± 4.9%	7.1E-05*
C56:5	916	0.9 ± 5.3%	1.0 ± 3.2%	1.8E-06*
C56:4	918	1.5 ± 5.1%	1.7 ± 2.9%	1.8E-06*
C56:3	920	2.3 ± 6.3%	2.8 ± 1.9%	1.2E-05*
C56:2	922	1.5 ± 4.6%	1.8 ± 4.6%	4.9E-06*

*Mean values are significantly different between the raw peak area data and the final corrected peak area data (p< 0.05).

The final corrected TAG percentage compositions of the Bunge and commercial edible oil samples are shown in Tables 4.10 and 4.11, respectively. The TAG profile of the five Bunge oil samples in Table 4.10 showed three major TAG groups: C52, C54 and C56. The most intense of the three TAG groups was C54:X with C54:3 being the most abundant TAG, with percentage compositions ranging from 30-52%. The distribution of

the TAGs in the oil samples based on the degree of unsaturations is shown in Figure 4.7; TAGs with 3 double bonds are the most abundant in all the five oils, with percentage compositions ranging from 36-58%. Overall, the Bunge samples compromise 17 TAG molecular ions with percentage compositions ranging from 0.3%-52%. Good repeatability of the TAG data was achieved in the five runs of each of the five oil samples ranging from 1.2-12.0%RSD. The changing pattern of the percentage compositions of the TAG distribution was the effect of hydrogenation on lowering the degrees of unsaturation of the successive Bunge oil samples as discussed in section 4.1.1.

Table 4.10 *Corrected average percentage compositions of TAGs in Bunge oil samples. The raw peak areas were corrected using isotopic correction factors, normalization with internal standards and RRF correction factors.*

TAG ID	m/z	Canola oil feed stock % TAG (Mean ± %RSD; n=5)	CAO4% TAG (Mean ± %RSD; n=5)	CAO9% TAG (Mean ± %RSD; n=5)	CA37% TAG (Mean ± %RSD; n=5)	CA67% TAG (Mean ± %RSD; n=5)
C52:5	860	0.9 ± 3.0%				
C52:4	862	2.5 ± 1.9%				
C52:3	864	3.8 ± 2.5%	3.2 ± 3.4%	2.9 ± 4.1%	1.5 ± 4.0%	
C52:2	866	4.8 ± 1.5%	7.9 ± 2.2%	8.3 ± 5.0%	8.4 ± 4.9%	5.6 ± 2.1%
C52:1	868	0.3 ± 8.7%	0.6 ± 6.7%	1.0 ± 3.7%	2.6 ± 5.8%	3.0 ± 2.9%
C52:0	870					0.6 ± 5.7%
C54:8	882	0.9 ± 6.9%				
C54:7	884	2.5 ± 2.7%				
C54:6	886	6.4 ± 1.5%	1.1 ± 6.4%			
C54:5	888	16.0 ±1.3%	4.2 ± 3.9%	2.8 ± 3.3%		
C54:4	890	21.2 ± 1.3%	19.1 ± 4.5%	15.6 ± 2.8%	6.0 ± 11%	1.8 ± 12%
C54:3	892	29.6 ± 1.2%	51.6 ± 4.4%	51.8 ± 3.7%	49.3 ± 11%	37.3 ± 9.7%
C54:2	894	2.9 ± 2.9%	6.2 ± 4.5%	9.9 ± 2.5%	21.6 ± 7.9%	32.5 ± 9.2%
C54:1	896	0.8 ± 4.9%	1.1 ± 3.0%	1.7 ± 6.9%	4.2 ± 12%	10.5 ± 7.9%
C54:0	898			1.5 ± 2.9%	1.8 ± 9.5%	2.9 ± 9.6%
C56:5	916	1.0 ± 3.2%				
C56:4	918	1.7 ± 2.9%				
C56:3	920	2.8 ± 1.9%	3.0 ± 3.5%	2.8 ± 3.6%	2.3 ± 4.3%	1.9 ± 4.5%
C56:2	922	1.8 ± 4.6%	2.1 ± 2.1%	1.9 ± 5.2%	2.3 ± 3.7%	2.6 ± 3.9%
C56:1	924					1.6 ± 6.0%
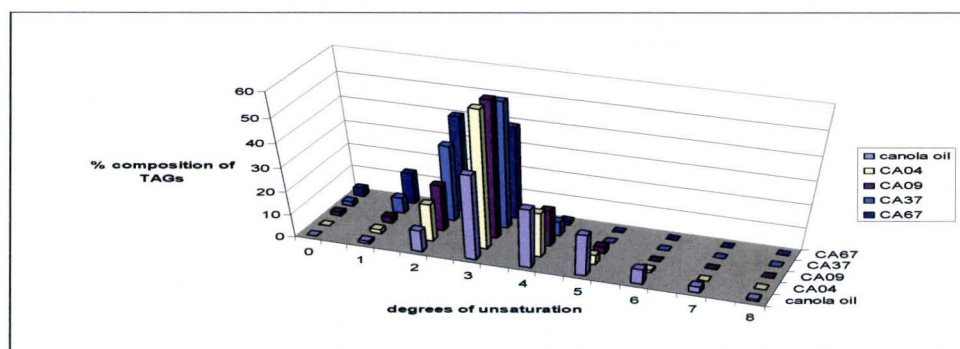
Figure 4.7 *Percentage compositions of TAGs in Bunge oil samples by degrees of unsaturation.*

The TAG percentage compositions of the edible oil samples is summarized in Table 4.11 and shows four major TAG groups: C52, C54, C55 and C57. One additional TAG group, C50, was detected in the olive oil sample. The most intense of the all TAG groups was C54:X with C54:6 being the most abundant TAG in walnut, hemp seed and grape seed oils ranging from about 20%-30%. For olive oil and sesame oil the most abundant TAGs were C54:3 and C54:5 with percentage compositions of about 26% and 16%, respectively. Overall, the edible oil samples compromised 26 TAG molecular ions with percentage compositions ranging from 0.3-30.5%. These samples were prepared and analyzed in the same way as the Bunge oil samples, however; their %RSDs were much higher than the Bunge oil samples. The increase in data variation could possibly be due to ion interferences from unknown components.

Table 4.11 *Final corrected average percentage compositions of TAGs in edible oil samples. The raw peak areas were corrected using the normalization, isotopic correction factors, LiCl adduct correction factors and RRF correction factors.*

TAG ID	M/Z	OLIVE OIL % TAG (Mean ± %RSD; n=5)	WALNUT OIL % TAG (Mean ± %RSD; n=5)	HEMP SEED OIL % TAG (Mean ± %RSD; n=5)	SESAME OIL % TAG (Mean ± %RSD; n=5)	GRAPESEED OIL % TAG (Mean ± %RSD; n=5)
C50:2	838	3.3 ± 18%				
C50:1	840	5.2 ± 14%				
C52:5	860		2.7 ± 6.4%	3.7 ± 1.4%		
C52:4	862	2.8 ± 4.6%	6.4 ± 4.8%	6.3 ± 2.1%	6.1 ± 3.5%	7.9 ± 4.8%
C52:3	864	10.9 ± 4.5%	2.6 ± 6.5%	2.0 ± 3.5%	6.5 ± 3.0%	3.7 ± 7.4%
C52:2	866	20.2 ± 2.9%			4.4 ± 3.4%	
C54:1	876		1.2 ± 23%	1.1 ± 26%		
C54:1	878		2.3 ± 28%	1.9 ± 26%	2.0 ± 31%	
C54:9	880		1.2 ± 26%	1.7 ± 14%	1.9 ± 31%	
C54:8	882		2.5 ± 8.8%	5.4 ± .8%	1.2 ± 28%	
C54:7	884		10.1 ± 6.1%	14.6 ± 5.9%	0.7 ± 6.3%	
C54:6	886		20.4 ± 6.9%	20.2 ± 4.4%	12.5 ± 5.5%	30.5 ± 39%
C54:5	888	4.6 ± 19%	12.2 ± 9.1%	12.1 ± 4.5%	16.2 ±6.3%	18.7 ± 35%
C54:4	890	14.1 ± 17%	6.3 ± 7.2%	6.5 ± 5.2%	14.2± 5.0%	12.0 ± 34%
C54:3	892	27.5 ± 17%	2.2 ± 9.5%	1.8 ± 10%	13.9 ± 4.6%	4.3 ± 30%
C54:2	894	3.9 ± 21%			3.1 ± 10%	
C54:0	898					
C55:6	900		5.9 ± 25%	6.2 ± 21%		1.5 ± 26%
C55:5	902		10.1 ± 29%	8.0 ± 20%		9.6 ± 27%
C55:4	904		6.2 ± 28%	4.8 ± 15%	6.5 ± 33%	6.3 ± 25%
C55:3	906	2.7 ± 44%	3.6 ± 27%	2.2 ± 22%	5.5 ± 27%	4.0 ± 25%
C55:2	908	4.8 ± 53%			5.3 ± 30%	1.6 ± 25%
C57:7	926		0.8 ± 19%	0.3 ± 5.6%		
C57:6	928		1.4 ± 11%	0.6 ± 6.0%		
C57:5	930		1.8 ± 11%	0.7 ± 9.9%		

Table 4.11 shows the composition and amount of the TAG species found in the five edible oils.

Olive oil: 11 TAG species were identified and the most significant TAGs were C54:3, C52:2, C54:4 and C52:3 in decreasing order with percentage compositions ranging from about 28-11%. The repeatability for all the TAGs in the oil ranged from 5-53 %RSD.

Walnut oil: 19 TAG species were identified and the most significant TAGs were C54:6, C54:5, C54:7and C55:5 in decreasing order with percentage compositions ranging from about 20-10%. The repeatability for all the TAGs in the oil ranged from 5-29 %RSD.

Hemp seed oil: 19 TAG species were identified and the most significant TAGs were C54:6, C54:7, C54:5and C55:5 in decreasing order with percentage compositions ranging from about 20-8%. The repeatability for all the TAGs in the oil ranged from 1-26 %RSD. Walnut oil and hemp seed oil had similar quantitative and qualitative TAG compositions.

Sesame oil: 15 TAG species were identified and the most significant TAGs were C54:5, C54:4, C54:3 and C54:6 in decreasing order with percentage compositions ranging from about 16-12%. The repeatability for all the TAGs in the oil ranged from 3-33 %RSD. The range of percentage compositions in sesame oil was very narrow and all of the high percentage TAGs were in the C54 TAG group.

Grape seed oil: 12 TAG species were identified and the most significant TAGs were C54:6, C54:5, C54:4 and C55:5 in decreasing order and ranging from about 30-10%. The repeatability for all the TAGs in the oil ranges from 5-39 %RSD.

Using the final TAG percentage compositions, the iodine values of the Bunge oil and edible oil samples were determined as presented in the following section.

4.2.4 Determination of Iodine Values of Oil Samples

The validity of the ESI/MS method was ultimately tested by the agreement of the measured iodine values with the calculated iodine values from the mass spectrometry data of the Bunge oil samples.

TAGs are often characterized by iodine values (or iodine numbers) which are the measures of the total unsaturations. The iodine value of a TAG is defined as the number of grams of iodine that are reacted with 100 grams of triacylglycerol [117, 118]. The higher the iodine value, the higher the number of double bonds in a given sample. The iodine value of a pure TAG can be calculated using equation 4.1 [119].

$$\text{Iodine value (IV)} = ((DOU) \times (MW\ I_2)/ (MW\ TAG))100 \qquad 4.1$$

Where, DOU and MW stand for "degrees of unsaturation" and "molecular weight", respectively. Thus the iodine value of an oil sample is the summation of the iodine values of the individual TAGs in the sample as shown in equation 4.2 [117, 119].

$$\text{Oil IV} = \sum ((DOU) \times (MW\ I_2) \times (\%TAG)/ (MW\ TAG))100 \qquad 4.2$$

Table 4.12 lists the calculated iodine values of the Bunge oil samples. The results were as expected in that an increase in degree of hydrogenation resulted in the decrease in degrees of unsaturation which was manifested in decreasing the iodine values for the successive partially hydrogenated oil samples.

Table 4.12 *Calculated iodine values (IVs) of each TAG ions and total iodine values of five Bunge oil samples based of MS.*

M/Z	TAG ID	CANOLA OIL			CA04			CA09			CA37			CA67		
		% comp	DOU	IV	% comp	DOU	IV	% comp	DOU	IV	% comp	DOU	IV	% comp	DOU	IV
860	C52:5	0.94	5	1.4												
862	C52:4	2.46	4	2.9												
864	C52:3	3.78	3	3.3	3.16	3	2.8	2.86	3	2.5	1.48	3	1.3			
866	C52:2	4.78	2	2.8	7.87	2	4.6	8.26	2	4.8	8.40	2	4.9	5.55	2	3.3
868	C52:1	0.32	1	0.1	0.59	1	0.2	0.98	1	0.3	2.55	1	0.7	2.95	1	0.9
870	C52:0													0.61	0	
882	C54:8	0.94	8	2.2												
884	C54:7	2.54	7	5.1												
886	C54:6	6.43	6	11.0	1.11	6	1.9									
888	C54:5	15.96	5	22.8	4.15	5	5.9	2.82	5	4.0						
890	C54:4	21.18	4	24.2	19.14	4	21.8	15.60	4	17.8	6.04	4	6.9	1.80	4	2.0
892	C54:3	29.64	3	25.3	51.62	3	44.1	51.78	3	44.2	49.27	3	42.1	37.26	3	31.8
894	C54:2	2.88	2	1.6	6.23	2	3.5	9.85	2	5.6	21.59	2	12.3	32.46	2	18.4
896	C54:1	0.82	1	0.2	1.13	1	0.3	1.72	1	0.5	4.23	1	1.2	10.45	1	3.0
898	C54:0							1.49	0		1.82	0		2.92	0	
916	C56:5	1.04	5	1.4												
918	C56:4	1.73	4	1.9												
920	C56:3	2.82	3	2.3	2.95	3	2.4	2.76	3	2.3	2.31	3	1.9	1.86	3	1.5
922	C56:2	1.75	2	1.0	2.06	2	1.1	1.89	2	1.0	2.31	2	1.3	2.59	2	1.4
924	C56:1													1.56	1	0.9
Calculated iodine values of oils				110			89			83			73			63

% comp = percentage composition; DOU = degrees of unsaturation; IV = iodine value.

Table 4.13 displays the calculated iodine values of the edible oil samples. The edible oil iodine values were usually given in a range in the literature, and the calculated iodine values were compared with the literature values as shown in Table 4.14. Olive oil, sesame oil and grape seed oil were in the ranges specified while hemp seed oil and walnut oil were not. It is worth to mention that these reported iodine values of the edible oils were not consistent as for example, different sources quoted different IVs for olive oil: 77-94 [120], 81 [121] and 75-94 [122] and for sesame oil: 110 [121] and 104-120 [122]. The reason for this wide range values could be due to the differences in the environmental factors i.e. climate conditions, degree of fruit ripening and time of harvesting [23-25] and possible adulteration of the oils which have significant effects on the chemical composition and quality of the edible oils [26-29]. Furthermore, the purity of the edible oils was not guaranteed as oil samples were obtained from local food stores as oppose to from quality assured laboratories.

Table 4.13 *Calculated iodine values (IVs) of each TAG ions and total iodine values of five edible oil samples based on MS data.*

m/z	TAG ID	SESAME OIL			HEMP SEED OIL			WALNUT OIL			GRAPE SEED OIL			OLIVE OIL		
		%	DOU	IV	% comp	DOU	IV	% comp	DOU	IV	% comp	DOU	IV	% comp	DOU	IV
838	C50:2													3.25	2	2.0
840	C50:1													5.18	1	1.6
860	C52:5				3.65	5	5.4	2.66	5	4.0	7.92	5	11.7	0.00	5	0.0
862	C52:4	6.05	4	7.1	6.28	4	7.0	6.37	4	7.3	3.73	4	4.1	2.82	4	3.3
864	C52:3	6.49	3	5.4	1.99	3	1.7	2.64	3	2.3	0.00	3	0.0	10.94	3	9.6
866	C52:2	4.42	2	2.5										20.24	2	11.9
868	C52:1															
876	C54:11				1.06	11	3.4	1.21	11	4.0						
878	C54:10	1.97	10	5.7	1.90	10	5.5	2.29	10	6.8						
880	C54:9	1.89	9	4.9	1.74	9	4.5	1.24	9	3.3						
882	C54:8	1.21	8	2.8	5.37	8	12.3	2.51	8	5.9						
884	C54:7	0.68	7	1.4	14.64	7	27.9	10.14	7	19.9						
886	C54:6	12.53	6	21.5	20.17	6	33.1	20.41	6	34.4	30.45	6	52.2			
888	C54:5	16.15	5	23.0	12.12	5	16.5	12.19	5	17.1	18.68	5	26.6	4.57	5	6.5
890	C54:4	14.18	4	16.1	6.49	4	7.5	6.27	4	7.5	11.99	4	13.6	14.06	4	16.0
892	C54:3	13.93	3	11.9	1.84	3	1.5	2.22	3	1.9	4.26	3	3.6	27.54	3	22.5
894	C54:2	3.08	2	1.7										3.86	2	2.2
896	C54:1															
898	C54:0															
900	C55:6				6.19	6	10.5	5.92	6	10.3	1.52	6	2.6			
902	C55:5				8.03	5	11.5	10.13	5	14.7	9.58	5	13.4			
904	C55:4	6.54	4	7.6	4.76	4	5.7	6.23	4	7.2	6.25	4	7.3			
906	C55:3	5.54	3	4.9	2.20	3	2.0	3.63	3	3.1	3.98	3	3.6	2.72	3	2.3
908	C55:2	5.35	2	3.1							1.64	2	0.9	4.83	2	2.7
926	C57:7				0.28	7	1.6	0.76	7	1.6						
928	C57:6				0.63	6	2.2	1.37	6	2.2						
930	C57:5				0.67	5	2.0	1.82	5	2.2						
Calculated iodine values				**120**			**162**			**156**			**136**			**82**

% comp = percentage composition; DOU = degrees of unsaturation; IV = iodine value.

Table 4.14 lists the literature and calculated iodine values from mass spectral data of commercial edible oils.

Table 4.14 *Literature and calculated iodine values from mass spectral data of edible oils.*

oils	Literature iodine values	Calculated Iodine values
Grape seed oil	(120-151) [123]	136
Olive oil	(77-94) [120], 81[121], (75-94) [122]	82
Sesame oil	110 [121], (104-120) [122]	120
Hemp seed oil	167 [124]	162
Walnut oil	150 [121]	156

4.2.4.1 Correlation of the Calculated and Measured Iodine Values of Bunge Oil Samples

The measured and calculated iodine values from mass spectral data of Bunge oil samples show an excellent correlation (see Table 4.15). The accuracy of the methodology was excellent with the average relative error of 1.6% for the five Bunge oil samples.

Table 4.15 *Measured iodine values (provided by Bunge Canada) and corresponding calculated iodine values from mass spectral data with % relative error of Bunge oil samples.*

Bunge oil samples	measured iodine values	calculated iodine values	%relative error
CA67	63	63	0
CA37	73	73	0
CA09	86	83	-3.5
CA04	89	89	0
Canola oil feedstock	115	110	-4.3

A plot of the calculated versus measured iodine values revealed a linear least squares line of best fit drawn through the data points providing a slope of 1.10 and correlation coefficient $R^2 = 0.995$ (Figure 4.8).
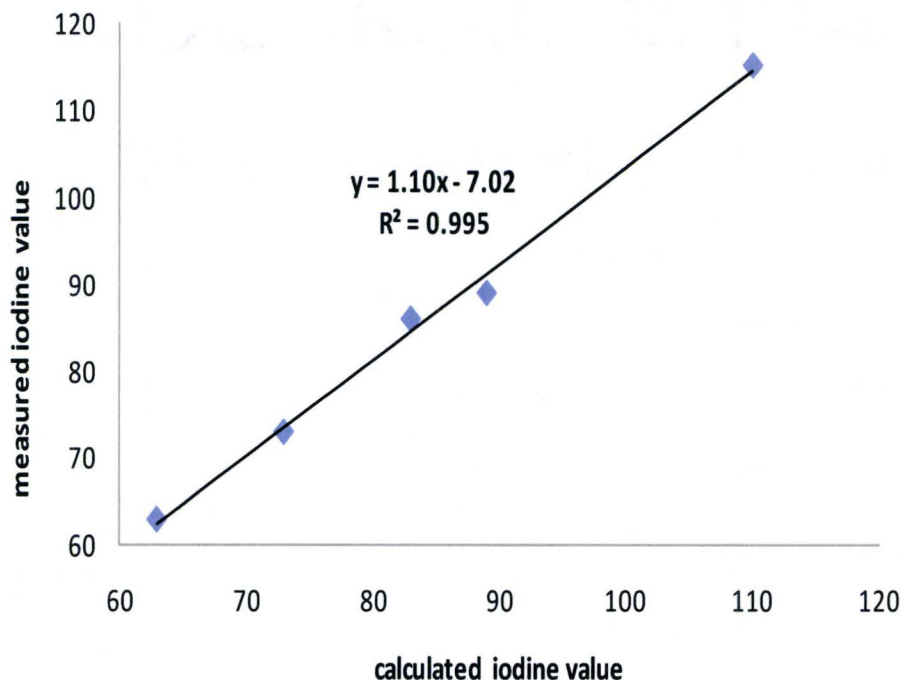
Figure 4.8 *Correlation plot of measured iodine values of Bunge oil samples versus calculated iodine values from mass spectral data.*

The validity of ESI/MS method in determining iodine values of oil samples was demonstrated. The MS method used a series of steps to correct the raw peak areas of the TAG components in order to get a better accuracy in the percentage compositions of the TAGs in the oil samples. The percentage TAG composition data was used to calculate iodine values of each TAG in particular and the oil sample in general. RRF correction had the greatest impact on the qunatitative determination of the TAG components, and on the other hand the LiCl adduct correction had the least effect.

In summary, the ESI/MS and ESI/MS/MS methodologies provided a rapid screening tool enabling the molecular mass identification, structural characterization and quantification of TAG species in oils without prior use of the time consuming and chromatographic step.

CONCLUSIONS AND FUTURE WORK

The quantitative and qualitative analysis of triacylglycerols in edible oils using direct infusion electrospray ionization mass spectrometry and tandem mass spectrometry has been demonstrated. The optimized method involves the infusion of an oil sample in chloroform-methanol (1:1) solution (~10-15 μg/mL of oil) in the presence of 0.5 mM LiCl which was found to be the optimal value. The raw peak areas of the lithiated molecular ions, $[M+Li]^+$, were converted to quantitative values using a sequence of correction factors to account for: (1) normalization of peak area data using three internal standards, (2) peak area contributions of M+2 isotopic peaks of TAGs with one more degree of unsaturation and (3) peak area contributions of LiCl adduct ions, $[M+Li+LiCl]^+$, when applicable. The fourth and the major correction factor involved application of the relative response factor (RRF) for that TAG. The RRFs for all TAGs containing between 48 and 63 carbons in their fatty acyl chains and between 0 and 9 degrees of unsaturation were extrapolated from experimentally determined response factors from a series of TAG standards. The RRFs were found to decrease linearly by 6.7% for each additional acyl chain carbon ($R^2 = 0.996$) but increased by 18.7% for each double bond. Comparison of these calculated RRFs to reported RRFs for a series of TAG standards [18] showed an excellent correlation (1.06% ± 10.20% RSD).

Relative response factors (RRFs) of the individual TAGs were used to calculate TAG percentage compositions and thereby used to determine the iodine values (IVs) of the oil samples. In this study, a linear least squares line of best fit with a slope of 1.10 and a correlation $R^2=0.995$ was obtained between the measured and calculated iodine

values for the Bunge oil samples. The iodine values of the edible oils were also calculated in the same manner and their values were compared to literature values. Olive, sesame and grape seed oils were in agreement with literature values whereas walnut and hemp oils were not. However, the literature IVs of the edible oils are not consistent in all sources, therefore the comparison lacks accuracy. To the best of our knowledge, it is the first time that a comprehensive quantitative approach that particularly encompasses RRF corrections, M+2 isotopic correction factors with the consideration of the isotopes that arise from the O, C and H elements and LiCl adduct correction factors have been applied in the analysis of "real" samples.

Product ion scan for the molecular mass identification and structural information of lithiated triacylglycerols in partially hydrogenated oil samples and edible vegetable oils was also demonstrated. Previous analytical techniques for the structural characterization of standard TAGs based on alkali metal adducts [19, 75, 93, 106] and ammonium adducts [75, 76] have been reported. However applications of these methods for complex TAG mixtures in oils have their own short comings entailed from the inability to separate isobaric and isomeric TAG components. In this study, the identification of the possible isobars of TAG molecular ion was determined by using the CID fragment ions that resulted from the neutral losses of the fatty acid substituents of the TAG species as fatty acids and lithium salt of the fatty acids. A logical combination of the identified fatty acids provided a basis to the affirmation of the possible isobaric ions existing in a given TAG molecular ion peak.

In conclusion, knowing the types and accurate amounts of TAGs in oil and biological samples has commercial, nutritional and diagnostic values as a result a reliable methodology is indispensible. ESI/MS method with tandem mass spectrometry has a great potential to be a rapid, robust and reliable routine technique for the identification and quantification of TAG mixture species and determination of IVs in oil samples. Another benefit of this methodology was simplicity and robustness. The sample preparation is simple and needs a single stage mass spectrometer for quantitative analysis without the need for an expensive triple quad mass spectrometer. Therefore, we envision that our simplistic model could easily be adopted and used to determine the structural identification and quantification of sample TAGs in a high throughput environment of industrial and clinical laboratories. However, this method has an inherent limitation in which isobaric and positional isomer TAGs are not differentiated; although, using the tandem mass spectrometer analyzer the possible structure of the isobaric TAGs is determined. To that end a research work is required in the future.

6. REFERENCES

[1] C. Dass. 2001. *Principles and Practice of Biological Mass Spectrometry*. John Wiley, New York, USA.

[2] A. J. Furth. 1980. *Lipids and Polysaccharides in Biology*. Edward Arnold, London, U.K.

[3] http://www.iseo.org 2006. Food Fats and Oils. 9th ed. Washington, D.C.

[4] http://lipidlibrary.aocs.org/Lipids/tag1/index.htm

[5] N. K. Andrikopoulos, A. Chiou, A. Mylona. 2004. Triacylglycerol species of less common edible vegetable oils. Food Rev. Int., **20**:389-405.

[6] http://www.natural-health-information-centre.com/hydrogenated-fats.html

[7] N. K. Andrikopoulos. 2000. Triacylglyceride species composition of common edible vegetable oils and methods used for their identification and quantification. Food Rev. Intl. **18**:71-102.

[8] K. Larsson. 1986. Physical Properties-Structural and Physical Characteristics, in The *Lipid Handbook*. F. D. Gunstone, J. L. Hawood, F. B. Padle, eds., Chapman and Hall, London, U.K, 321-384.

[9] M. I. Gurr, A. T. James. 1975. *Lipid Biochemistry: An Introduction*. 2nd ed., John Wiley, New York, USA.

[10] W. W. Christie. 1982. *Lipid Analysis*. 2nd ed., Pergamon Press, Oxford, England.

[11] R. P. Evershed. 1994. Application of modern mass spectrometric techniques to the analysis of lipids, in *Developments in the Analysis of Lipids*. J. H. P. Tyman, M. H. Gordon, eds., The Royal Society of Chemistry, Cambridge, U.K.

[12] http://www.nutristrategy.com/nutrition/calories.html

[13] A. Valenzuela, N. Morgado. 1999. *Trans* fatty acid isomers in human health and in the food industry. Biol. Res. **32**:273-287.

[14] http://www.cem.msu.edu/~reusch/VirtualText/lipids.htm

[15] http://www.ext.colostate.edu/pubs/foodnut/09315.html

[16] D. F. Horrobin. 1992. Nutritional and medical importance of gamma-linolenic acid. Prog. Lipid Res., **31**:163-194.

[17] A. Grandgirard, J. M. Bourre, F. Julliard, P. Homayoun, O. Dumont, M. Piciotti, J. L. Sebedio. 1994. Incorporation of trans long-chain n-3 ployunsaturated fatty acids in rat brain structures and retina. Lipids, **24**:251-258.

[18] X. Han, R. W. Gross. 2001. Quantitative analysis and molecular species fingerprinting of triacylglycerol molecular species directly from lipid extracts of biological samples by electrospray ionization tandem mass spectrometry. Analytical Biochemistry, **295**:88-100.

[19] A. M. McAnoy, C. C. Wu, R. C. Murphy. 2005. Direct qualitative Analysis of triacylglycerols by electrospray mass spectrometry using a linear ion trap. J. Am. Soc. Spectrom., **16**:1498-1509.

[20] P. Kallo, A. Kemppinen, V. Ollilainen. 2009. Determination of triacylglycerols in butterfat by normal-phase HPLC and electrospray-tandem mass spectrometry. Lipids, **44**:169-195.

[21] S. C. Cunha, M. B. P. P. Oliveira. 2006. Discrimination of vegetable oils by triacylglycerols evaluation of profile using HPLC/ELSD. Food Chemistry, **95**:518-524.

[22] S. D Segall, W. E. Artz, D. S. Raslan, G. N. Jham, J. A. Takahashi. 2005. Triacylglycerol composition of coffee beans (coffea canephora p.) by reversed phase liquid chromatography and positive electrospray tandem mass spectroscopy. J. Agric. Food. Chem., **53**:9650-9655.

[23] M. J. Lerma-Garcia, J. M. Herrero-Martinez, G. Ramis-Ramos, E. F. Simo-Alfonso. 2008. Evaluation of the quality of olive oil using fatty acid profiles by direct infusion electrospray ionization mass spectrometry. Food Chemistry, **107**:1307-1313.

[24] M. D. Salvador, F. Aranda, S. Gomez-Alonso, G. Fregapane. 2003. Influence of extraction system, production year and area on Cornicabra virgin olive oil: A study of five crop seasons. Food Chemistry, **80**:359-366.

[25] M. M. Torres, D. M. Maestri. 2006. The effect of genotype and extraction methods of chemical composition of virgin oils from Traslasierra Valley (Cordoba, Argentina). Food Chemistry, **96**:507-511.

[26] Z. Wu, R. P. Rodgers, A. G. Marshall. 2004. Characterization of vegetable oils: Detailed compositional fingerprints derived from electrospray ionization fourier transform ion cyclotron resonance mass spectrometry. Food Chemistry, **52**:5322-5328.

[27] J. B. Rossell. 1994. Purity criteria in edible oils and fats, in *Developments in the Analysis of Lipids*. J. H. P. Gordon, ed., The Royal Society of Chemistry, Cambridge, U.K.

[28] A. K. Shukla, A. K. Dixit, R. P. Singh. 2005. Detection of adulteration in edible oils. J. Oleo. Sci., **54**:317-324.

[29] R. R. Catharino, R. Haddad, L. G. Cabrini, I. B. S. Cunha, A. C. H. F. Sawaya, M. N. Eberlin. 2005. Characterization of vegetable oils by electrospray ionization mass spectrometery finger printing: classification, quality adulteration and aging. Anal. Chem., **77**:7429-7433.

[30] V. K. S. Shukla. 2003. A designer oil for a better health. INFORM, **14**:340-341.

[31] E. W. Hammond. 1994. Physical, chemical and chromatographic methods for the analysis of symmetrical triacylglycerols- analytical application to an understanding of cocoa butter performance, in *Developments in the Analysis of Lipids*. J. H. P. Gordon, ed., The Royal Society of Chemistry, Cambridge, U.K.

[32] E. Geeraert, P. Sandra. 1984. On the potential of CGC in triacylglycerides analysis. J. High Resol. Chromatogr., **7**:431-432.

[33] E. Geeraert, P. Sandra. 1987. Capillary GC of triglycerides in fats and oils using a high temperature phenylmethylsilicone stationary phase. PART II. The analysis of chocolate fats. J. Am. Oil Chem. Soc., **64**:100-105.

[34] T. Rezanka, P. Mares. 1991. Determination of plant triglycerols using capillary gas chromatography, high performance liquid chromatography and mass spectrometry. J. Chromatogr., **542**:145-159.

[35] A. Kemppinen, P. Kallo. 2006. Quantification of triacylglycerols in butterfat by gas chromatography-electron impact mass spectrometry using molar correction factors for [M-RCOO]$^+$ ions. J. Chromatogr. A, **1134**:260-283.

[36] M. Hermansson, A. Uphoff, R. Kakela, P. Somerharju. 2005. Automated quantitative analysis of complex lipidomes by liquid chromatography/mass spectrometry. Anal. Chem., **77**:2166-2175.

[37] R. D. Plattner. 1981. High performance liquid chromatography of triglycerides: controlling selectivity with reverse phase columns. J. Am. Oil Chem. Soc., **58**:638-664.

[38] K. Aitzetmuller. 1982. Recent progress in the high performance liquid chromatography of lipids. Prog. Lipid Res., **21**:171-193.

[39] V. K. S. Shukla. 1988. Recent advances in the high performance liquid chromatography of lipds. Prog. Lipid Res., **27**:5-38.

[40] A. A Carelli, A. Cert. 1993. Comparative study of the dertermination of triacylglycerol in vegetable oils using chromatographic techniques. J. Chromatogr., **630**:213-222.

[41] S. Thurnhoter, W. Vetter, A gas chromatography/electron ionization-mass spectrometry-selected ion monitoring method for determining fatty acid pattern in food after formation of fatty acid methyl esters. J. Agric. Food Chem., **53**:8896-8903.

[42] V. Ruiz-Gutierrez, L. J. R. Barron. 1995. Methods for the analysis of triacylglycerols. J. Chromatogr., **671**:133-168.

[43] W. W. Christie. 2003. *Lipid Analysis. Isolation, Separation, Identification and Structural Analysis of Lipids.* 3rd ed., The Oily Press, Bridgewater, England.

[44] J. S. Buckner, W. P. Kemp, J. Bosch. 2004. Characterization of triacylglycerols from overwintering prepupae of the alfalfa pollinator *megachile rotundata* (hymenoptera: megachilidae). Archives of Insect Biochemistry and Physiology, **57**:1-14.

[45] I. Brondz. 2002. Development of fatty acid analysis by high-performance liquid chromatography, gas chromatography and related techniques. Anal. Chim. Acta, **465**:1-37.

[46] G. N. Jham, M. A. Berhow, L. K. Manthey, D. A. Palmquist, S. F. Vaughn. 2008. The use of fatty acid profile as a potential maker for Brazilian coffee (coffee arabica L.) for corn adultration. J. Braz. Chem. Soc., **19**:1462-1467.

[47] A. L. Bailley, S. Southon. 1998. Determination of total long chain fatty acids in human plasma and lipoproteins, before and during copper stimulated oxidation, by high performance liquid chromatography. Anal. Chem., **70**:415-419.

[48] S. d. Koning, H. G. Janssen, U. A. Th. Brinkman. 2006. Characterization of triacylglycerides from edible oils and fats using single and multidimensional techniques. LCGC Europe, **19**, issue 11, www.chromatographyonline.com.

[49] R. Ryhage, E. Stenhagen. 1960. Mass spectrometry in lipid research. J. Lipid Res., **1**:361-390.

[50] N. K. Andrikopoulos. 2002. Chromatographic and spectroscopic methods in the analysis of triacylglycerol species and regiospecific isomers of oils and fats. Crit. Rev. Food Sci. Nutr., **42**:473-505.

[51] P. Mares. 1988. High temperature capillary gas liquid chromatography of triacylglycerol and other intact lipids. Prog. Lipid Res., **27**:107-133.

[52] J. Parcerisa, J. Boatella, R. Codony, M. Rafecas, A. I. Castellote, J. Gracia, A. Lopez, A. Romero. 1995. Comparison of fatty acid and triacylglycerol composition of different hazelnut varieties (corylus avellana L.) cultivated in Catalonia (Spain). J. Agric. Food Chem., **43**:13-16.

[53] R. D. Plattner, K. Paya-Wahl. 1978. Separation of triacylglycerides by chain length and degree of unsaturation on silica HPLC columns. Lipids, **14**:152-153.

[54] H. Y. Kim, N. Salem, Jr. 1993. Liquid chromatography-mass spectrometry of lipids. Prog. Lipid Res. **32**:221-245.

[55] H. R. Mottram, R. P. Evershed. 2001. Elucidation of the composition of bovine milk fat triacylglycerols using high-performance liquid chromatography-atmospheric pressure chemical ionization mass spectrometry. J. Chromatogr., **926**:239-253.

[56] S. D. Segall, W. E. Artz, D. S. Rasian, V. P. Ferraz, J. A. Takahashi. 2004. Analysis of triacylglycerol isomers in Malaysian cocoa butter using HPLC-mass spectrometry. Food Res. Int., **38**:167-174.

[57] W. E. Neff, W. C. Byrdwell. 1995. Triacylglycerol analysis by high performance liquid chromatography-atmospheric chemical ionization mass spectrometry: crepis alpine and Veronia glamensis seed oil. J. Liq. Chromatogr. **18**:4165-4181.

[58] P. Laakso, P. Voutilainen. 1996. Analysis of triacyglycerols by silver ion high performance liquid chromatography-atmospheric pressure chemical ionization mass spectrometry. Lipids, **31**:1311-1322.

[59] http://www.waters.com/waters/nav.htm?cid=10125009

[60] (http://www.phenomenex.com/cms400min/kinetex.aspx)

[61] W. M. A. Hax, W. S. M Guurts van Kessel. 1977. High performance liquid chromatography separation and photometric detection of phospholipids. J. Chromatogr., **142**:735-741.

[62] F. B. Jungalwala, J. E. Evans, R. H. McCluer. 1976. High performance liquid chromatography of phosphatidylcholine and sphingomyelin with detection in the region of 200nm. J. Biochem., **155**:55-60.

[63] G. N. Jham, R. Velikova, B. Nikolovo-Damyavova, S. C. Rabelo, J. C. T. Silva, K.A. P. Souza, V. M. M. Valente, P. R. Cecon. 2005. Preparative silver ion TLC/RP-

HPLC determination of coffee triacylglycerol molecular species. Food Res. Int., **38**:21-126.

[64] R. Rombaut, N. D. Clercq, I. Foubert, K. Dewettinck. 2009. Triacylglycerol analysis of fats and oils by evaporative light scattering detection. J. Am. Oil Chem. Soc., **86**:19-25.

[65] S. D. Segall, W. E. Artz, D. S. Raslan, V. P. Ferraz, J. A. Takahashi. 2006. Triacylglycerol analysis of pequi (caryocar brasiliensis camb.) oil by electrospray and tandem mass spectrometery. J. Sci. Food Agric, **86**:445-452.

[66] S. S. Cai, J. A. Syage. 2006. Comparison of atmospheric pressure photoionization, atmospheric pressure chemical ionization and electrospray ionization mass spectrometry for analysis of lipids. Anal. Chem., **78**:1191-1199.

[67] B. M. Ham, J. T. Jacob, M. M. Keese, R. B. Cole. 2004. Identification, quantification and comparison of major non polar lipids in normal and dry eye tear lipidomes by electrospray tandem mass spectrometry. J. Mass Spectrom., **39**:1321-1336.

[68] S. de Koning, H. G. Janssen, M. Van Deursen. U. A. Th. Brinkman. 2004. Automated on-line comprehensive two-dimensional LCXGC-ToF MS instrument design and application to edible oil and fat analysis. J. Sep. Sci., **27**:397-409.

[69] H. G. Janssen, S. de Koning, U.A. Th. Brinkman. 2004. On-line LC-GC and comprehensive two-dimensional LCXGC-ToF MS for the analysis of complex samples. Anal. Bioanal. Chem., **378**:1944-1947.

[70] M. de. Murbuker, L. G. Blomberg, N. U. Olsson, M. Bergqvist, B. G. Herslof, F. A. Jacobs. 1992. Characterization of triacylglycerols in the seed of *Aquilegia vulgaris* by chromatographic and mass spectrometric methods. Lipids, **27**:436-441.

[71].M. Hori, Y. Sahashi, S. Koike, R. Yamaoka, M. Sago. 1994. Molecular species analysis of polyunsaturated fish triacylglycerol by high-performance liquid chromatography/ fast atom bombardment mass spectrometry. Anal. Sci., **10**:719-724.

[72] M. Lamberto, M. Saitta. 1995. Principal component analysis in fast atom bombardment-mass spectrometry of triacylglycerols in edible oils. J. Am. Oil Chem. Soc., **72**:867-871.

[73] W. C. Byrdwell, W. E. Neff. 1996. Analysis of genetically modified canola varieties by atmospheric pressure chemical ionization mass spectrometric and flame ionization detection. J. Liq. Chromatogr., **19**:2203-2225.

[74] W. C. Byrdwell, E. A. Emken, W. E. Neff, R. O. Adolf. 1996. Quantiative analysis of triacylglycerides using atmospheric pressure chemical ionization-mass spectrometry. Lipids, **31**:919-935.

[75] K.L. Duffin, J. D. Henion. 1991. Electrospray and tandem mass spectrometric characterization of acyglycerol mixtures that are dissolved in non polar solvents. Anal. Chem., **63**:1781-1788.

[76] C. Cheng, M. L. Gross, E. Pittenauer. 1998. Complete structural elucidation of triacylglycerols by tandem mass spectrometry. Anal Chem., **70**:4417-4426.

[77] R. B. Cody. 2002. Electrospray ionization mass spectrometry: history, theory and instrumentation, in *Applied Electrospray Mass Spectrometry*. B. N. Pramanik, A. K. Ganguly, M. L. Gross, eds., Marcel Dekker Inc., New York, USA.

[78] M. Dole, L. L. Mack, R. L. Hines, R. C. Mobley, L. D. Ferguson, M. A. Alice. 1968. Molecular beams of macroions. J. Chem. Phys., **49**:2240-2249.

[79] M Yamashita, J. B. Fenn. 1984. Electrospray ion source-another variation on the free-jet theme. J. Phys. Chem., **88**:4451-4459.

[80] G. Siuzdak. 2003. The Expanding Role of Mass Spectrometry in Biotechnology. MCC Press, San Diego, USA.

[81] A. D. Postel. 2006. Electrospray mass spectrometry of lipids. Lipid Technology, **18**:181-185.

[82] S. J. Gaskell. 1997. Electrospray: principles and practice. J. Mass Spectrom. **32**:677-688.

[83] X. Han, R. W. Gross. 2005. Shotgun lipidomics: Electrospray ionization mass spectrometric analysis and quantitation of cellular lipodomes directly from crude extracts of biological samples. Mass Spectrom. Rev., **24**:367-412.

[84] X. Han, R. W. Gross. 2003. Global analysis of cellular lipodomes directly from crude extracts of biological samples by ESI mass spectrometry: A bridge to lipodomics. J. Lipid Res., **44**:1071-1079.

[85] C. A. Schalley, A. Springer. 2009. *Mass Spectrometry and Gas-Phase Chemistry of Non-Covalent Complexes*. John Wiley, New Jersey, USA.

[86] M. Mann. 1990. Electrospray mass spectrometry, in *Mass Spectrometry in the Biological Sciences: A Tutorial*. M. L. Gross, ed., Kluwer Academic Publishers, London, U.K.

[87] R. D. Smith, K. J. Light-Wahl. 1993. The observation of non covalent interaction in solution by electrospray ionization mass spectrometry: promise, pitfalls and prognosis. Bio. Mass Spectrom., **22**:493-501.

[88] J. V. Iribarne, B. A. Thomson. 1976. On the evaporation of small ions from charged droplets. Journal of Chemical Physics, **64**:2287-2294.

[89] A. H. Payne, G. L. Glish. 2005. Tandem mass spectrometry in quadrupole ion trap and ion cyclotron resonance mass spectrometers, in *Methods in Enzymology Vol 402 Biological Mass Spectrometry*. A. L. Burlingame, ed., Elsevier Inc., San Diego, USA.

[90] R.A.Yost, C. G. Enke. 1978. Selected ion fragmentation with a tandem quadrupole mass spectrometer. J. Am. Soc. Mass. Spectrom., **100**:2274-2275.

[91] V. H. Wysocki. 1990. Triple quadrupole mass spectrometry, in *Mass Spectrometry in the Biological Sciences: A Tutorial*. M. L. Gross, ed., Kluwer Academic Publishers, London, U.K.

[92] A. Somogyi. 2008. Mass spectrometry instrumentation and techniques, in *Medical Applications of Mass Spectrometry*. K. Vekey, A. Telekes, A. Vertes, ed., Elsevier, Amsterdam, The Netherlands.

[93] F. F. Hsu, J. Turk. 1999. Structural characterization of triacylglycerols as lithiated adducts by electrospray ionization mass spectrometry using low energy collisionally activated dissociation on a triple stage quadrupole instrument. J. Am. Soc. Mass Spectrom., **10**:587-599.

[94] W. J. Griffiths. 2003. Tandem mass spectrometry in the study of fatty acids, bile acids and steroids. Mass Spectrom. Rev., **22**:81-152.

[95] R. C. Murphy, J. Fiedler, J. Hevko. 2001. Analysis of nonvolatile lipids by mass spectrometry. Chem. Rev., **101**:479-526.

[96] R. Welti, J. Shah, W. Li, M. Li, J. Chen, J. J. Burke, M. L. Fauconnier, K. Chapman, M. L. Chye, X. Wang. 2007. Plant lipidomics: discerning biological functions by profiling plant complex lipids using mass spectrometry. Frontiers in Bioscience, **12**:2494-2506.

[97] H. Song, J. Ladenson, J. Turk. 2008. Algorithms for automatic processing of data from mass spectrometric analyses of lipids. J. Chromatogr., **877**:2847-2854.

[98] W. W. Christie. 2009. Lipidomics-a personal view. Lipid Technology, **21**:58-60.

[99] X. Han, R. W. Gross. 2008. New development in multidimensional mass spectrometry-based shotgun lipidomics, in *Metabolomics, Metabonomics and Metabolite Profiling*. W. J. Griffiths, ed., Thomas Graham House, Cambridge, U.K.

[100] K. Yang, H. Cheng, R. W. Gross, X. Han. 2009. Automated lipid identification and quantitation by multidimensional mass spectrometry-based shotgun lipidomics. Anal. Chem., **81**:4356-4368.

[101] X. Han, A. R. Abendschein, J. G. Kelley, R. W. Gross. 2000. Diabetes-induced changes in specific lipid molecular species in rat myocardium. J. Biol. Chem., **352**:79-89.

[102] E. Hvattum. 2001. Analysis of triacylglycerols with non-aqueous reversed phase liqiuid chromatography and positive ion electrospray tandem mass spectrometry. Rapid Commun. Mass Spectrom., **15**:187-190.

[103] J. Adams, M. L. Gross. 1987. Tandem mass spectrometry for collisional activation of alkali-metal-cationized fatty acids: A method for determining double bond location. Anal. Chem., **59**:1576-1582.

[104] J. E. Del. Bene. 1979. A molecular orbital study of lithium ion association with bases. I. The carbonyl bases R_2CO. Chem. Phys., **40**:329-335.

[105] A. Qinghong, J. Adams. 1993. Structure-specific collision-induced fragmentations of ceremides cationized with alkali-metal ions.Anal. Chem., **65**:7-13.

[106] S. D. Segall, W. E. Artz, D. S. Rasian, V. P. Ferraz, J. A. Takahashi. 2004. Ouricuri (syagrus coronata) TAG analysis using HPLC and positive ion electrospray tandem MS. J. Am. Oil Chem. Soc., **81**:143-149.

[107] H. L. Callender, J. S. Forrester, P. Ivanova, A. Preininger, S. Milne, H. A. Brown. 2007. Quantification of diacylglycerol species from cellular extracts by electrospray ionization mass spectrometry using a linear regression algorithm. Anal. Chem., **79**:263-272.

[108] A. Zacarias, D. Bolanowski, A. Bhatnagar. 2002. Comparative measurements of multicomponent phospholipid mixtures by electrospray mass spectroscopy: Relating ion intensity to concentration. Anal. Biochem., **308**:152-159.

[109] U. Sommer, H. Herscouitz, F. K. Welty, C. E. Castello. 2006. LC-MS based method for qualitative and quantitative analysis of complex lipid mixtures. J. Lipid Res., **47**:804-814.

[110] A. Uphoff, M. Hermanson, P. Haimi, P. Somerharju. 2008. Analysis of complex lipidomes, in *Medical Applications of Mass Spectrometry*. K. Vekey, A. Telekes, A. Vertes, eds., Jordan Hill, Oxford, U.K.

[111] P. Kallo, A. Kemppinen, V. Ollilainen, A. Kuksis. 2004. Regiospecific determination of short-chain triacylglycerols in butterfat by normal-phase HPLC with on-line electrospray-tandem mass spectrometry. Lipids, **39**:915-928.

[112] L. A. Marzilli, L. B. Fay, F. Dionisi, P. Vouros. 2003. Structural characterization of triacylglycerols using electrospray ionization-MS^n ion trap MS. J. Am. Oil Chem. Soc., **80**:195-202.

[113] H. Kallio, K. Y. Jokipii, J. P. Kurvinen, O. Sjovall, R. Tahvonen. 2001. Regioisomerism of triacylglycerols in lard, tallow, yolk, chicken skin, palm oil, palm olein, palm stearin, and a transesterified blend of palm stearin and coconut oil analyzed by tandem mass spectrometry. J. Agric. Food Chem., **49**:3363-3369.

[114] J. P. Kurvinen, H. Mu, H. Kallio, X. Xu, C. E. Hoy. 2001. Regioisomers of octanoic acid-containing structured triacylglycerols analyzed by tandem mass spectrometry using ammonia negative ion chemical ionization. Lipids, **36**:1377-1382.

[115] M. Jie, J. Mustafa. 1997. High resolution nuclear magnetic resonance spectroscopy-application to fatty acids and triacylglycerols. Lipids, **32**:1019-1034.

[116] A. Manz, N. Pamme, D. Iossifidis. 2004. *Bioanalytical Chemistry*. Imperial College Press, London, U.K.

[117] http://www.righthealth.com/topic/iodine-value

[118] F. Mozayeni, G. Szajer, M. Walters. 1996. Determination of iodine value without chlorinated solvents. JAOCS, **73**:519-522.

[119] G. Knothe. 2002. Structural indices in FA chemistry. How relevant is iodine value? JAOCS, **79**:847-854.

[120] http://www.journeytoforever.org/biodiesel_yield.html

[121] http://www.natural-skincare-made-easy.org/iodine-value.html

[122] http://vegburner.co.uk/oils.htm

[123] http://www.alibaba.com/product-tp/101274646/Refined_Grape_Seed_Oil.html

[124] http://www.hemptraders.com/properties_of_hemp_analysis.php

7. APPENDICES

Appendix 1

Sample Spreadsheet for Calculation of Percentage Compositions of Triacylglycerols in Bunge Canola Feedstock Oil

Sample

The spreadsheet shows uncorrected mass spectral peak areas for five infusions. All peak areas in sample were isotopically corrected and normalized using C51:0 and C57:0 TAG standards (co-infused).The mean normalized peak areas (n=5) were calculated and then divided by the relative response factors for the TAGs to give an RRF-normalized values for each TAG. Using these data a percentage composition was calculated.

Canola oil feedstock (Bunge Canada)

TAG ID	m/z	Analysis 1			Analysis 2			Analysis 3			Analysis 4			Analysis 5			AVE NORM	STD	%RSD	RRF	RRF NORM	%COMP
		AREA1	IC1	NORM1	AREA2	IC2	NORM2	AREA3	IC3	NORM3	AREA4	IC4	NORM4	AREA5	IC5	NORM5						
C51:0	856	2.E+06			2.E+06			2.E+06			2.E+06			2.E+06								
C52:5	860	4.E+05	4.E+05	0.19	4.E+05	4.E+05	0.20	4.E+05	4.E+05	0.19	4.E+05	4.E+05	0.19	4.E+05	4.E+05	0.20	0.19	0.01	3.0	2.24	0.09	0.94
C52:4	862	1.E+06	9.E+05	0.46	1.E+06	1.E+06	0.47	1.E+06	1.E+06	0.46	1.E+06	9.E+05	0.45	1.E+06	1.E+06	0.46	0.46	0.01	1.9	2.05	0.22	2.46
C52:3	864	1.E+06	1.E+06	0.62	2.E+06	1.E+06	0.64	2.E+06	1.E+06	0.64	1.E+06	1.E+06	0.64	2.E+06	1.E+06	0.66	0.64	0.02	2.5	1.86	0.34	3.78
C52:2	866	2.E+06	1.E+06	0.71	2.E+06	2.E+06	0.74	2.E+06	2.E+06	0.72	2.E+06	1.E+06	0.74	2.E+06	2.E+06	0.74	0.73	0.01	1.5	1.67	0.44	4.78
C52:1	868	4.E+05	9.E+04	0.05	4.E+05	9.E+04	0.04	4.E+05	1.E+05	0.05	4.E+05	8.E+04	0.04	4.E+05	1.E+05	0.05	0.04	0.00	8.7	1.49	0.03	0.32
C54:8	882	4.E+05	4.E+05	0.25	4.E+05	4.E+05	0.24	4.E+05	4.E+05	0.21	4.E+05	4.E+05	0.23	4.E+05	4.E+05	0.22	0.23	0.02	6.9	2.68	0.09	0.94
C54:7	884	1.E+06	1.E+06	0.60	1.E+06	1.E+06	0.58	1.E+06	1.E+06	0.56	1.E+06	1.E+06	0.58	1.E+06	1.E+06	0.56	0.58	0.02	2.7	2.49	0.23	2.54
C54:6	886	2.E+06	2.E+06	1.36	3.E+06	2.E+06	1.37	3.E+06	3.E+06	1.33	2.E+06	2.E+06	1.36	3.E+06	3.E+06	1.33	1.35	0.02	1.5	2.30	0.59	6.43
C54:5	888	6.E+06	5.E+06	3.04	6.E+06	6.E+06	3.13	7.E+06	6.E+06	3.04	6.E+06	5.E+06	3.07	6.E+06	6.E+06	3.11	3.08	0.04	1.3	2.12	1.46	15.96
C54:4	890	7.E+06	6.E+06	3.65	8.E+06	7.E+06	3.77	9.E+06	7.E+06	3.70	7.E+06	6.E+06	3.76	8.E+06	7.E+06	3.75	3.72	0.05	1.3	1.93	1.93	21.18
C54:3	892	9.E+06	8.E+06	4.66	1.E+07	8.E+06	4.79	1.E+07	9.E+06	4.70	9.E+06	8.E+06	4.71	1.E+07	9.E+06	4.67	4.71	0.05	1.2	1.74	2.70	29.64
C54:2	894	2.E+06	7.E+05	0.40	2.E+06	7.E+05	0.40	3.E+06	8.E+05	0.40	2.E+06	7.E+05	0.43	3.E+06	8.E+05	0.41	0.41	0.01	2.9	1.55	0.26	2.88
C54:1	896	3.E+05	2.E+05	0.11	3.E+05	2.E+05	0.10	4.E+05	2.E+05	0.10	3.E+05	2.E+05	0.10	4.E+05	2.E+05	0.10	0.10	0.01	4.9	1.37	0.08	0.82
C56:5	916	3.E+05	3.E+05	0.19	3.E+05	3.E+05	0.19	4.E+05	4.E+05	0.18	3.E+05	3.E+05	0.20	4.E+05	4.E+05	0.19	0.19	0.01	3.2	2.00	0.09	1.04
C56:4	918	6.E+05	5.E+05	0.29	6.E+05	5.E+05	0.29	6.E+05	5.E+05	0.27	6.E+05	5.E+05	0.29	6.E+05	5.E+05	0.28	0.28	0.01	2.9	1.81	0.16	1.73
C56:3	920	8.E+05	7.E+05	0.43	8.E+05	7.E+05	0.42	9.E+05	8.E+05	0.41	8.E+05	7.E+05	0.42	9.E+05	8.E+05	0.42	0.42	0.01	1.9	1.62	0.26	2.82
C56:2	922	6.E+05	4.E+05	0.24	6.E+05	4.E+05	0.23	6.E+05	4.E+05	0.22	5.E+05	4.E+05	0.23	6.E+05	4.E+05	0.22	0.23	0.01	4.6	1.43	0.16	1.75
C57:0	940	2.E+06			2.E+06			2.E+06			2.E+06			2.E+06								

Total=9.12

TAG ID: triacylglycerol identification

AREA#: uncorrected peak areas of TAGs in sample analyses (1-5).

IC#: isotopically corrected peak areas of TAGs in sample runs number 1-5.

NORM#: normalized peak areas using isotopically corrected peak area of TAGs in sample runs 1-5.

AVE NORM: isotopically corrected and internal standard normalized mean peak area (n=5)

STD: standard deviation (n=5)

%RSD: percent relative standard deviation (n=5)

RRF: relative response factor of TAGs

RRF NORM: RRF normalized peak area (from AVE. NORM peak areas)

% COMP: percentage composition of each TAG in the sample

C51:0 and C57:0 are internal standards used to normalize the peak areas of the TAGs (shown in bold face type)

Total = the sum of the RRF NORM

Appendix 2

Calculation of Percentage Compositions of Triacylglycerols in Five Bunge Oil Samples

The spreadsheets show the last six columns as shown in Appendix 1 (AVE NORM, STD, (%RSD), RRF, RRF NORM and % COMP) in the five Bunge oil samples (canola feed stock, CA04, CA09, CA37 and CA67).

Canola oil feed stock (Bunge Canada)

TAG ID	m/z	1	2	3	4	5	6
C51:0	**856**						
C52:5	860	0.19	0.0057	3.0	2.24	0.09	0.94
C52:4	862	0.46	0.0086	1.9	2.05	0.22	2.46
C52:3	864	0.64	0.016	2.5	1.86	0.34	3.78
C52:2	866	0.73	0.011	1.5	1.67	0.44	4.78
C52:1	868	0.04	0.0038	8.7	1.49	0.03	0.32
C54:8	882	0.23	0.016	6.9	2.68	0.09	0.94
C54:7	884	0.58	0.016	2.7	2.49	0.23	2.54
C54:6	886	1.35	0.020	1.5	2.30	0.59	6.43
C54:5	888	3.08	0.041	1.3	2.12	1.46	15.96
C54:4	890	3.72	0.050	1.3	1.93	1.93	21.18
C54:3	892	4.71	0.054	1.2	1.74	2.70	29.64
C54:2	894	0.41	0.012	2.9	1.55	0.26	2.88
C54:1	896	0.10	0.051	4.9	1.37	0.08	0.82
C56:5	916	0.19	0.0060	3.2	2.00	0.09	1.04
C56:4	918	0.28	0.0083	2.9	1.81	0.16	1.73
C56:3	920	0.42	0.0078	1.9	1.62	0.26	2.82
C56:2	922	0.23	0.011	4.6	1.43	0.16	1.75
C57:0	**940**						
					Total=9.12		

1 = AVE NORM: isotopically corrected and internal standard normalized mean peak area (n=5)

2 = STD: standard deviation (n=5)

3 = %RSD: percent relative standard deviation (n=5)

4 = RRF: relative response factor of TAGs

5 = RRF NORM: RRF normalized peak area

6 =% COMP: percentage composition of each TAG in the sample

CA04

TAG ID	m/z	1	2	3	4	5	6
C51:0	**856**						
C52:3	864	0.56	0.019	3.4	1.86	0.30	3.16
C52:2	866	1.25	0.028	2.2	1.67	0.75	7.87
C52:1	868	0.08	0.0055	6.7	1.49	0.06	0.59
C54:6	886	0.24	0.016	6.4	2.30	0.11	1.11
C54:5	888	0.83	0.032	3.9	2.12	0.39	4.15
C54:4	890	3.49	0.16	4.5	1.93	1.81	19.14
C54:3	892	8.51	0.38	4.4	1.74	4.89	51.62
C54:2	894	0.92	0.041	4.5	1.55	0.59	6.23
C54:1	896	0.15	0.0044	3.0	1.37	0.11	1.13
C56:3	920	0.45	0.0157	3.5	1.62	0.28	2.95
C56:2	922	0.28	0.061	21.8	1.43	0.19	2.06
C57:0	**940**						
						Total=9.47	

CA09

TAG ID	m/z	1	2	3	4	5	6
C51:0	**856**						
C52:3	864	0.50	0.021	4.1	1.86	0.27	2.86
C52:2	866	1.30	0.066	5.0	1.67	0.78	8.26
C52:1	868	0.14	0.0050	3.7	1.49	0.09	0.98
C54:5	888	0.56	0.019	3.3	2.12	0.27	2.82
C54:4	890	2.83	0.080	2.8	1.93	1.47	15.60
C54:3	892	8.50	0.32	3.7	1.74	4.88	51.78
C54:2	894	1.44	0.036	2.5	1.55	0.93	9.85
C54:1	896	0.22	0.015	6.9	1.37	0.16	1.72
C54:0	898	0.17	0.0047	2.9	1.18	0.14	1.49
C56:3	920	0.42	0.015	3.6	1.62	0.26	2.76
C56:2	922	0.26	0.013	5.2	1.43	0.18	1.89
C57:0	**940**						

Total=9.43

CA37

TAGS	m/z	1	2	3	4	5	6
C51:0	**856**						
C52:3	864	0.26	0.010	4.0	1.86	0.14	1.48
C52:2	866	1.31	0.065	4.9	1.67	0.78	8.40
C52:1	868	0.35	0.021	5.8	1.49	0.24	2.55
C54:4	890	1.09	0.12	10.8	1.93	0.56	6.04
C54:3	892	7.99	0.85	10.6	1.74	4.59	49.27
C54:2	894	3.13	0.25	7.9	1.55	2.01	21.59
C54:1	896	0.54	0.065	12.0	1.37	0.39	4.23
C54:0	898	0.20	0.019	9.5	1.18	0.17	1.82
C56:3	920	0.35	0.015	4.3	1.62	0.22	2.31
C56:2	922	0.31	0.011	3.7	1.43	0.21	2.31
C57:0	**940**						
						Total=9.32	

CA67

TAG ID	m/z	1	2	3	4	5	6
C51:0	**856**						
C52:2	866	1.17	0.024	2.1	1.67	0.70	5.55
C52:1	868	0.55	0.016	2.9	1.49	0.37	2.95
C52:0	870	0.10	0.0057	5.7	1.30	0.08	0.61
C54:4	890	0.44	0.050	11.5	1.93	0.23	1.80
C54:3	892	8.16	0.79	9.7	1.74	4.69	37.26
C54:2	894	6.35	0.58	9.2	1.55	4.08	32.46
C54:1	896	1.80	0.14	7.9	1.37	1.31	10.45
C54:0	898	0.43	0.042	9.6	1.18	0.37	2.92
C56:3	920	0.38	0.017	4.5	1.62	0.23	1.86
C56:2	922	0.47	0.018	3.9	1.43	0.33	2.59
C56:1	924	0.24	0.015	6.0	1.247	0.20	1.56
C57:0	**941**						
						Total=12.58	

Appendix 3

Calculation of Percentage Compositions of Triacylglycerols in Edible Oil Samples

The spreadsheets show the last six columns as shown in Appendix 1 (AVE NORM, STD, (%RSD), RRF, RRF NORM and % COMP) in the five edible oil samples (sesame oil, hemp seed oil, walnut oil, grape seed oil and olive oil).

Sesame oil

TAG ID	m/z	1	2	3	4	5	6
C51:0	**856**						
C52:4	862	0.53	0.018	3.5	2.05	0.26	6.1
C52:3	864	0.52	0.015	2.9	1.86	0.28	6.5
C52:2	866	0.32	0.018	5.6	1.67	0.19	4.4
C54:10	878	0.26	0.079	30.6	3.05	0.08	2.0
C54:9	880	0.23	0.072	31.2	2.86	0.08	1.9
C54:8	882	0.14	0.038	27.5	2.68	0.05	1.2
C54:7	884	0.07	0.0045	6.3	2.49	0.03	0.7
C54:6	886	1.23	0.068	5.5	2.30	0.54	12.5
C54:5	888	1.46	0.092	6.3	2.12	0.69	16.2
C54:4	890	1.17	0.058	5.0	1.93	0.61	14.2
C54:3	892	1.04	0.048	4.6	1.74	0.60	13.9
C54:2	894	0.20	0.021	10.0	1.55	0.13	3.1
C55:4	904	0.52	0.18	34.1	1.87	0.28	6.5
C55:3	906	0.40	0.12	29.0	1.68	0.24	5.5
C55:2	908	0.34	0.11	31.8	1.49	0.23	5.3
C57:0	**940**						
						Total=4.28	

1 = AVE NORM: isotopically and LiCl adduct corrected and internal standard normalized mean peak area (n=5)

2 = STD: standard deviation (n=5)

3 = %RSD: percent relative standard deviation (n=5)

4 = RRF: relative response factor of TAG

5 = RRF NORM: RRF normalized peak area

6 =% COMP: percentage composition of each TAG in the sample

Hemp seed oil

TAG ID	m/z	1	2	3	4	5	6
C51:0	**856**						
C52:5	860	0.34	0.0047	1.4	2.24	0.15	3.7
C52:4	862	0.53	0.011	2.1	2.05	0.26	6.3
C52:3	864	0.15	0.0054	3.5	1.86	0.08	2.0
C54:11	876	0.14	0.037	25.7	3.24	0.04	1.1
C54:10	878	0.24	0.063	26.3	3.05	0.08	1.9
C54:9	880	0.21	0.029	14.1	2.86	0.07	1.7
C54:8	882	0.60	0.047	7.8	2.68	0.22	5.4
C54:7	884	1.52	0.089	5.9	2.49	0.61	14.6
C54:6	886	1.93	0.085	4.4	2.30	0.84	20.2
C54:5	888	1.07	0.048	4.5	2.12	0.50	12.1
C54:4	890	0.52	0.027	5.2	1.93	0.27	6.5
C54:3	892	0.13	0.014	10.2	1.74	0.08	1.8
C55:6	900	0.58	0.12	21.4	2.24	0.26	6.2
C55:5	902	0.69	0.14	20.6	2.06	0.33	8.0
C55:4	904	0.37	0.060	16.3	1.87	0.20	4.8
C55:3	906	0.15	0.037	24.2	1.68	0.09	2.2
C57:7	926	0.03	0.0046	17.3	2.31	0.01	0.3
C57:6	928	0.06	0.0070	12.6	2.12	0.03	0.6
C57:5	930	0.05	0.011	21.1	1.94	0.03	0.7
C57:0	**940**						
						Total=4.16	

Walnut oil

TAG ID	m/z	1	2	3	4	5	6
C51:0	**856**						
C52:5	860	0.29	0.019	6.4	2.24	0.13	2.7
C52:4	862	0.64	0.031	4.8	2.05	0.31	6.4
C52:3	864	0.24	0.016	6.5	1.86	0.13	2.6
C54:11	876	0.19	0.044	22.7	3.24	0.06	1.2
C54:10	878	0.34	0.097	28.3	3.05	0.11	2.3
C54:9	880	0.17	0.045	26.0	2.86	0.06	1.2
C54:8	882	0.33	0.029	8.8	2.68	0.12	2.5
C54:7	884	1.24	0.076	6.1	2.49	0.50	10.1
C54:6	886	2.30	0.16	6.9	2.30	1.00	20.4
C54:5	888	1.26	0.11	9.1	2.12	0.60	12.2
C54:4	890	0.59	0.042	7.2	1.93	0.31	6.3
C54:3	892	0.19	0.018	9.5	1.74	0.11	2.2
C55:6	900	0.65	0.16	25.3	2.24	0.29	5.9
C55:5	902	1.02	0.29	28.9	2.06	0.50	10.1
C55:4	904	0.57	0.16	28.3	1.87	0.31	6.2
C55:3	906	0.30	0.079	26.4	1.68	0.18	3.6
C57:7	926	0.09	0.018	20.4	2.31	0.04	0.8
C57:6	928	0.14	0.014	9.8	2.12	0.07	1.4
C57:5	930	0.17	0.016	9.2	1.94	0.09	1.8
C57:0	**940**						
					Total=4.90		

Grape seed oil

TAG ID	m/z	1	2	3	4	5	6
C51:0	**856**						
C52:4	862	0.68	0.033	4.8	2.05	0.33	7.9
C52:3	864	0.29	0.021	7.3	1.86	0.16	3.7
C54:6	886	2.95	1.2	38.9	2.30	1.28	30.5
C54:5	888	1.67	0.58	35.0	2.12	0.79	18.7
C54:4	890	0.97	0.34	34.4	1.93	0.51	12.0
C54:3	892	0.31	0.095	30.3	1.74	0.18	4.3
C55:6	900	0.14	0.037	25.5	2.24	0.06	1.5
C55:5	902	0.83	0.23	27.1	2.06	0.40	9.6
C55:4	904	0.49	0.13	26.7	1.87	0.26	6.3
C55:3	906	0.28	0.076	26.9	1.68	0.17	4.0
C55:2	908	0.10	0.027	25.6	1.49	0.07	1.6
C57:0	**940**						
						Total=4.21	

Olive oil

TAG ID	m/z	1	2	3	4	5	6
C50:2	838	0.19	0.033	17.4	1.79	0.10	3.2
C50:1	840	0.27	0.038	14.1	1.61	0.17	5.2
C51:0	**856**						
C52:4	862	0.19	0.0086	4.6	2.05	0.09	2.8
C52:3	864	0.66	0.030	4.5	1.86	0.35	10.9
C52:2	866	1.09	0.032	2.9	1.67	0.65	20.2
C54:5	888	0.31	0.060	19.2	2.12	0.15	4.6
C54:4	890	0.88	0.15	17.2	1.93	0.45	14.1
C54:3	892	1.55	0.27	17.2	1.74	0.89	27.5
C54:2	894	0.19	0.040	20.6	1.55	0.12	3.9
C55:3	906	0.15	0.065	53.6	1.68	0.09	2.7
C55:2	908	0.23	0.12	67.6	1.49	0.16	4.8
C57:0	**940**						
						Total=3.23	

Appendix 4

Table of TAGFatty Acid Compositions of the Identified Triacylglycerol Species in Edible Oil Samples as Determined by

ESI/MS/MS

TAG ID	[M+Li]+ m/z	TAG Fatty Acid Compositions				
		Olive oil	Walnut oil	Hemp seed oil	Sesame oil	Grapeseed oil
C50:2	838	C16:0/C16:0/C18:2 C16:0/C16:1/C18:1				
C50:1	840	C16:0/C16:0/C18:1				
C52:5	860		C16:0/C18:2/C18:3	C16:0/C18:2/C18:3		
C52:4	862	C16:0/C18:2/C18:2 C16:0/C18:1/C18:3 C16:1/C18:1/C18:2	C16:0/C18:2/C18:2	C16:0/C18:2/C18:2	C16:10C18:2/C18:2	C16:0/C18:2/C18:2
C52:3	864	C16:1/C18:1/C18:1 C16:0/C18:1/C18:2	C16:0/C18:1/C18:2	C16:0/C18:2/C18:1	C16:0/C18:2/C18:1	C16:0/C18:1/C18:2
C52:2	866	C16:0/C18:1/C18:1			C16:0/C18:1/C18:1	C16:0/C18:1/C18:1
C54:11	876		C16:2/C18:3/C20:6	C18:2/C18:2/C18:7		
C54:10	878		C18:2/C18:4/C18:4 C18:3/C18:3/C18:4	C18:3/C18:3/C18:4	C16:0/C18:5/C20:5	
C54:9	880		C18:3/C18:3/C18:3 C18:2/C18:3/C18:4	C18:3/C18:3/C18:3 C18:0/C18:2/C18:7	C16:0/C18:5/C20:4	
C54:8	882		C18:2/C18:3/C18:3	C18:2/C18:3/C18:3 C16:0/C18:2/C20:6	C16:0/C18:2/C20:6 C16:0/C18:4/C20:4 C18:2/C18:2/C18:4 C18:1/C18:3/C18:4	
C54:7	884		C18:2/C18:2/C18:3	C18:2/C18:2/C18:3	C16:0/C18:3/C20:4 C16:0/C18:4/C20:3	
C54:6	886		C18:2/C18:2/C18:2	C18:2/C18:2/C18:2	C18:2/C18:2/C18:2	C18:2/C18:2/C18:2
C54:5	888	C18:2/C18:2/C18:1	C18:2/C18:2/C18:1	C18:2/C18:2/C18:1 C18:1/C18:1/C18:3 C18:0/C18:2/C18:3	C18:1/C18:2/C18:2	C18:1/C18:2/C18:2
C54:4	890	C18:2/C18:1/C18:1	C18:2/C18:1/C18:1 C18:2/C18:2/C18:0	C18:2/C18:1/C18:1 C18:2/C18:2/C18:0	C18:2/C18:1/C18:1	C18:2/C18:1/C18:1 C18:2/C18:2/C18:0

C54:3	892	C18:1/C18:1/C18:1	C18:1/C18:1/C18:1 C18:0/C18:1/C18:2	C18:1/C18:1/C18:1 C18:0/C18:1/C18:2	C18:1/C18:1/C18:1	C18:1/C18:1/C18:1 C18:0/C18:1/C18:2
C54:2	894	C18:0/C18:1/C18:1			C18:0/C18:1/C18:1	C18:0/C18:1/C18:1
C54:1	896					C18:0/C18:0/C18:1
C54:0	898					
C55:6	900		C18:2/C18:2/C19:2	C18:2/C18:3/C19:1		C18:3/C18:3/19:0
C55:5	902		C18:2/C18:3/C19:0	C18:2/C18:2/C19:1		C18:2/C18:3/19:0
C55:4	904		C18:1/C18:2/C19:1 C18:2/C18:2/C19:0	C18:2/C18:2/C19:0 C18:1/C18:3/C19:0	C18:2/C18:2/C19:0 C18:2/C18:1/C19:1	C18:1/C18:3/19:0
C55:3	906	C18:1/C18:2/C19:0	C18:1/C18:2/C19:0	C18:1/C18:2/C19:0	C18:1/C18:2/C19:0	C18:1/C18:2/C19:0
C55:2	908	C18:1/C18:1/C19:0			C18:1/C18:1/C19:0	C18:1/C18:1/C19:0
C57:7	924		C19:2/C19:2/C19:3 C19:1/C19:3/C19:3	C19:2/C19:2/C19:3 C19:1/C19:3/C19:3		
C57:6	926		C19:2/C19:2/C19:2	C19:0/C19:2/C19:4 C19:1/C19:1/C19:4 C19:2/C19:2/C19:2 C19:1/C19:2/C19:3 C19:0/C19:3/C19:3		
C57:5	928		C19:1/C19:2/C19:2	C19:1/C19:2/C19:2		

NB: more than one TAG composition confirms the presence of isobaric composition. The order of fatty acids does not imply an order for *sn-1, sn-2* and *sn-3* in the TAG.